Supporting Information

Role of the (Pseudo)Halido Ligand in Ruthenium(II) *p*-Cymene α-Amino Acid Complexes on Speciation, Protein Reactivity and Cytotoxicity

Lorenzo Biancalana,[a] Emanuele Zanda,[a] Mouna Hadiji,[b] Stefano Zacchini,[c] Alessandro Pratesi,[a] Guido Pampaloni,[a] Paul J. Dyson [b] and Fabio Marchetti [a]

[a] University of Pisa, Dipartimento di Chimica e Chimica Industriale, Via G. Moruzzi 13, I-56124 Pisa, Italy.

[b] Institut des Sciences et Ingénierie Chimiques, Ecole Polytechnique Fédérale de Lausanne (EPFL), Switzerland.

[c] University of Bologna, Dipartimento di Chimica Industriale "Toso Montanari", Viale Risorgimento 4, I-40136 Bologna, Italy.

Table of contents **Pages**

Synthesis of $[RuX_2(\eta^6\text{-}p\text{-cymene})]_2$ (X = Br, I)

$[RuBr_2(\eta^6\text{-}p\text{-cymene})]_2$ (Chart S1).

Chart S1. Structure of $[RuBr_2(\eta^6\text{-}p\text{-cymene})]_2$ (numbering refers to C atoms).

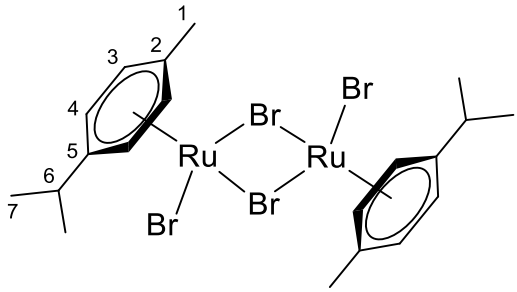

A suspension of $[RuCl_2(\eta^6\text{-}p\text{-cymene})]_2$ (186 mg, 0.304 mmol) and NaBr (164 mg, 1.59 mmol) in a H_2O/MeOH 1:1 *v*/*v* mixture (*ca*. 10 mL) was vigorously stirred at room temperature for 2 h. Next, volatiles were removed under vacuum and the residue was suspended in CH_2Cl_2. The mixture was filtered through celite and the filtrate was dried under vacuum. NaBr (*ca*. 160 mg) was added, and the procedure was repeated (×3). The final residue was suspended in Et_2O and filtered. The resulting bright orange-red solid was washed with Et_2O and dried under vacuum (40 °C, over P_2O_5). Yield: 232 mg, 97%. Soluble in acetone, CH_2Cl_2, $CHCl_3$, poorly soluble in H_2O and E_2O. Anal. Calcd. For $C_{20}H_{28}Br_4Ru_2$: C, 30.40; H, 3.57. Found: C, 29.96; H, 3.38. IR (solid state): $\tilde{\upsilon}/cm^{-1}$ = 3048w, 3034m, 2956m, 2924m-sh, 2867w, 1527w, 1493m, 1469s, 1442s-sh, 1407m, 1385s, 1377s-sh, 1363m-sh, 1324m, 1274m, 1198m, 1156m, 1114m, 1087m, 1055s, 1028s-sh, 1004m, 957w, 825wm 903w, 876s, 861s,803s, 727s, 692m, 689m, 667m. ^1H NMR ($CDCl_3$): δ/ppm = 5.49 (d, $^3J_{HH}$ = 5.9 Hz, 2H, C^4H), 5.37 (d, $^3J_{HH}$ = 5.9 Hz, 2H, C^3H), 2.95 (h, $^3J_{HH}$ = 6.9 Hz, 1H, C^6H), 2.21 (s, 3H, C^1H), 1.26 (d, $^3J_{HH}$ = 6.9 Hz, 6H, C^7H).

[$RuI_2(\eta^6$-*p*-cymene)]$_2$ (Chart S2).

Chart S2. Structure of [$RuI_2(\eta^6$-*p*-cymene)]$_2$ (numbering refers to C atoms).

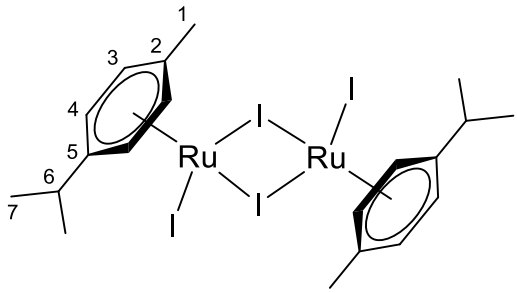

A suspension of [$RuCl_2(\eta^6$-*p*-cymene)]$_2$ (401 mg, 0.550 mmol) and NaI (597 mg, 3.98 mmol) in acetone (35 mL) was stirred at reflux temperature for 2.5 h. The resulting red/violet suspension was cooled to room temperature and taken to dryness under vacuum. The residue was suspended in CH_2Cl_2 and the suspension was filtered twice on a celite pad. Volatiles were removed under vacuum from the filtrate solution, affording a dark Bordeaux-red solid. The solid was washed with hexane then dried under vacuum (40 °C, over P_2O_5). Yield: 577 mg, 90%. Soluble in acetone, CH_2Cl_2, $CHCl_3$, poorly soluble in EtOH, Et_2O, insoluble in H_2O, petroleum ether and MeOH. Anal. Calcd. For $C_{20}H_{28}I_4Ru_2$: C, 24.56; H, 2.89. Found: C, 24.79; H, 2.77. IR (solid state): $\tilde{\upsilon}/cm^{-1}$ = 3028w, 2961m, 2924w, 2866w, 1902w, 1865w, 1785w, 1759w, 1735w, 1689w, 1530w, 1496w, 1469s, 1441w, 1407w, 1381s, 1375s, 1359m-sh, 1324w, 1296m, 1277m, 1211m, 1197m, 1156m, 1141m, 1115m, 1085m, 1055s, 1025s, 1006m, 958w, 923m, 888m, 866s, 801m, 734w, 659w. ^{1}H NMR ($CDCl_3$): δ/ppm = 5.53 (d, $^3J_{HH}$ = 5.9 Hz, 2H, C^4H), 5.43 (d, $^3J_{HH}$ = 5.8 Hz, 2H, C^3H), 3.01 (hept, $^3J_{HH}$ = 6.9 Hz, 1H, C^6H), 2.36 (s, 3H, C^1H), 1.25 (d, $^3J_{HH}$ = 6.9 Hz, 6H, C^7H).

Comparison of diastereomeric ratios and spectroscopic data.

Table S1. Diastereomeric ratios of [RuX(κ²*N*,*O*-amino carboxylate)(η⁶-*p*-cymene)] complexes in CD_3OD or D_2O solution by ^1H NMR.

Compound	Amino acid	Monodentate ligand	Diastereomeric ratio	
			Methanol (CD_3OD)	Water (D_2O) [a]
1a	L-proline	Cl^-	6.5 [b]	7
1b	"	Br^-	8	6
1c	"	I^-	6.5	16
1d	"	NCS^-	2	1
1e	"	N_3^-	4	2.5
1f	"	NO_2^-	5	*n.d.*
1g	"	CN^-	8	*n.d.*
[1w]⁺	"	H_2O	*n.d.*	2.6
2a	*trans*-4-hydroxy-L-proline	Cl^-	2 [b]	3.5
2b	"	Br^-	4	5
2c	"	I^-	5	6.5
2d	"	NCS^-	1	1.5
2e	"	N_3^-	1.5	2
[2w]⁺	"	H_2O	*n.d.*	1.5
3a	L-serine	Cl^-	1.4 [b]	1.4
[3-PPh₃]⁺ [c]	"	PPh_3	5 [b]	5 [b]
[3i]⁺	"	pta	1.3	1.3

[a] In the presence of excess Cl^- (**1-3a**), Br^- (**1-2b**) or I^- (**1-2c**). [b] Data taken from the literature.[1] [c] [**3-PPh₃**]⁺ = [Ru(κ²*N*,*O*-L-Ser)(PPh_3)(η⁶-*p*-cymene)]⁺.

Table S2. IR/NMR fingerprints of SCN^-, N_3^-, CN^-, NO_2^- coordination in $[RuX_2(\eta^6\text{-}p\text{-cymene})]_2$ and $[RuX(\kappa^2N,O\text{-amino carboxylate})(\eta^6\text{-}p\text{-cymene})]$ complexes and reference sodium/potassium salts.

Compound	Amino acid	Monodentate ligand X	^{13}C NMR:[a] δ / ppm	^{14}N NMR:[a] δ / ppm	IR (solid state):[b] ũ / cm^{-1}
KSCN	-	**SCN^-**	133	− 180	ν(NCS): 2043, *2002*
$[Ru(SCN)_2(\eta^6\text{-}p\text{-cymene})]_2$	-		137, 136, 134 (**N**CS) 125 (**S**CN)	− 279	ν(NCS): 2146 (**S**CN), 2094 (**N**CS)
1d	Pro		139	− 264	ν(NCS): 2094, *2054*
2d	Hyp		139	− 264	ν(NCS): 2089, *2050*
NaN_3	-	**N_3^-**	-	− 134, − 285	$\nu(N_3)$: 2140 [c]
$[Ru(N_3)_2(\eta^6\text{-}p\text{-cymene})]_2$	-		-	− 129, − 234	$\nu(N_3)$: 2059, 2040
$[Ru(N_3)_2(\eta^6\text{-}C_6Me_6)]_2$	-		-	-	$\nu(N_3)$: 2064, 2024 [c]
1e	Pro		-	− 130, − 241	$\nu(N_3)$: 2027
2e	Hyp		-	− 130, − 240	$\nu(N_3)$: 2025
$NaNO_2$	-	**NO_2^-**	-	230	$\nu_{asym}(NO_2)$: 1324sh. $\nu_{sym}(NO_2)$: 1226
1f	Pro		-	− 349	$\nu_{asym}(NO_2)$: 1365 $\nu_{sym}(NO_2)$: 1304
KCN	-	**CN^-**	98 [d]	-	ν(CN): 2077 [c]
1g	Pro		139	-	ν(CN): 2105

[a] NMR data in CD_3OD except $[Ru(SCN)_2(\eta^6\text{-}p\text{-cymene})]_2$, $[Ru(N_3)_2(\eta^6\text{-}p\text{-cymene})]_2$ (^{13}C, ^{14}N NMR) and **1d** (^{14}N NMR) (in acetone) and KCN (in water). [b] Shoulder peak of the SCN absorption in *italic*. [c] IR data taken from the literature.[2] [d] NMR data taken from the literature.[3]

IR (solid state) and $^{1}H/^{13}C/^{14}N/^{31}P$ NMR spectra.

Figure S1. Solid-state IR spectrum (650-4000 cm^{-1}) of $[RuBr_2(\eta^6\text{-}p\text{-cymene})]_2$.

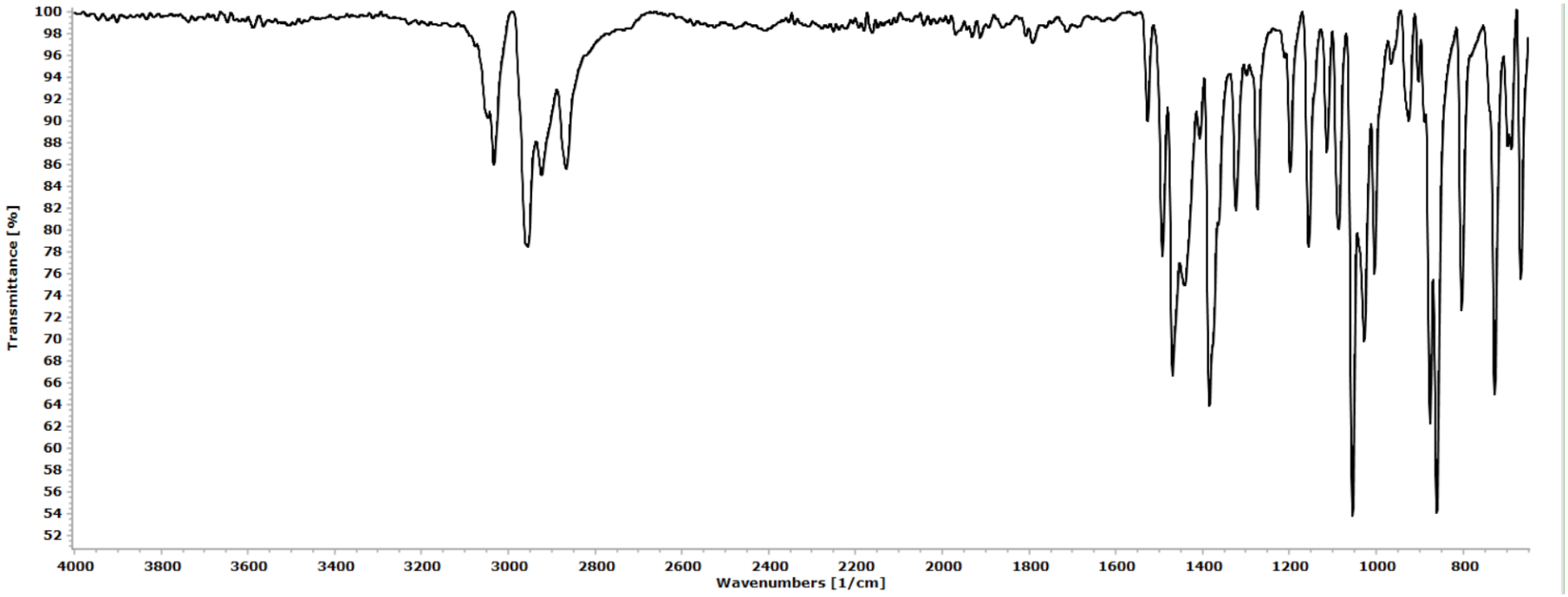

Figure S2. Solid-state IR spectrum (650-4000 cm^{-1}) of $[RuI_2(\eta^6\text{-}p\text{-cymene})]_2$.

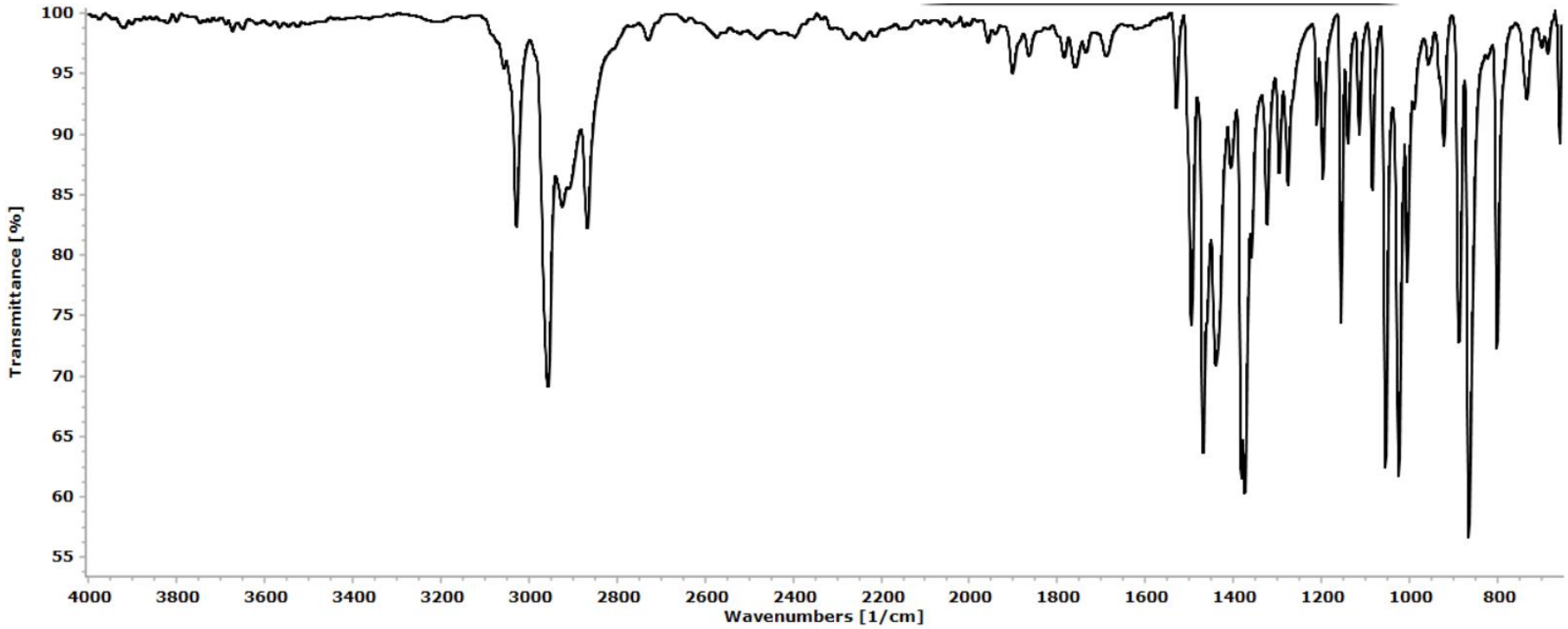

Figure S3. Solid-state IR spectrum (650-4000 cm^{-1}) of $[Ru(SCN)_2(\eta^6\text{-}p\text{-cymene})]_2$.

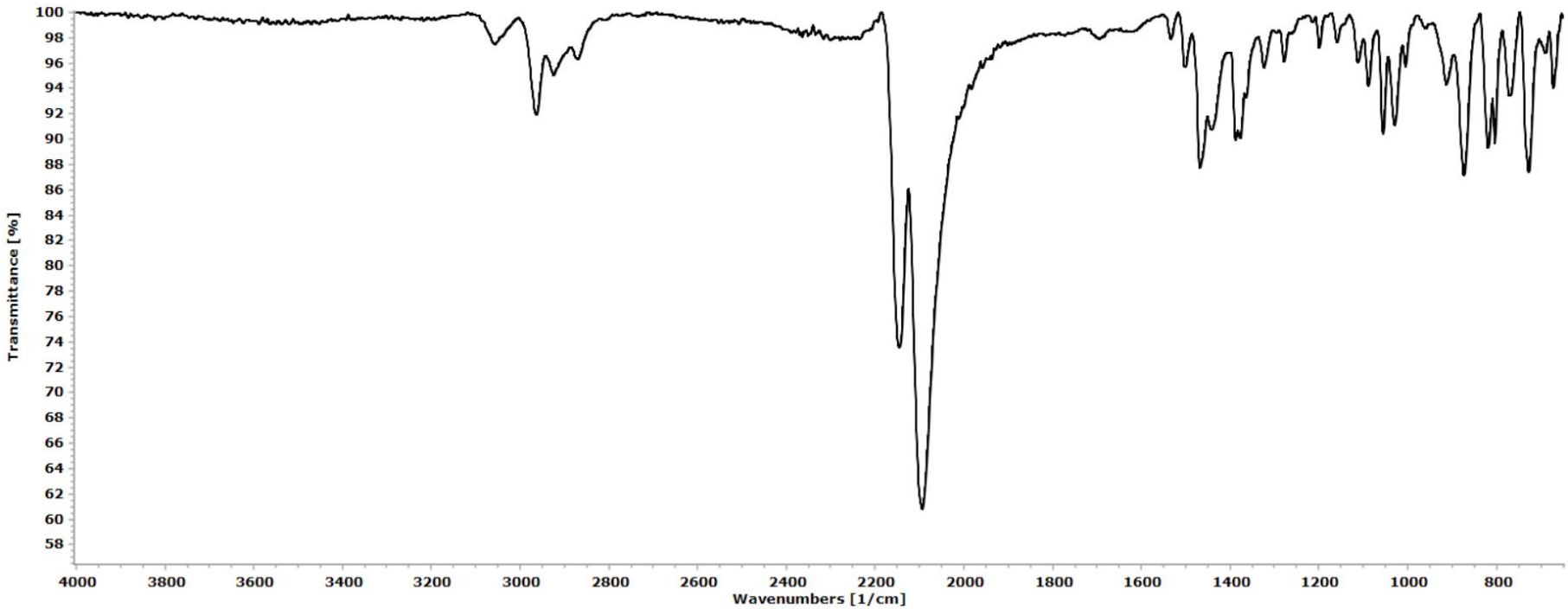

Figure S4. Solid-state IR spectrum (650-4000 cm^{-1}) of $[Ru(N_3)_2(\eta^6\text{-}p\text{-cymene})]_2$.

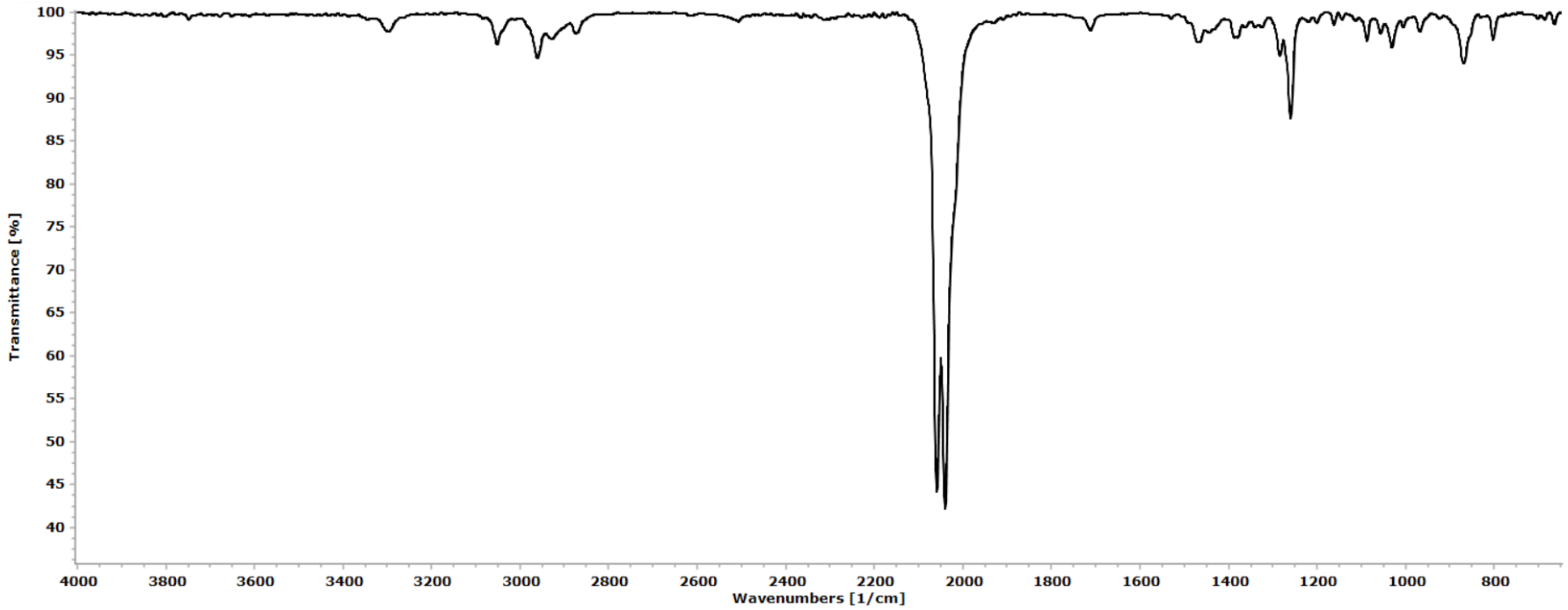

Figure S5. Solid-state IR spectrum (650-4000 cm^{-1}) of [RuBr(κ^2*N*,*O*-Pro)(η^6-*p*-cymene)], **1b**.

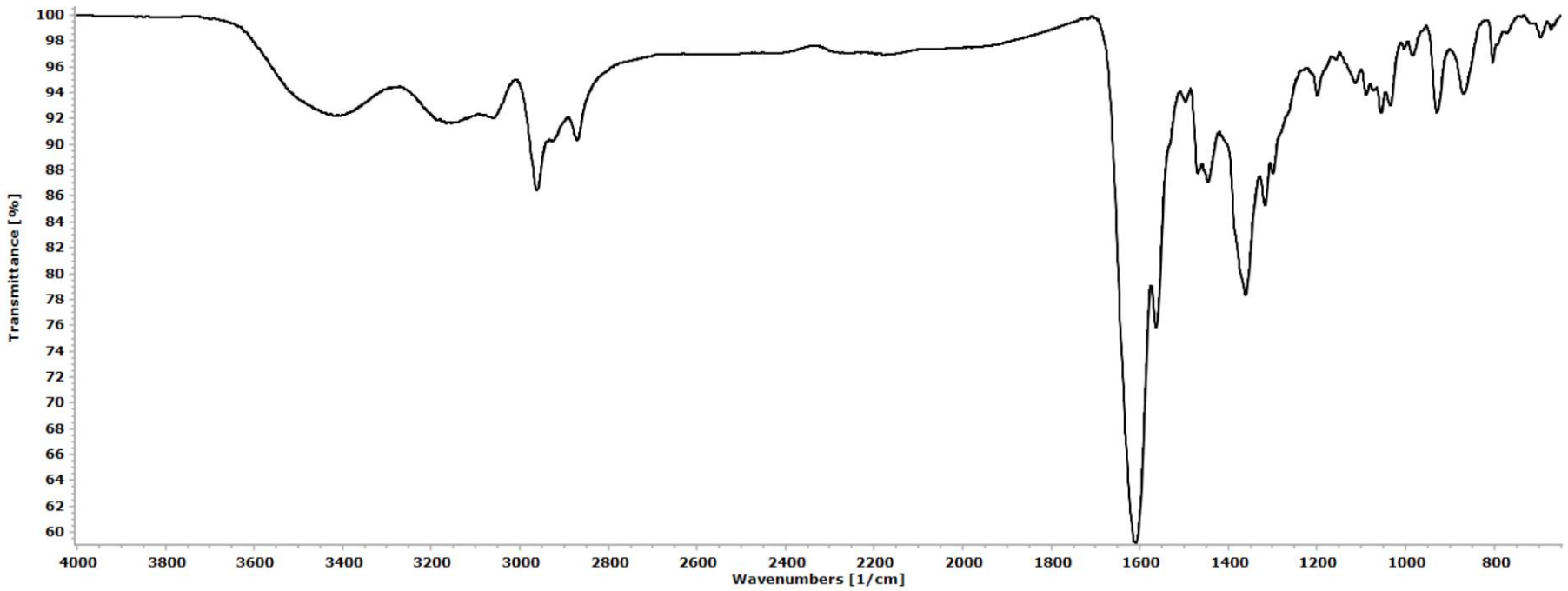

Figure S6. Solid-state IR spectrum (650-4000 cm^{-1}) of [RuI(κ^2*N*,*O*-Pro)(η^6-*p*-cymene)], **1c**.

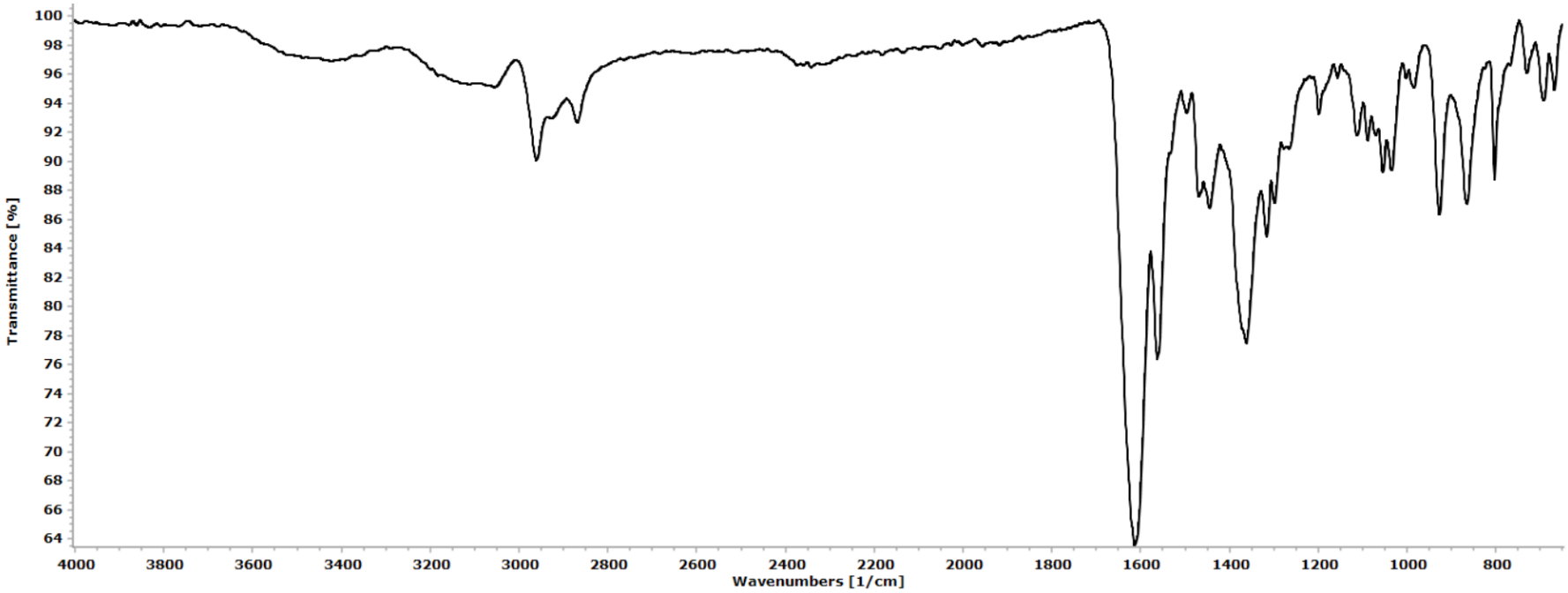

Figure S7. Solid-state IR spectrum (650-4000 cm^{-1}) of [Ru(κ*N*-NCS)(κ^2*N*,*O*-Pro)(η^6-*p*-cymene)], **1d**.

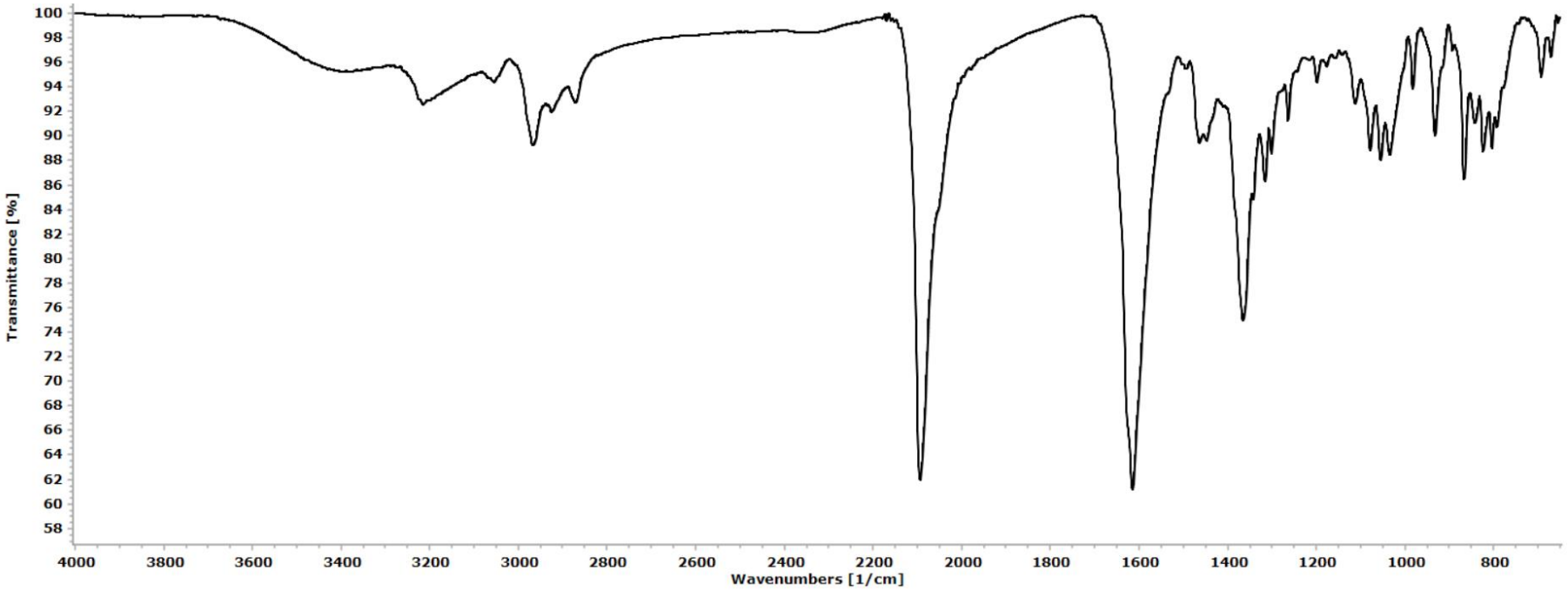

Figure S8. Solid-state IR spectrum (650-4000 cm^{-1}) of [Ru(N_3)(κ^2*N*,*O*-Pro)(η^6-*p*-cymene)], **1e**.

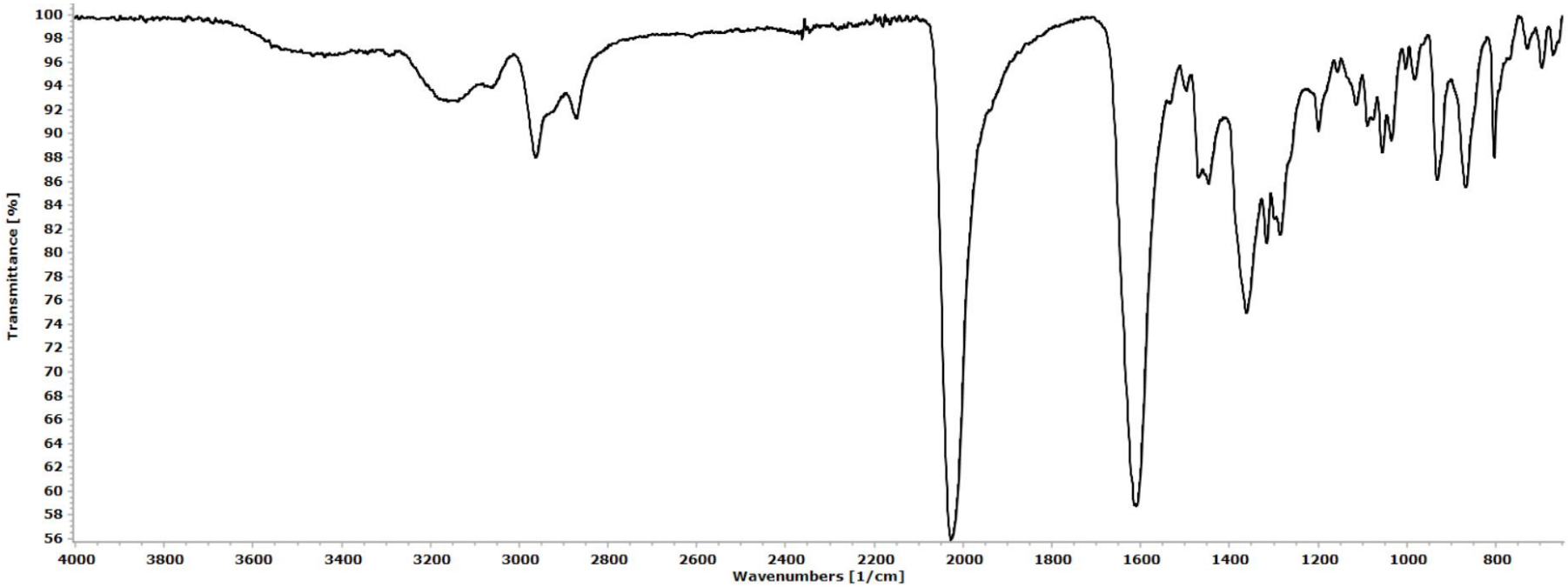

Figure S9. Solid-state IR spectrum (650-4000 cm^{-1}) of [Ru(κ*N*-NO_2)(κ^2*N*,*O*-Pro)(η^6-*p*-cymene)], **1f**.

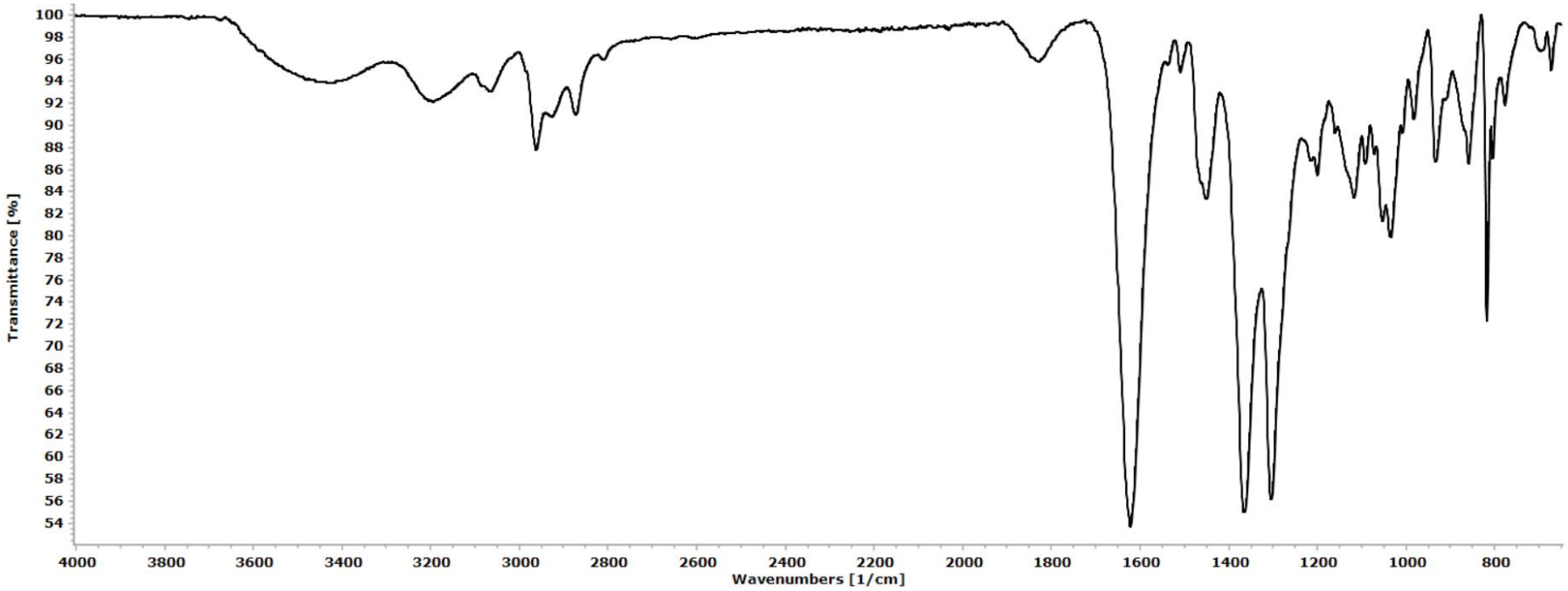

Figure S10. Solid-state IR spectrum (650-4000 cm^{-1}) of [Ru(CN)(κ^2*N*,*O*-Pro)(η^6-*p*-cymene)], **1g**.

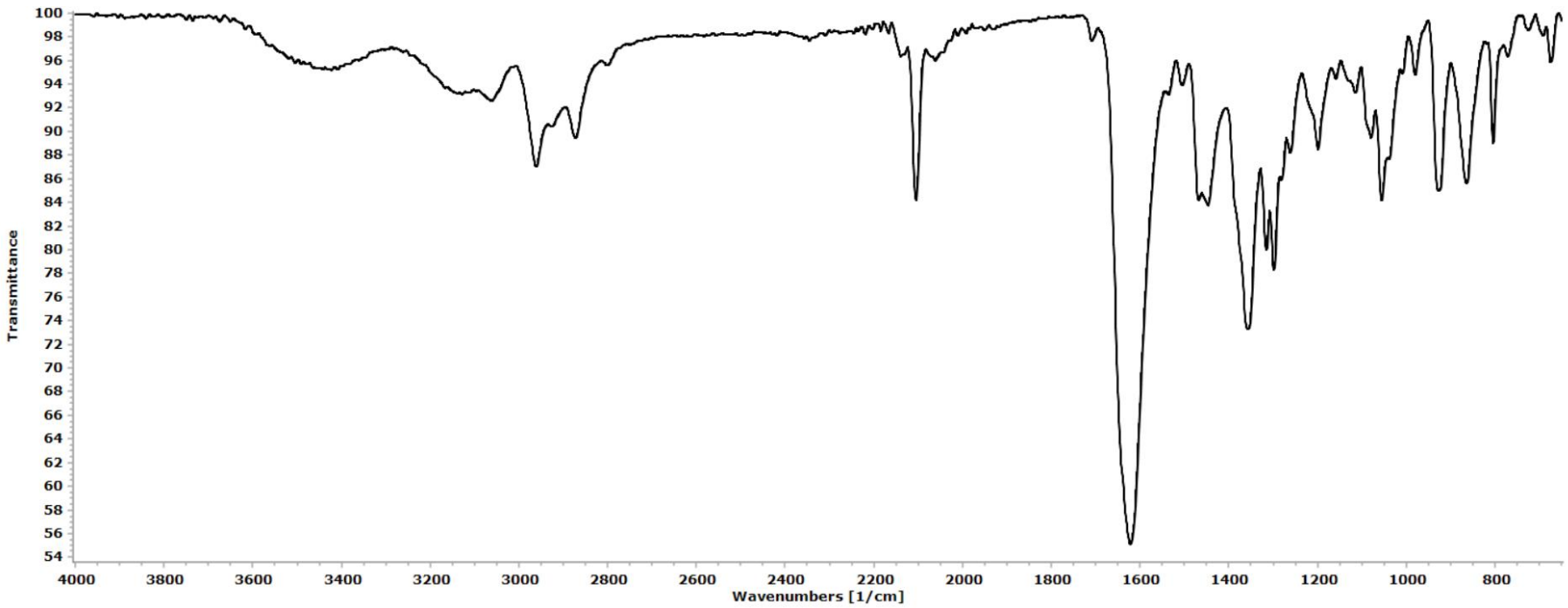

Figure S111. Solid-state IR spectrum (650-4000 cm^{-1}) of [RuBr(κ²*N*,*O*-Hyp)(η⁶-*p*-cymene)], **2b**.

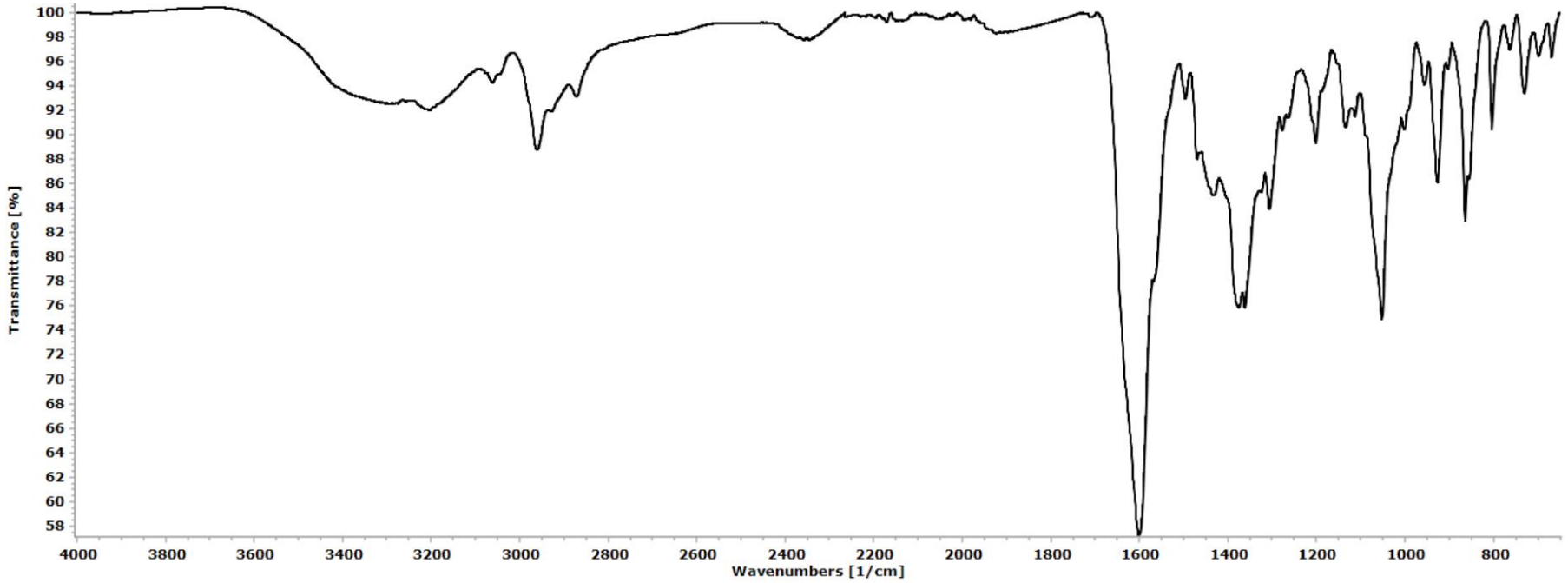

Figure S12. Solid-state IR spectrum (650-4000 cm^{-1}) of [RuI(κ^2*N*,*O*-Hyp)(η^6-*p*-cymene)], **2c**.

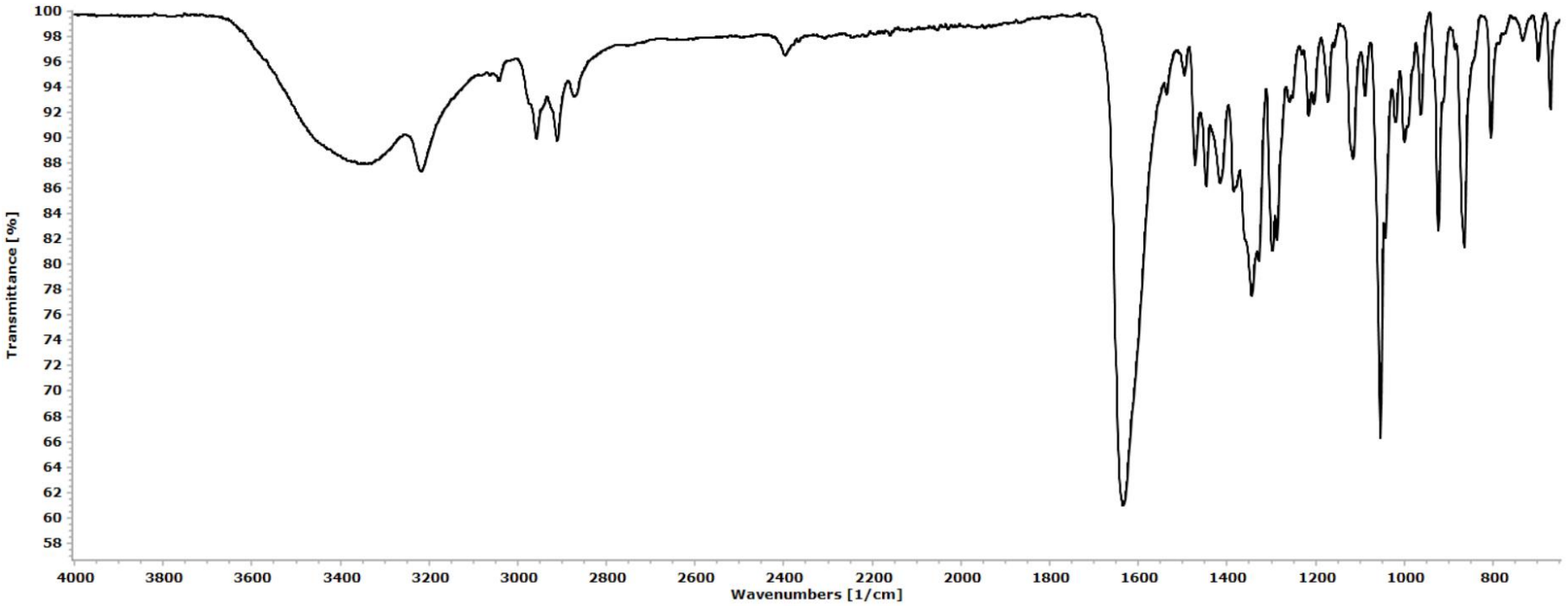

Figure S13. Solid-state IR spectrum (650-4000 cm^{-1}) of [Ru(κ*N*-NCS)(κ^2*N*,*O*-Hyp)(η^6-*p*-cymene)], **2d**.

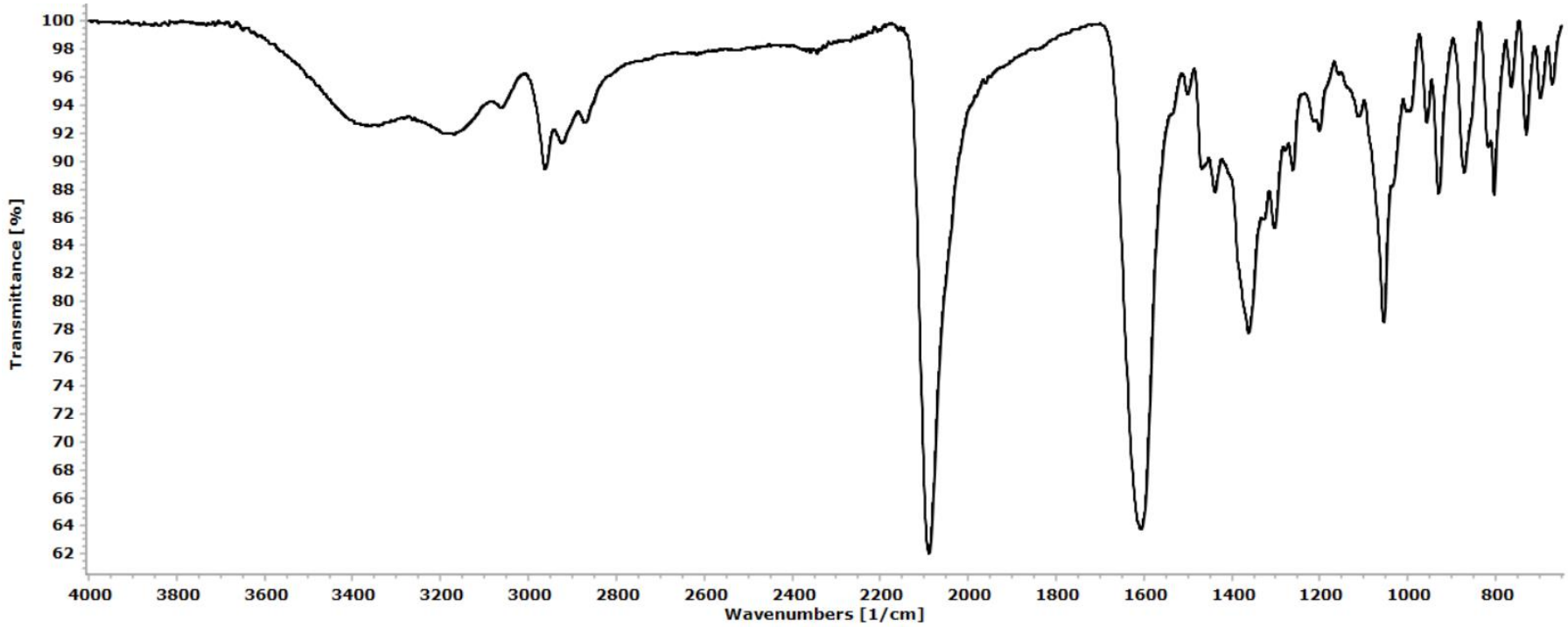

Figure S14. Solid-state IR spectrum (650-4000 cm^{-1}) of [Ru(N_3)(κ^2*N*,*O*-Hyp)(η^6-*p*-cymene)], **2e**.

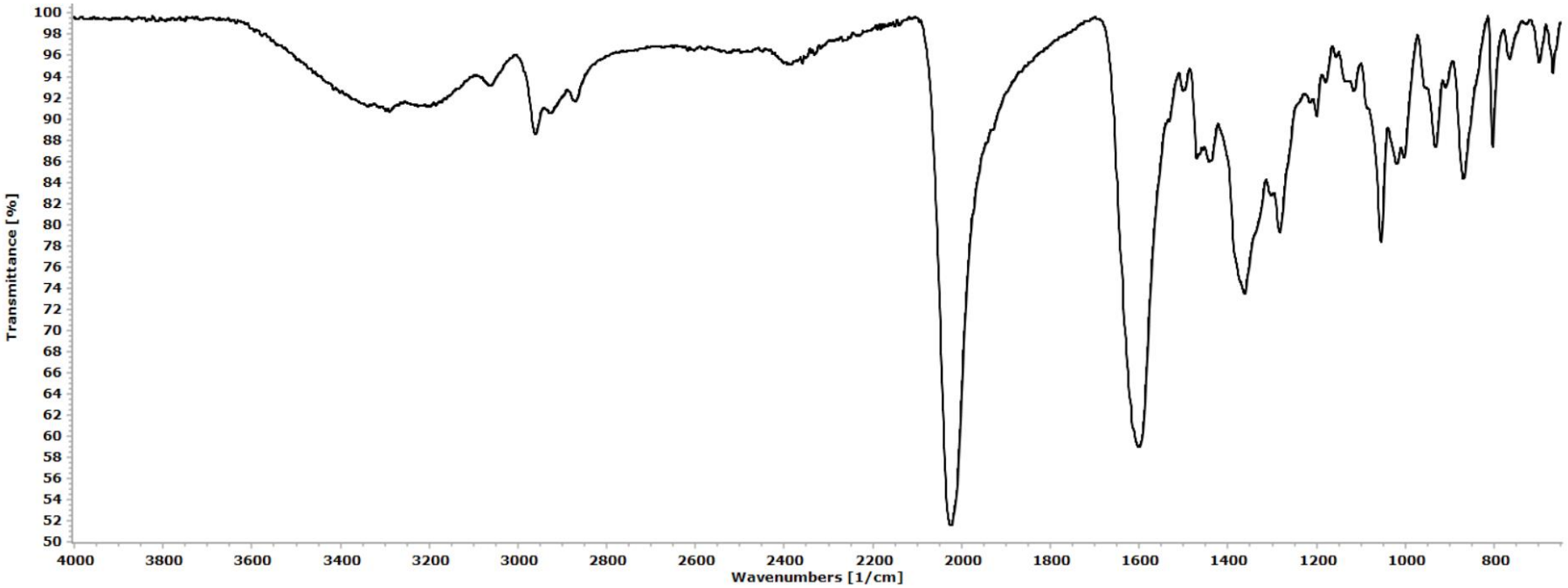

Figure S15. Solid-state IR spectrum (650-4000 cm^{-1}) of [Ru(κ^3*N*,*O*,*O'*-Ser)(η^6-*p*-cymene)], **3h**.

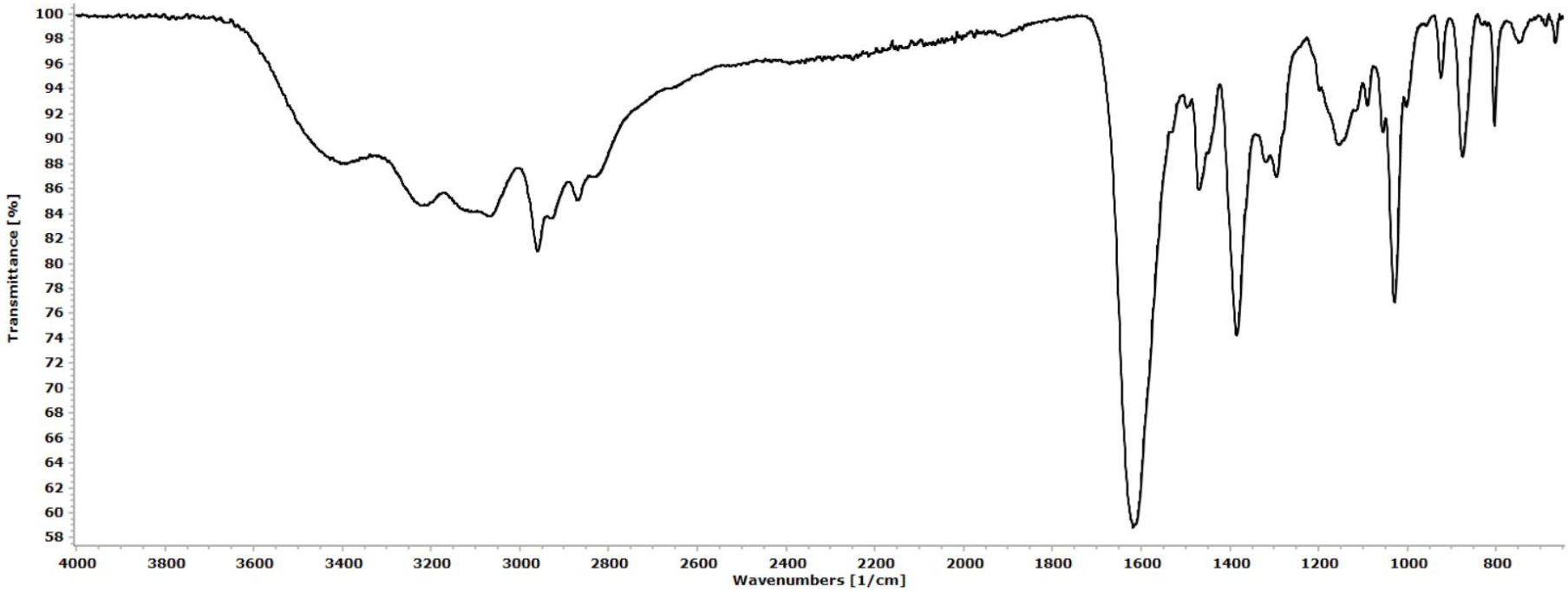

Figure S16. Solid-state IR spectrum (650-4000 cm^{-1}) of [Ru(κ^3*N*,*O*,*O'*-Thr)(η^6-*p*-cymene)], **4h**.

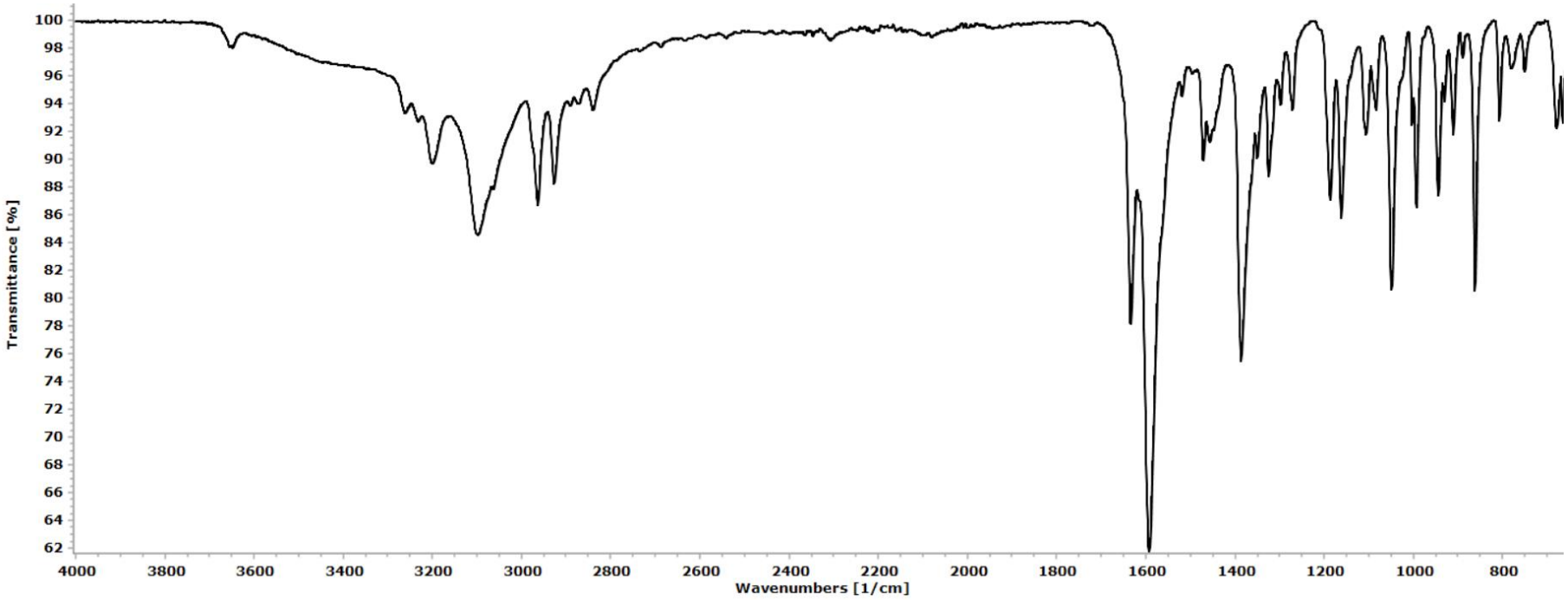

Figure S17. Solid-state IR spectrum (650-4000 cm^{-1}) of [Ru(κ^3*N*,*O*,*O'*-Hom)(η^6-*p*-cymene)], **5h**.

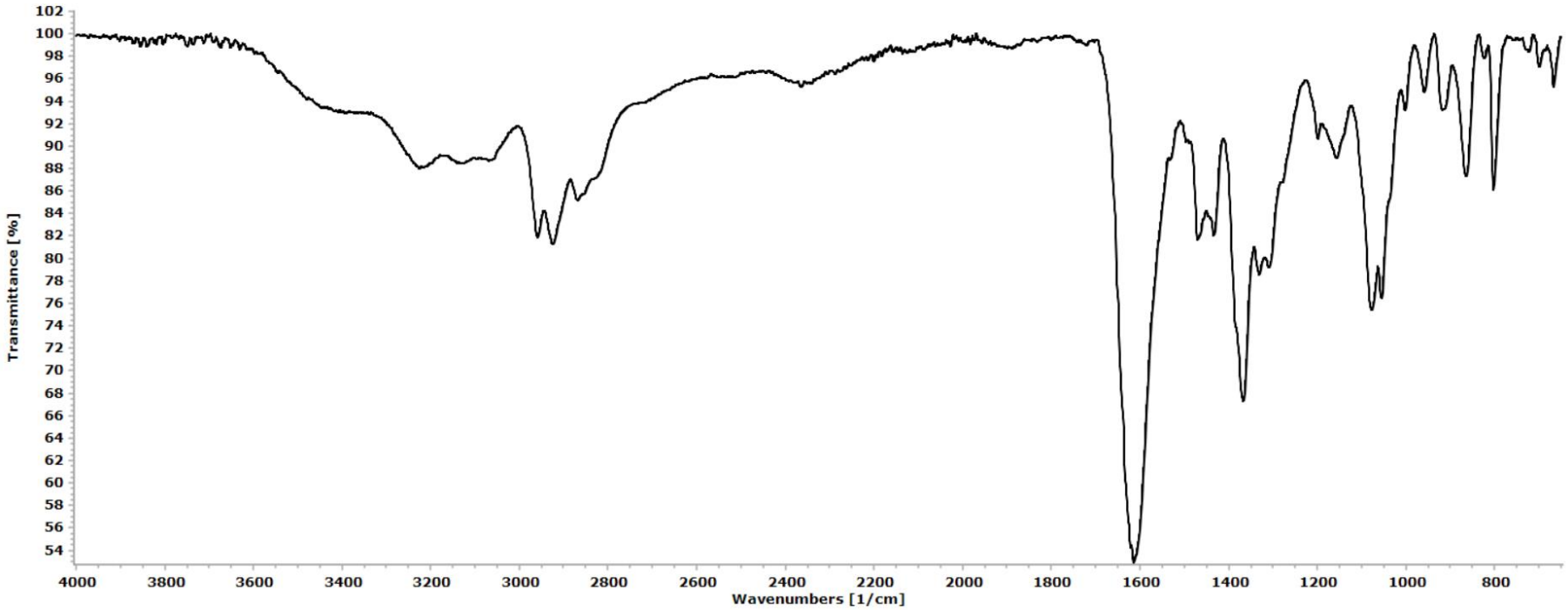

Figure S18. Solid-state IR spectrum (650-4000 cm^{-1}) of [Ru(κ^2*N*,*O*-Ser)(κ*P*-pta)(η^6-*p*-cymene)]Cl, [**3i**]Cl.

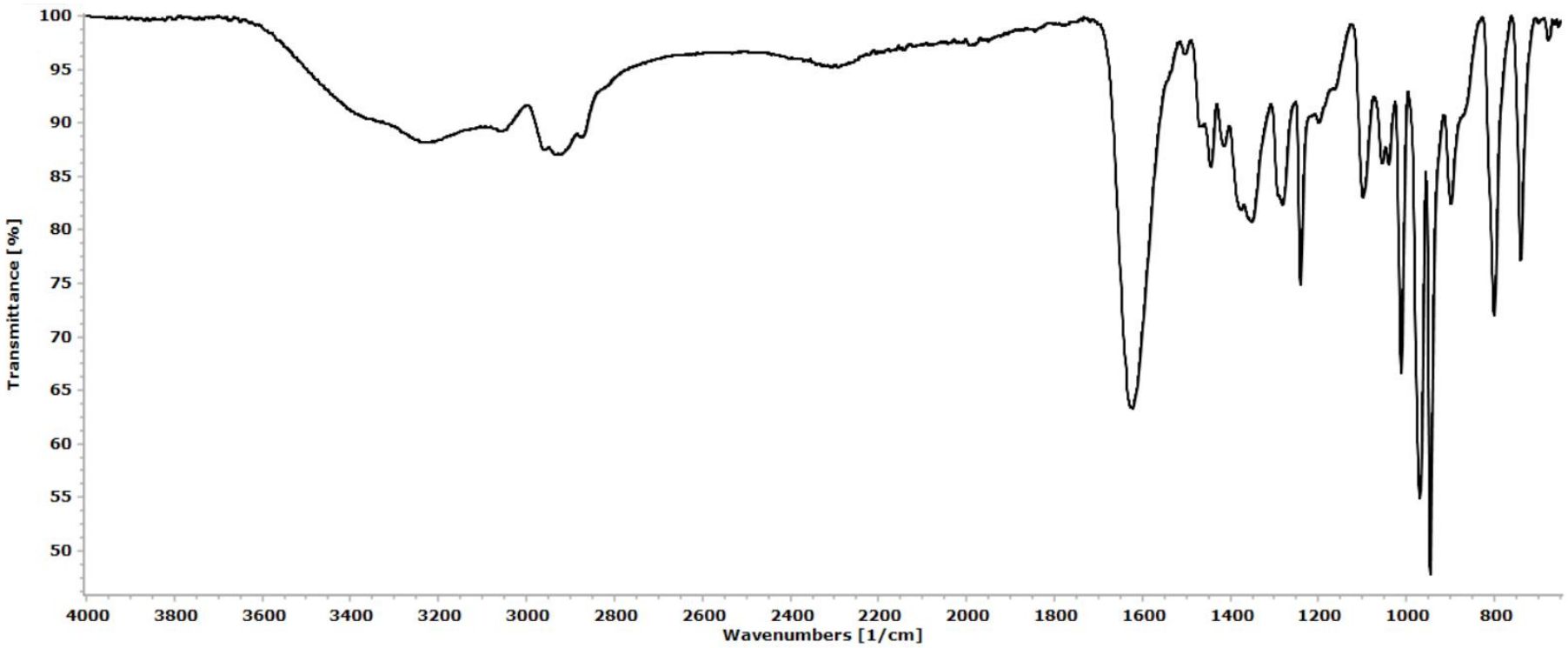

Figure S19. ^{1}H NMR spectrum (401 MHz, $CDCl_3$) of $[RuBr_2(\eta^6\text{-}p\text{-cymene})]_2$.

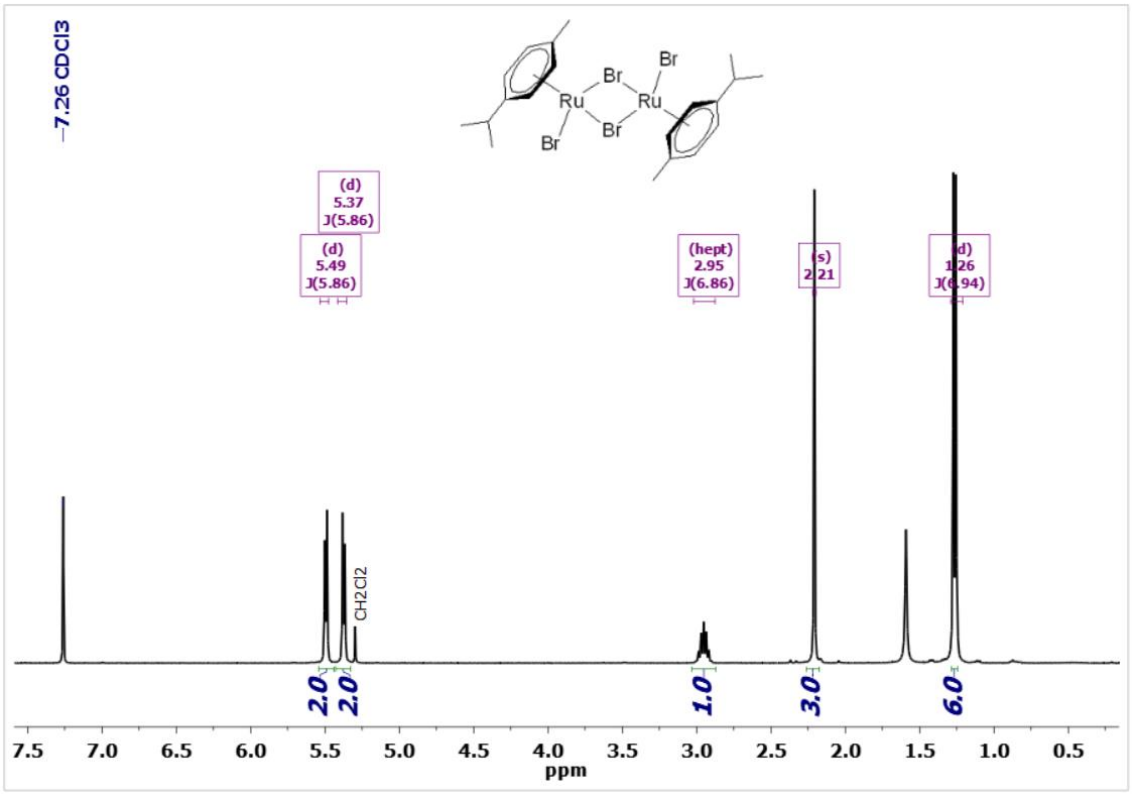

Figure S20. ^{1}H NMR spectrum (401 MHz, $CDCl_3$) of $[RuI_2(\eta^6\text{-}p\text{-cymene})]_2$.

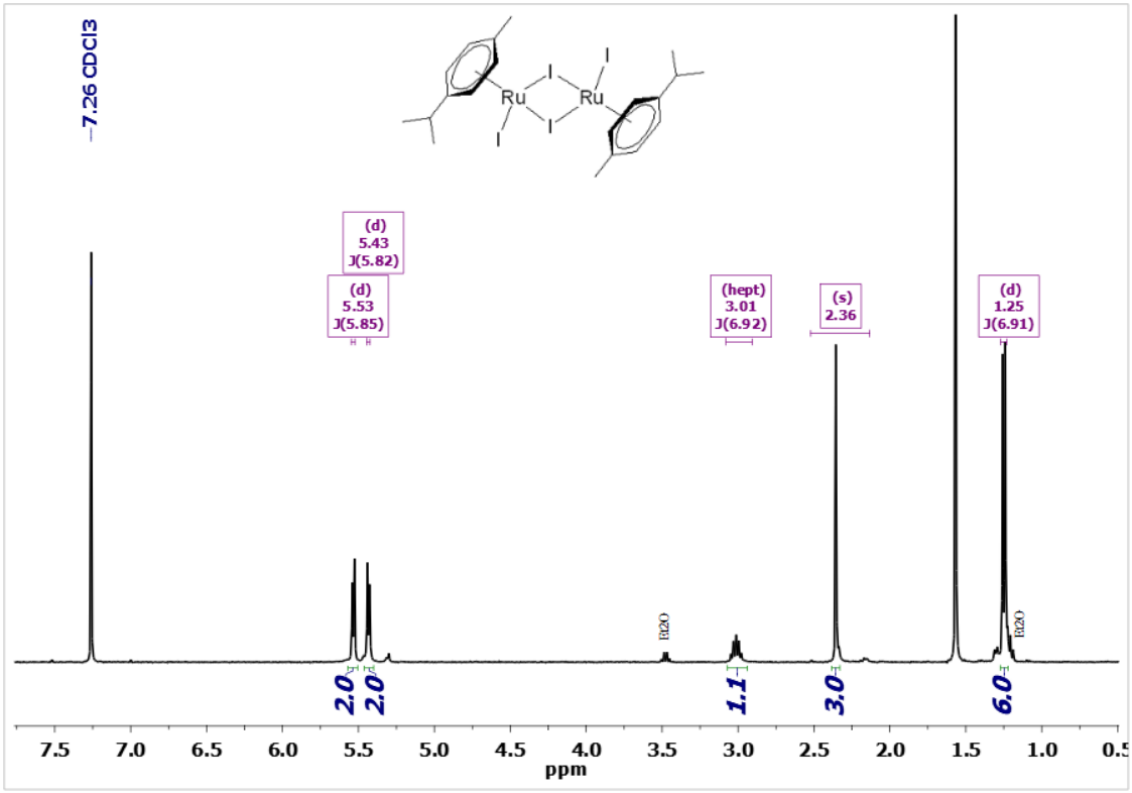

Figure S21. ^{1}H NMR spectrum (401 MHz, acetone-d_6) of $[Ru(SCN)_2(\eta^6\text{-}p\text{-cymene})]_2$.

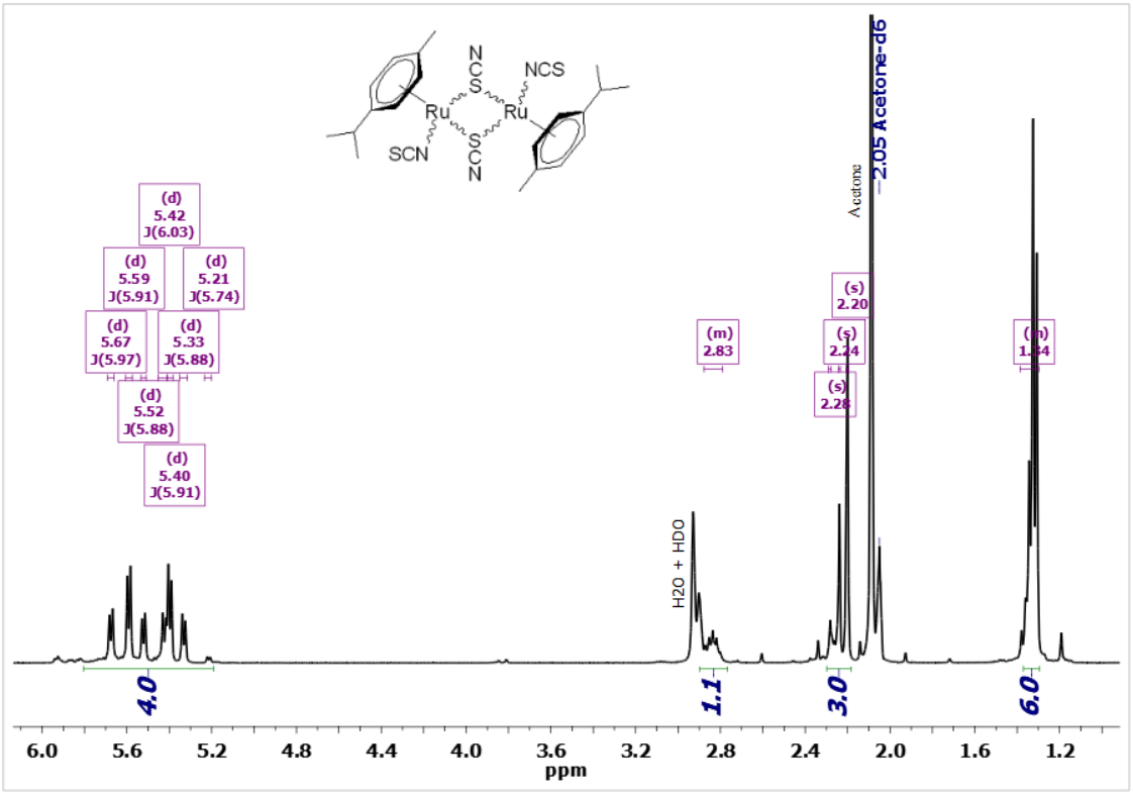

Figure S22. $^{13}C\{^{1}H\}$ NMR spectrum (101 MHz, acetone-d_6) of $[Ru(SCN)_2(\eta^6\text{-}p\text{-cymene})]_2$.

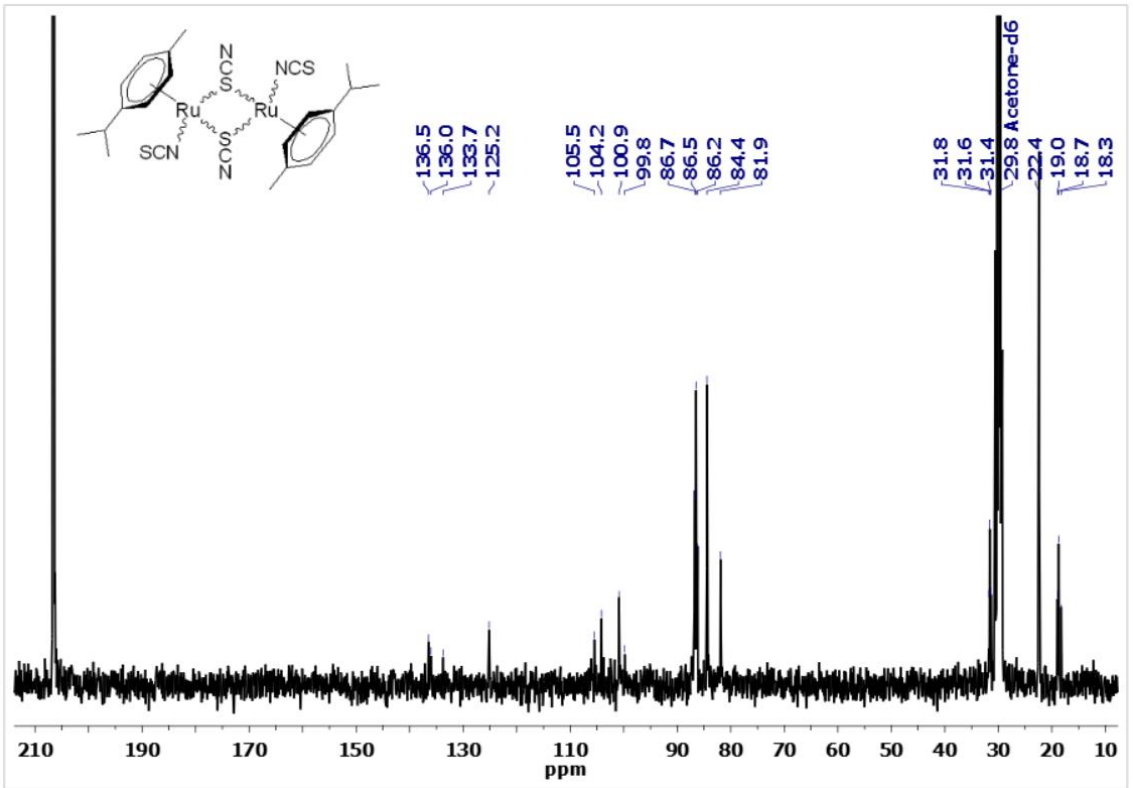

Figure S23. ^{1}H NMR spectrum (401 MHz, $CDCl_3$) of $[Ru(N_3)_2(\eta^6\text{-}p\text{-cymene})]_2$.

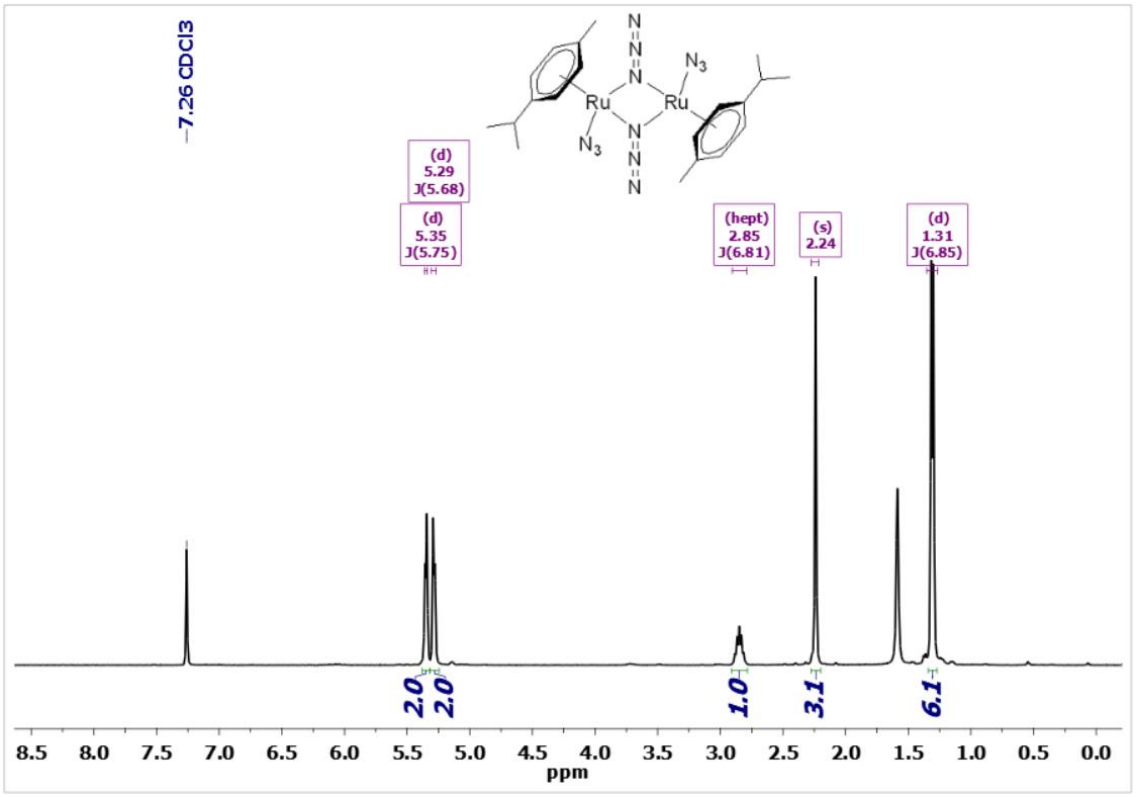

Figure S24. ^{1}H NMR spectrum (401 MHz, CD_3OD) of [RuBr(κ^2*N*,*O*-Pro)(η^6-*p*-cymene)], **1b**. Only resonances due to the major isomer are marked.

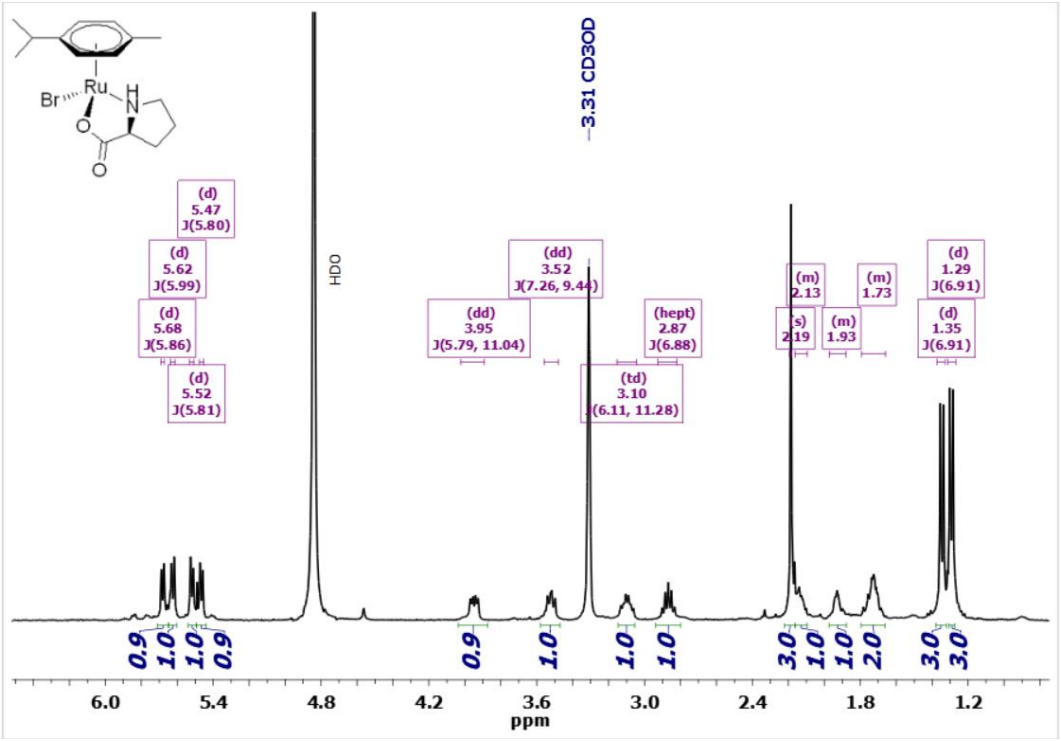

Figure S25. $^{13}C\{^{1}H\}$ NMR spectrum (101 MHz, CD_3OD) of [RuBr(κ²*N*,*O*-Pro)(η⁶-*p*-cymene)], **1b**.

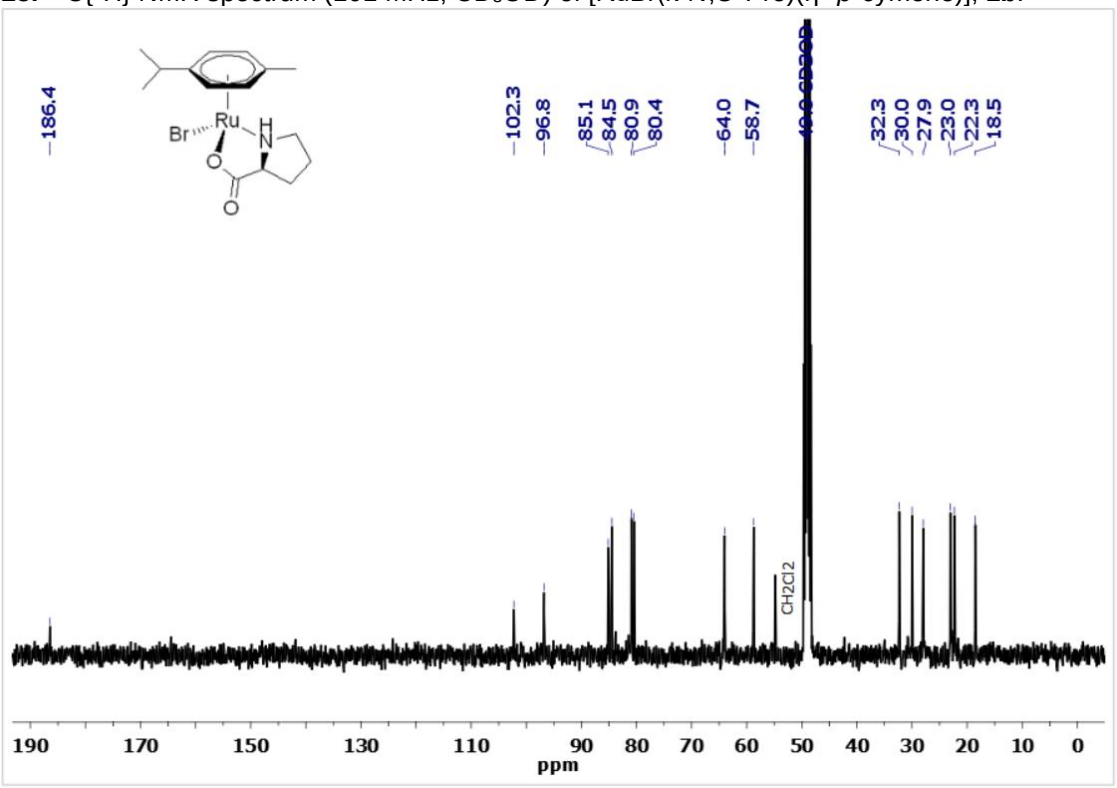

Figure S26. ^{1}H NMR spectrum (401 MHz, CD_3OD) of [RuI(κ²*N*,*O*-Pro)(η⁶-*p*-cymene)], **1c**. Only resonances due to the major isomer are marked.

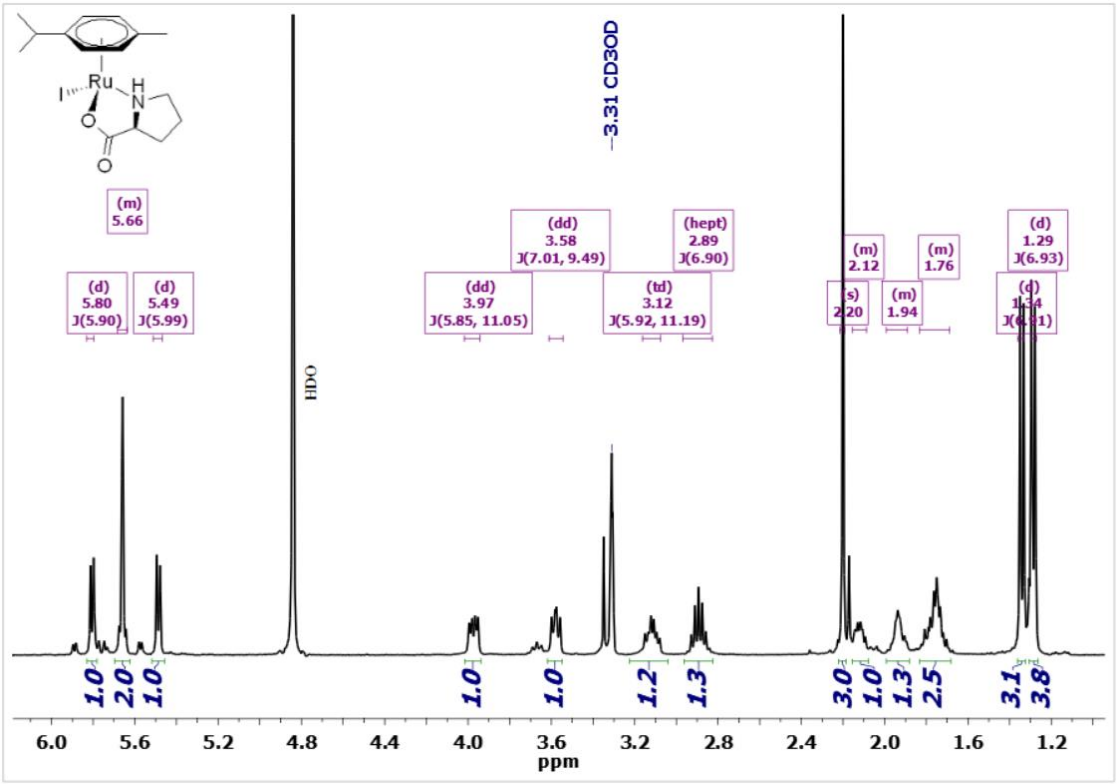

Figure S27. $^{13}C\{^{1}H\}$ NMR spectrum (101 MHz, CD_3OD) of [RuI(κ^2*N*,*O*-Pro)(η^6-*p*-cymene)], **1c**.

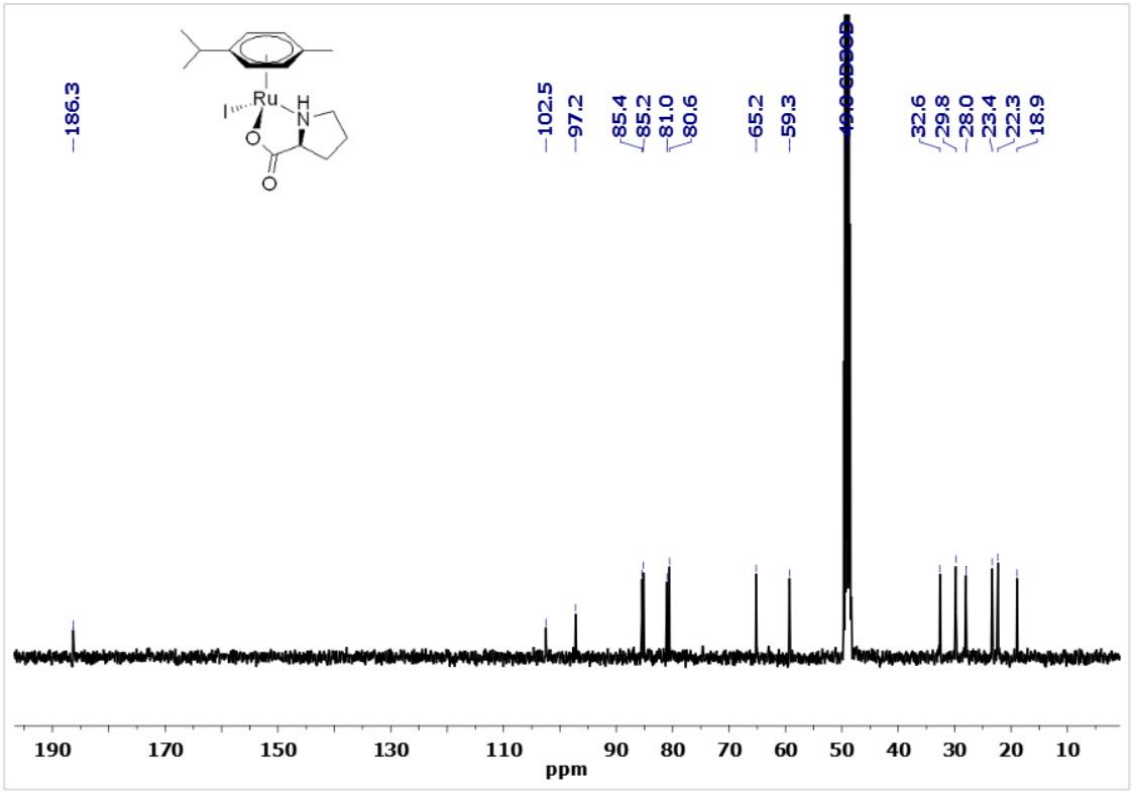

Figure S28. ^{1}H NMR spectrum (401 MHz, CD_3OD) of [Ru(κ*N*-NCS)(κ^2*N*,*O*-Pro)(η^6-*p*-cymene)], **1d**.

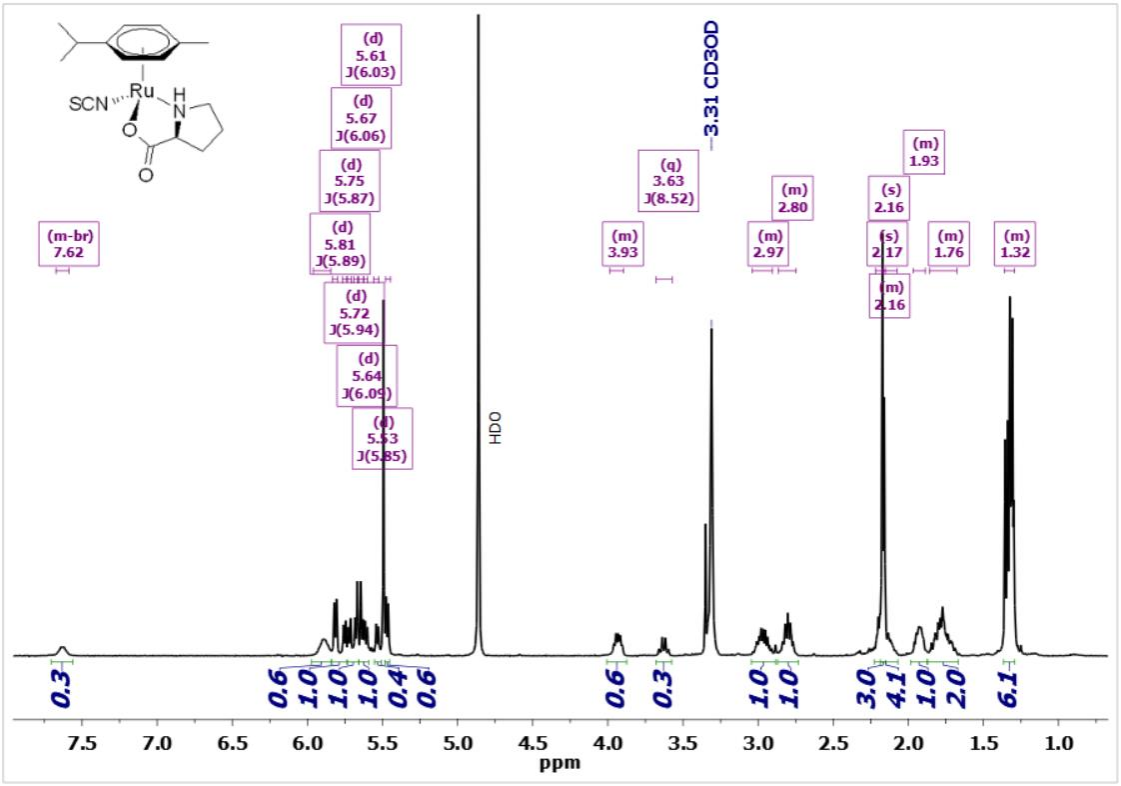

Figure S29. $^{13}C\{^{1}H\}$ NMR spectrum (101 MHz, CD_3OD) of [Ru(κ*N*-NCS)(κ^2*N*,*O*-Pro)(η^6-*p*-cymene)], **1d**.

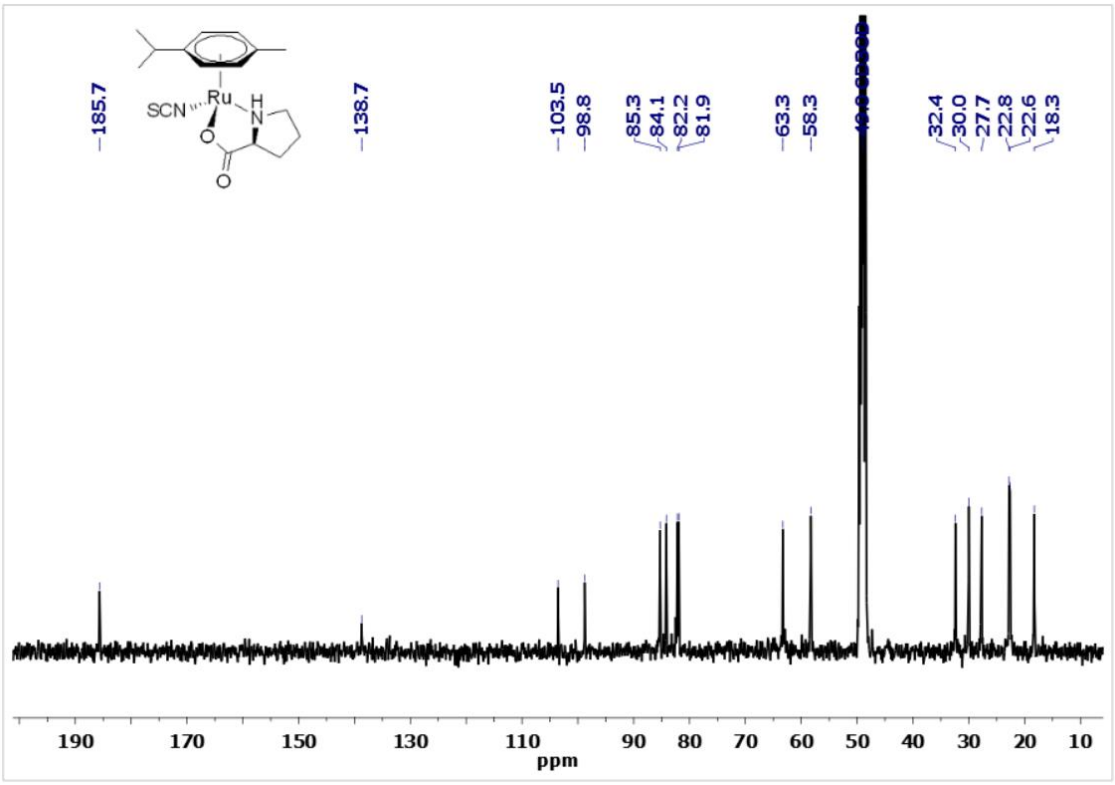

Figure S30. ^{1}H NMR spectrum (401 MHz, CD_3OD) of [Ru(N_3)(κ^2*N*,*O*-Pro)(η^6-*p*-cymene)], **1e**.

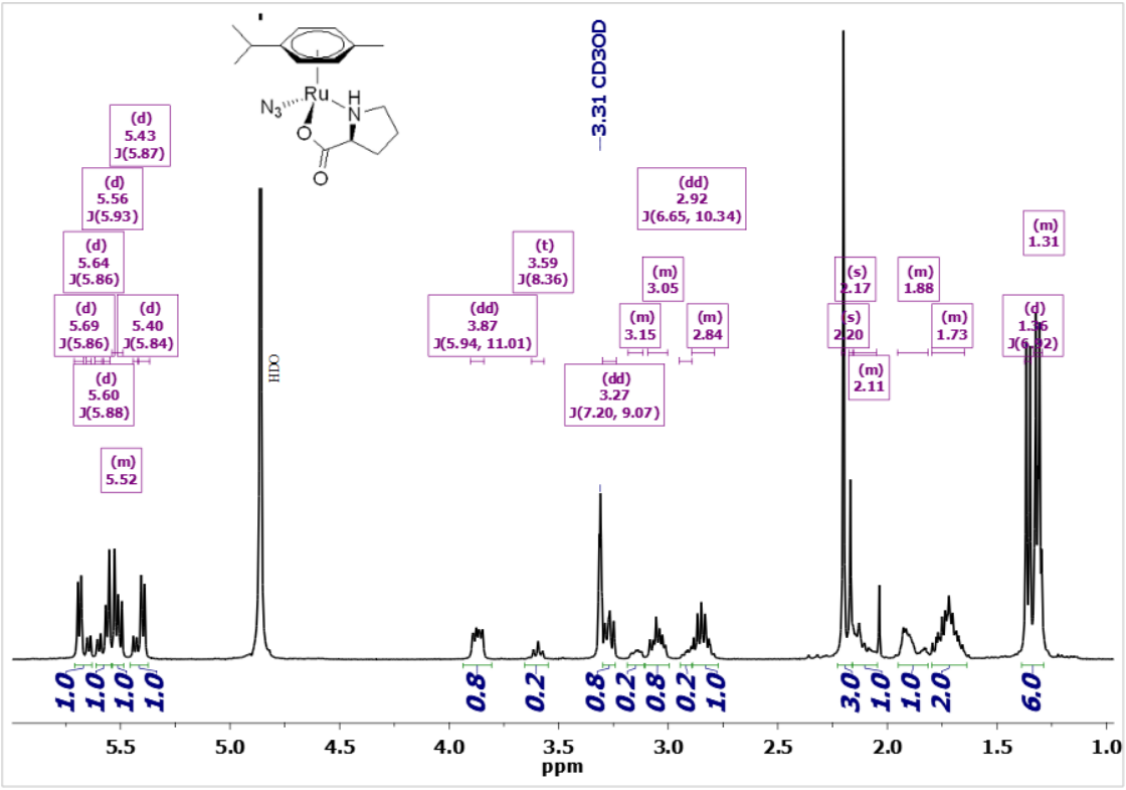

Figure S31. $^{13}C\{^{1}H\}$ NMR spectrum (101 MHz, CD_3OD) of [Ru(N_3)(κ^2*N*,*O*-Pro)(η^6-*p*-cymene)], **1e**.

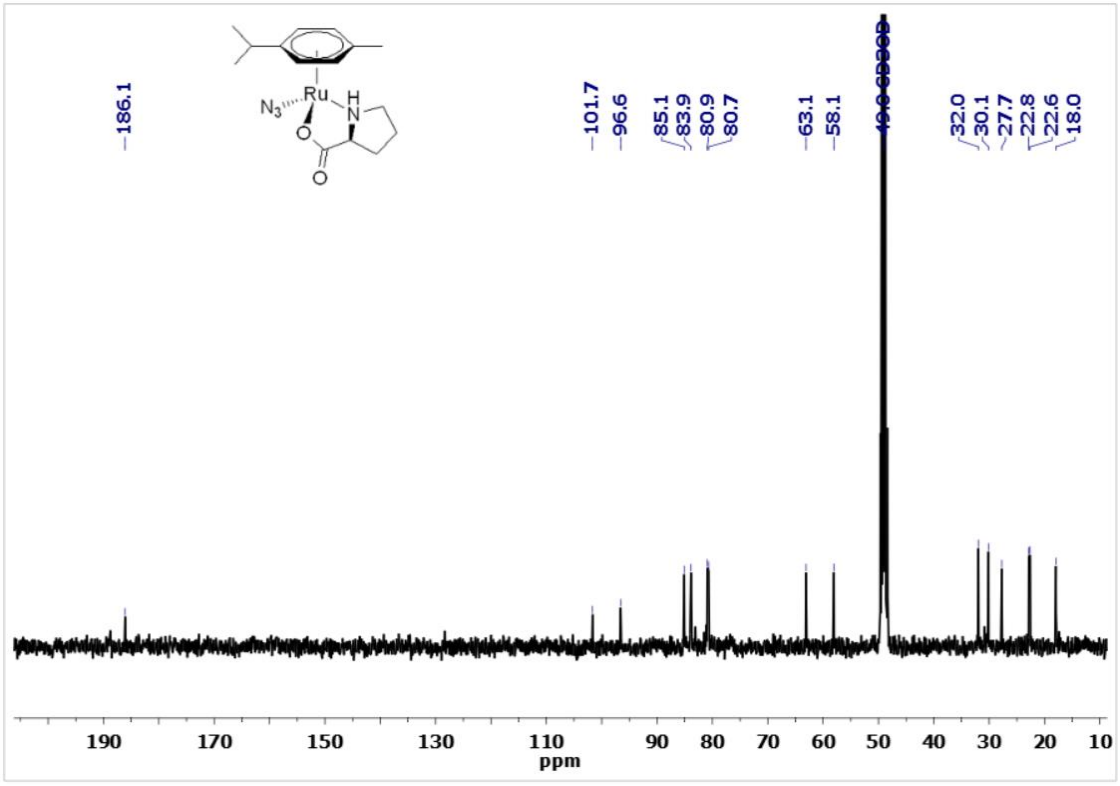

Figure S32. ^{1}H NMR spectrum (401 MHz, CD_3OD) of [Ru(κ*N*-NO_2)(κ^2*N*,*O*-Pro)(η^6-*p*-cymene)], **1f**. Only resonances due to the major isomer are marked.

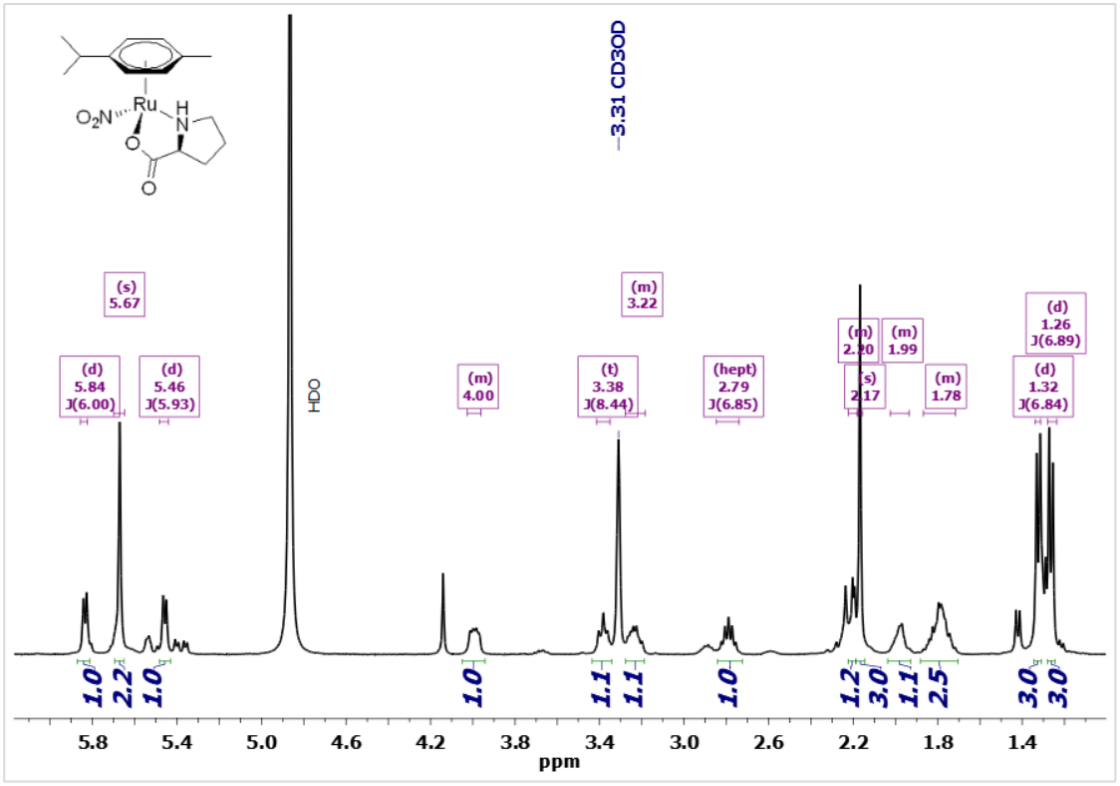

Figure S33. $^{13}C\{^{1}H\}$ NMR spectrum (101 MHz, CD_3OD) of [Ru(κ*N*-NO_2)(κ^2*N*,*O*-Pro)(η^6-*p*-cymene)], **1f**.

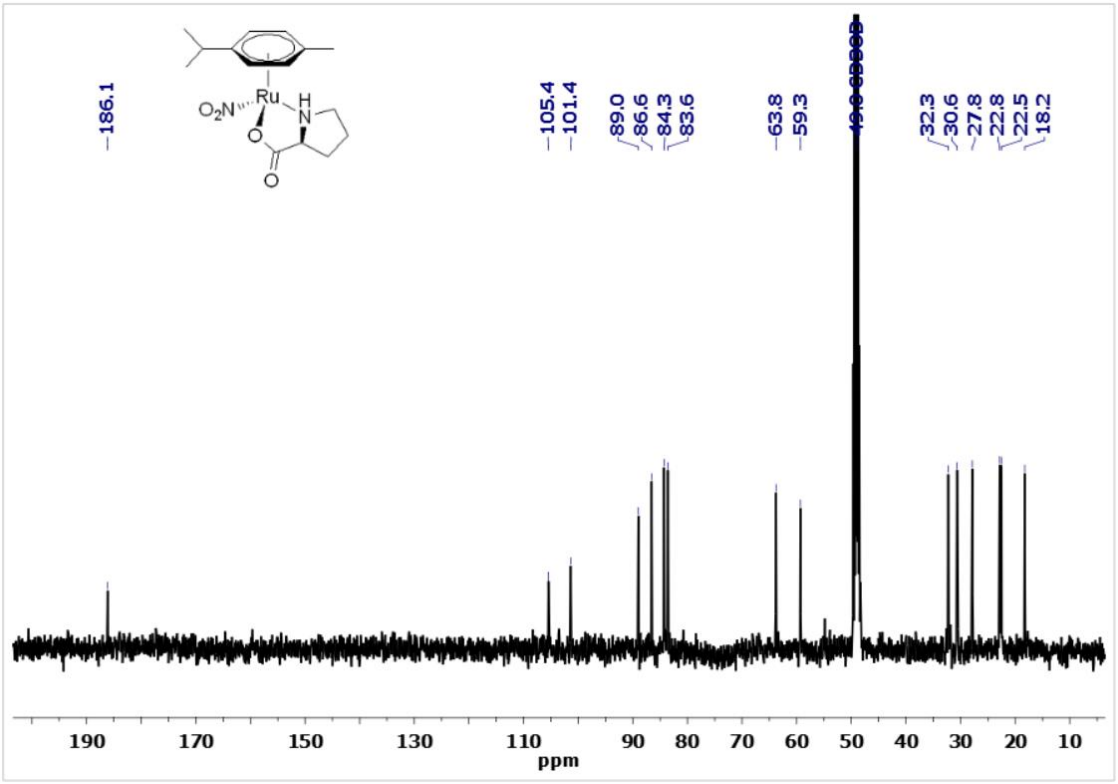

Figure S34. ^{1}H NMR spectrum (401 MHz, CD_3OD) of [Ru(CN)(κ^2*N*,*O*-Pro)(η^6-*p*-cymene)], **1g**. Only resonances due to the major isomer are marked.

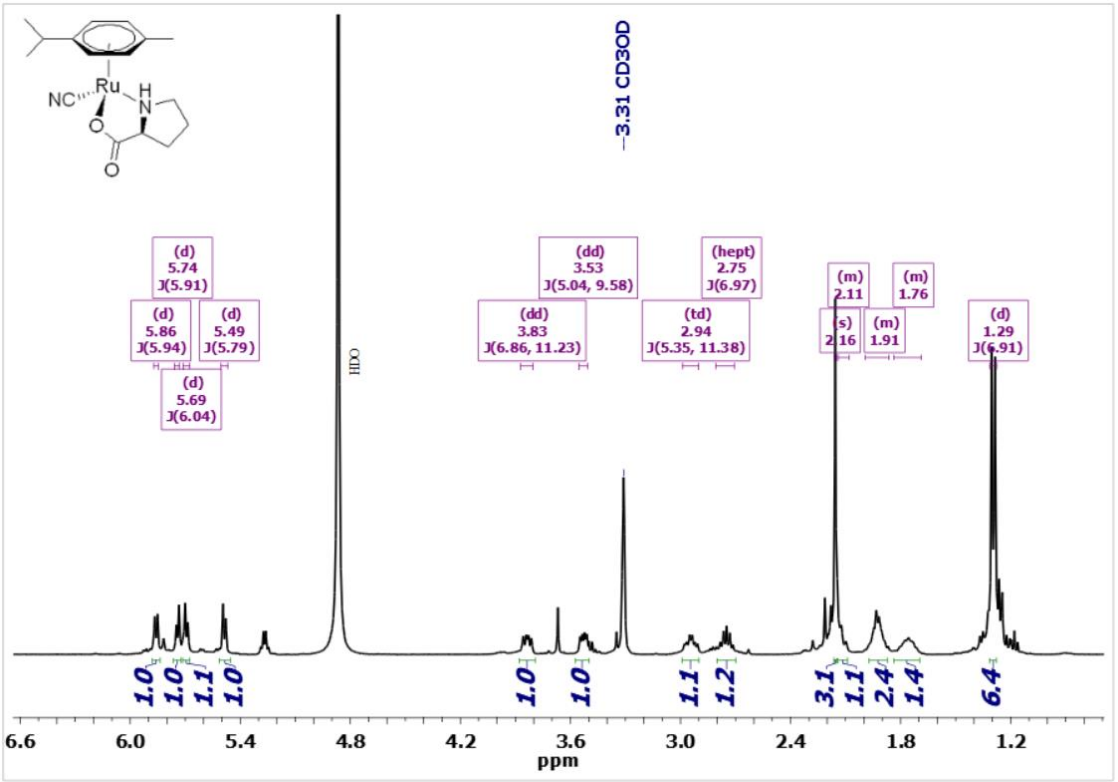

Figure S35. $^{13}C\{^{1}H\}$ NMR spectrum (101 MHz, CD_3OD) of [Ru(CN)(κ²*N*,*O*-Pro)(η⁶-*p*-cymene)], **1g**.

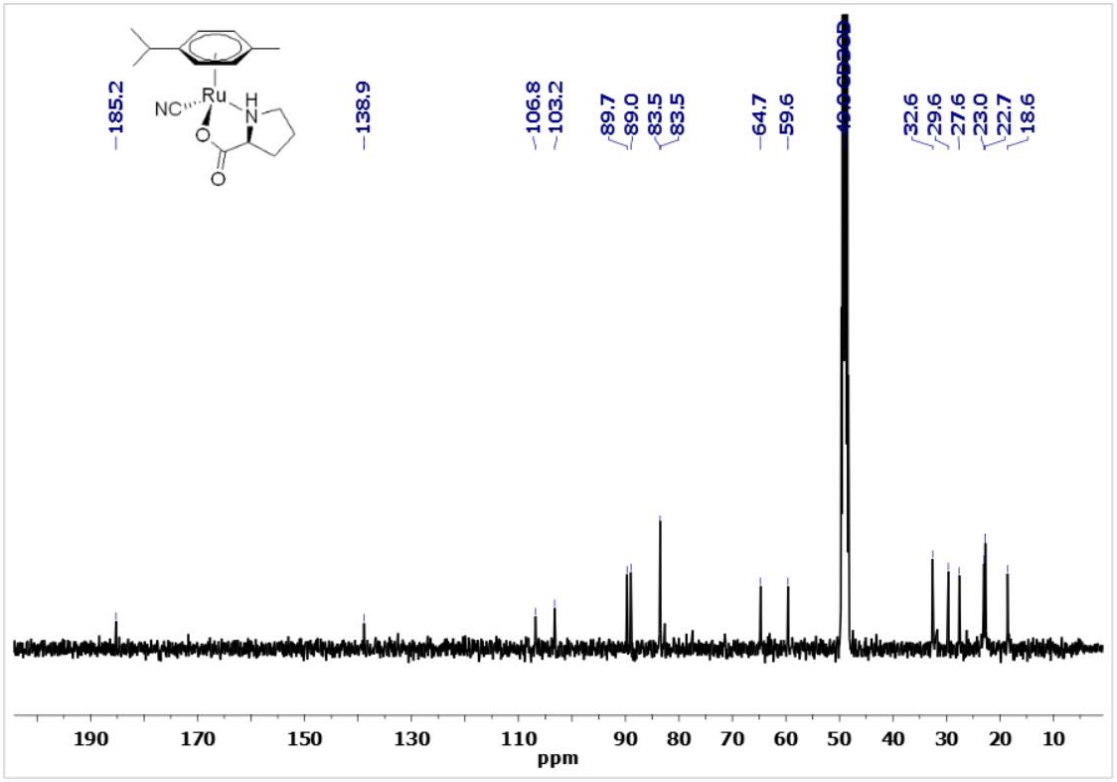

Figure S36. ^{1}H NMR spectrum (401 MHz, CD_3OD) of [RuBr(κ²*N*,*O*-Hyp)(η⁶-*p*-cymene)], **2b**. Only resonances due to the major isomer are marked.

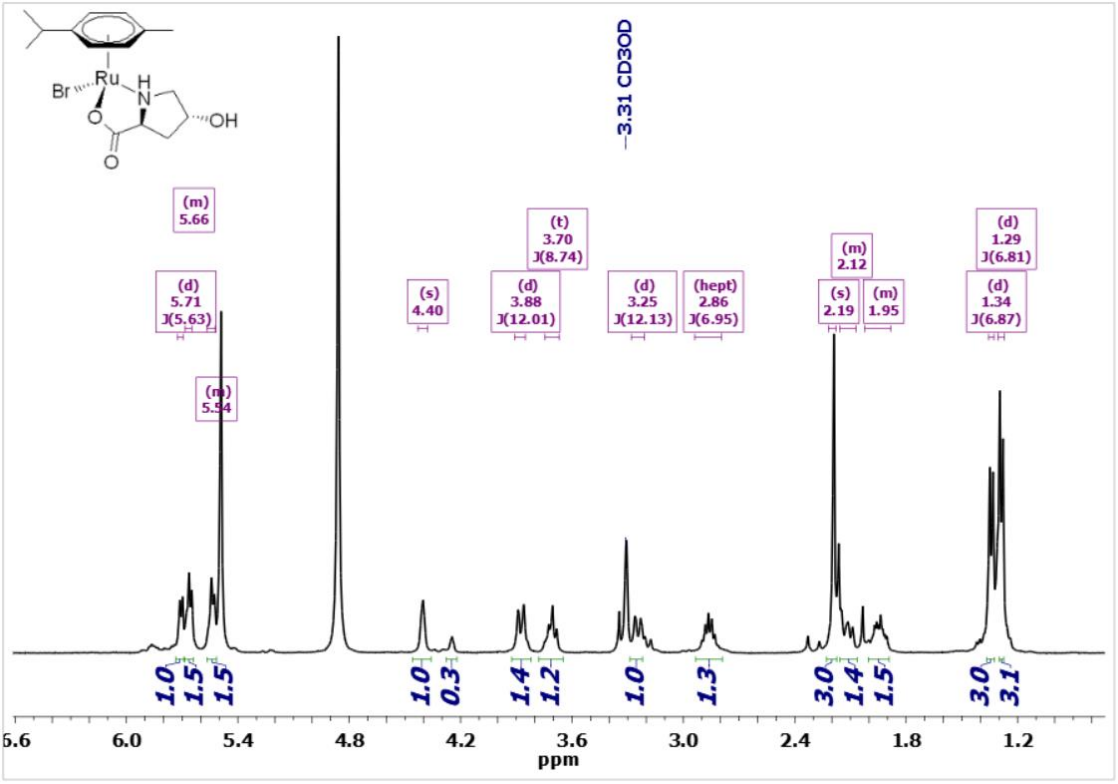

Figure S37. $^{13}C\{^{1}H\}$ NMR spectrum (101 MHz, CD_3OD) of [RuBr(κ²*N*,*O*-Hyp)(η⁶-*p*-cymene)], **2b**. Only resonances due to the major isomer are marked.

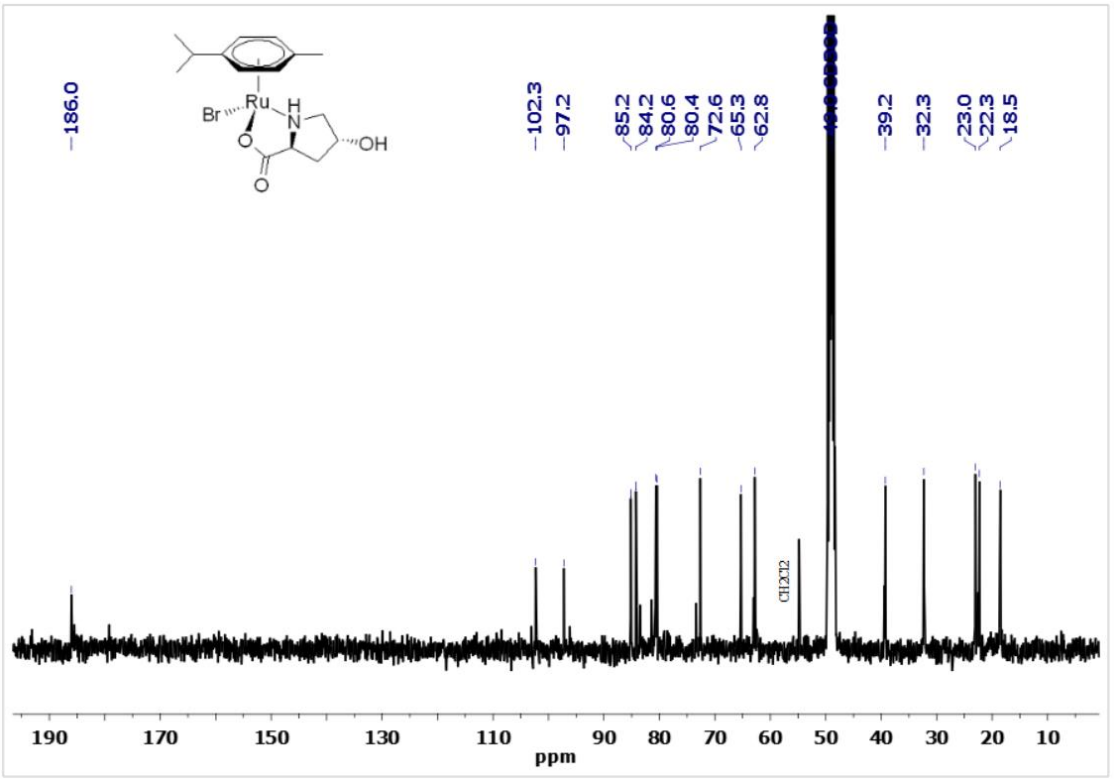

Figure S38. ^{1}H NMR spectrum (401 MHz, CD_3OD) of [RuI(κ²*N*,*O*-Hyp)(η⁶-*p*-cymene)], **2c**. Only resonances due to the major isomer are marked.

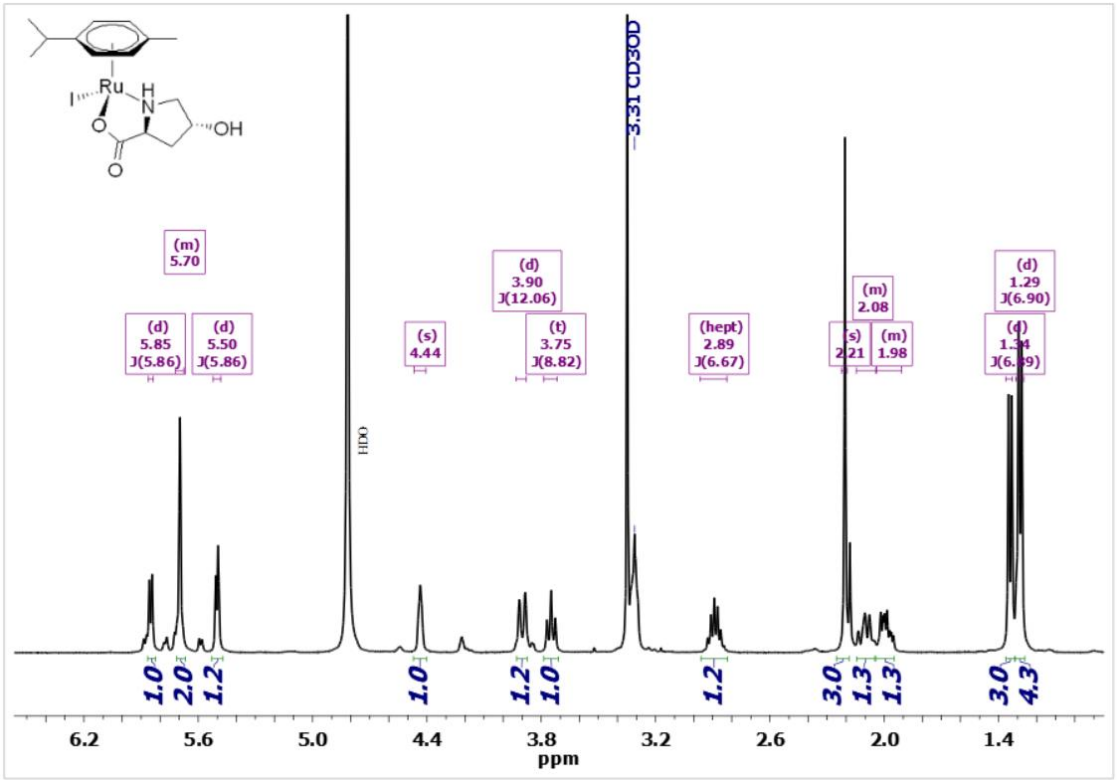

Figure S39. $^{13}C\{^{1}H\}$ NMR spectrum (101 MHz, CD_3OD) of [RuI(κ²*N*,*O*-Hyp)(η⁶-*p*-cymene)], **2c**. Only resonances due to the major isomer are marked.

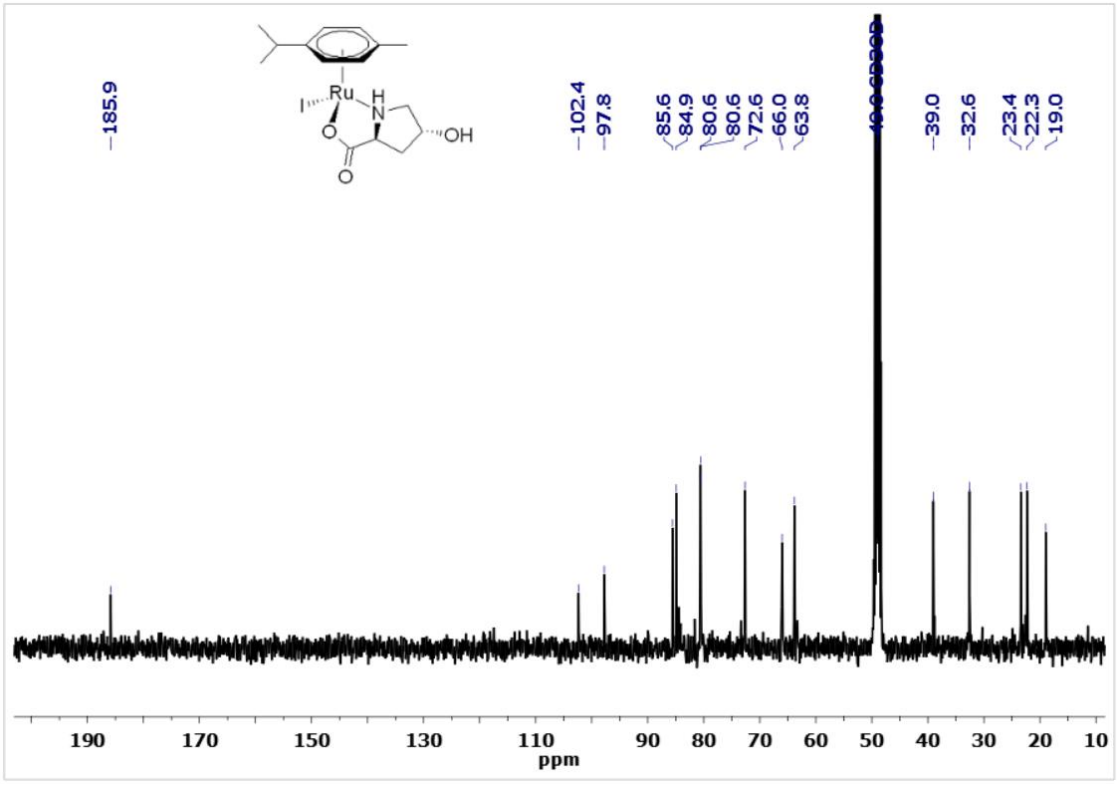

Figure S40. ^{1}H NMR spectrum (401 MHz, CD_3OD) of [Ru(κ*N*-NCS)(κ²*N*,*O*-Hyp)(η⁶-*p*-cymene)], **2d**.

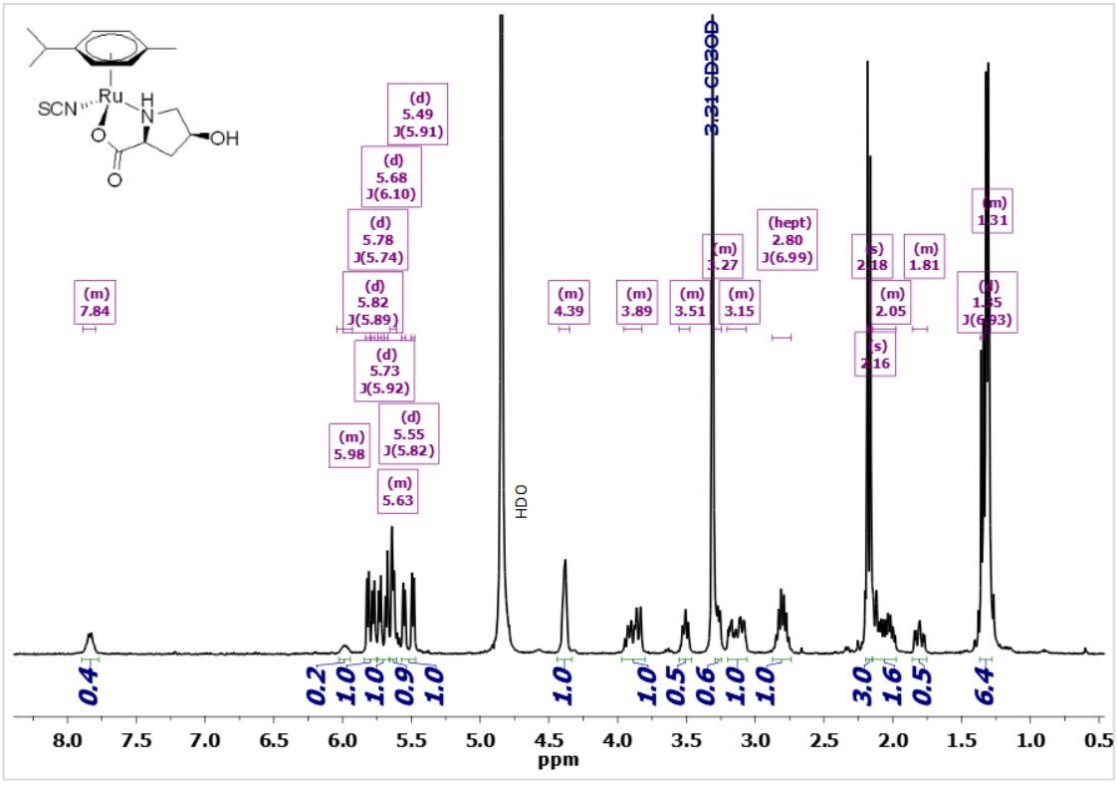

Figure S41. $^{13}C\{^{1}H\}$ NMR spectrum (101 MHz, CD_3OD) of [Ru(κ*N*-NCS)(κ^2*N*,*O*-Hyp)(η^6-*p*-cymene)], **2d**.

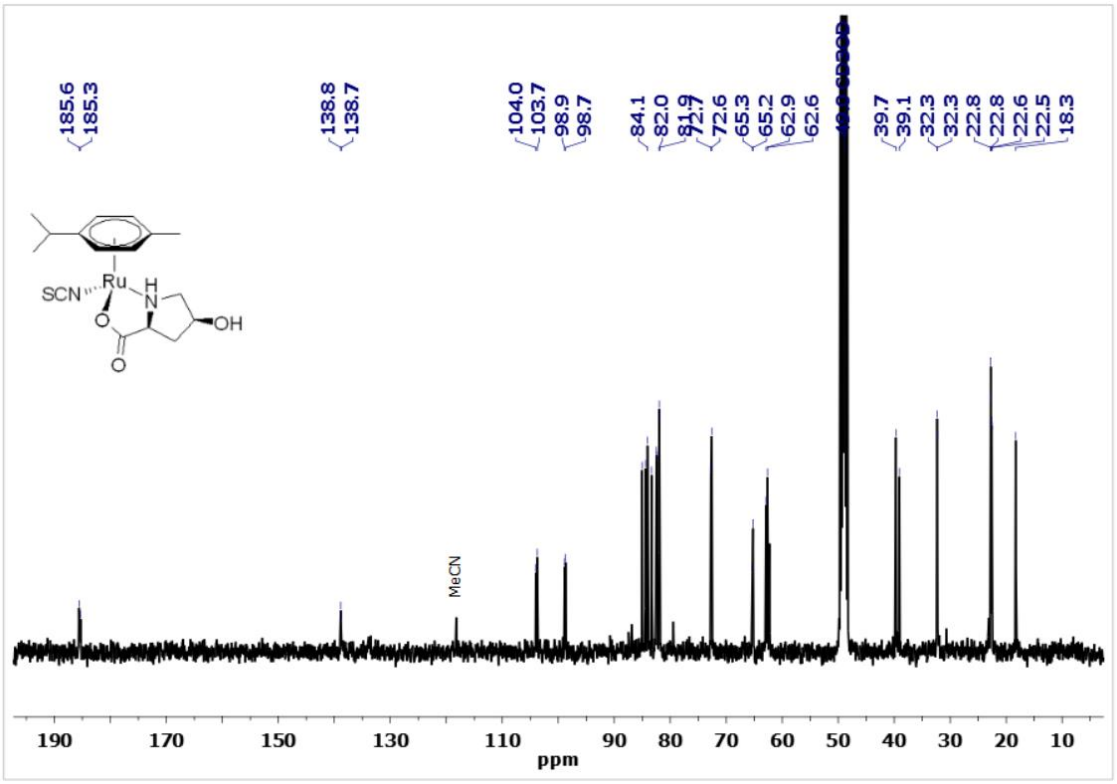

Figure S42. ^{1}H NMR spectrum (401 MHz, CD_3OD) of [Ru(N_3)(κ^2*N*,*O*-Hyp)(η^6-*p*-cymene)], **2e**.

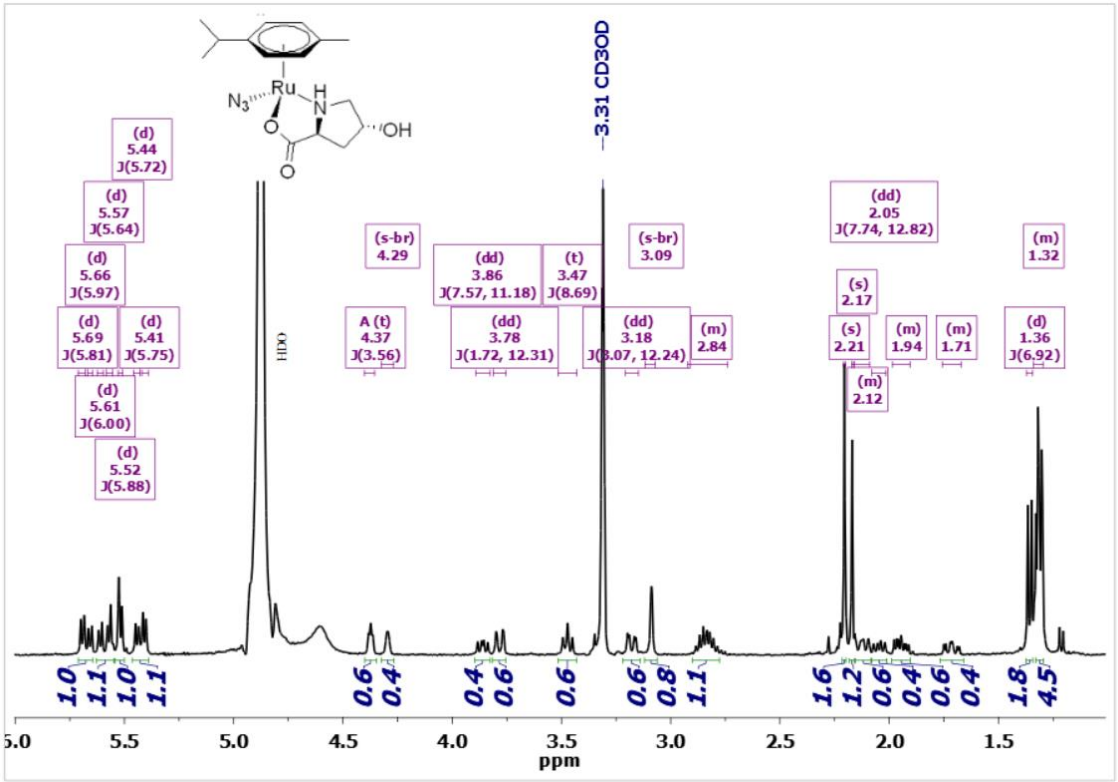

Figure S43. $^{13}C\{^{1}H\}$ NMR spectrum (101 MHz, CD_3OD) of [Ru(N_3)(κ^2*N*,*O*-Hyp)(η^6-*p*-cymene)], **2e**. Only resonances due to the major isomer are marked.

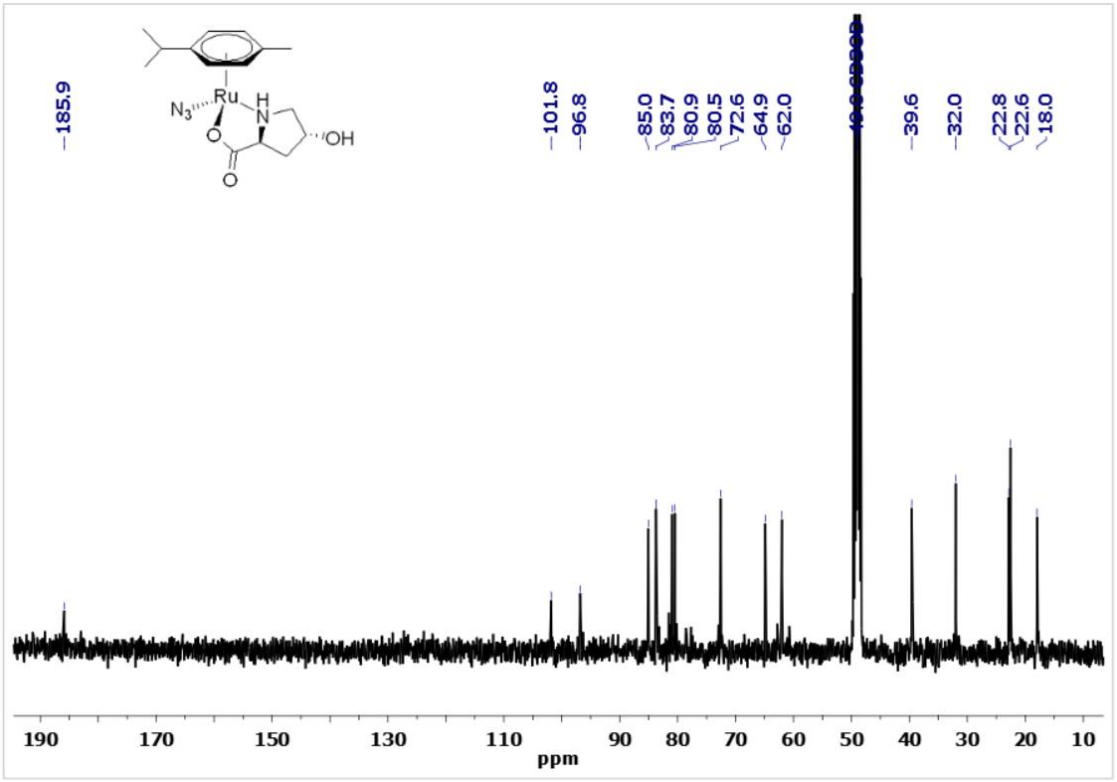

Figure S44. ^{1}H NMR spectrum (401 MHz, CD_3OD) of [Ru(κ^3*N*,*O*,*O'*-Ser)(η^6-*p*-cymene)], **3h**.

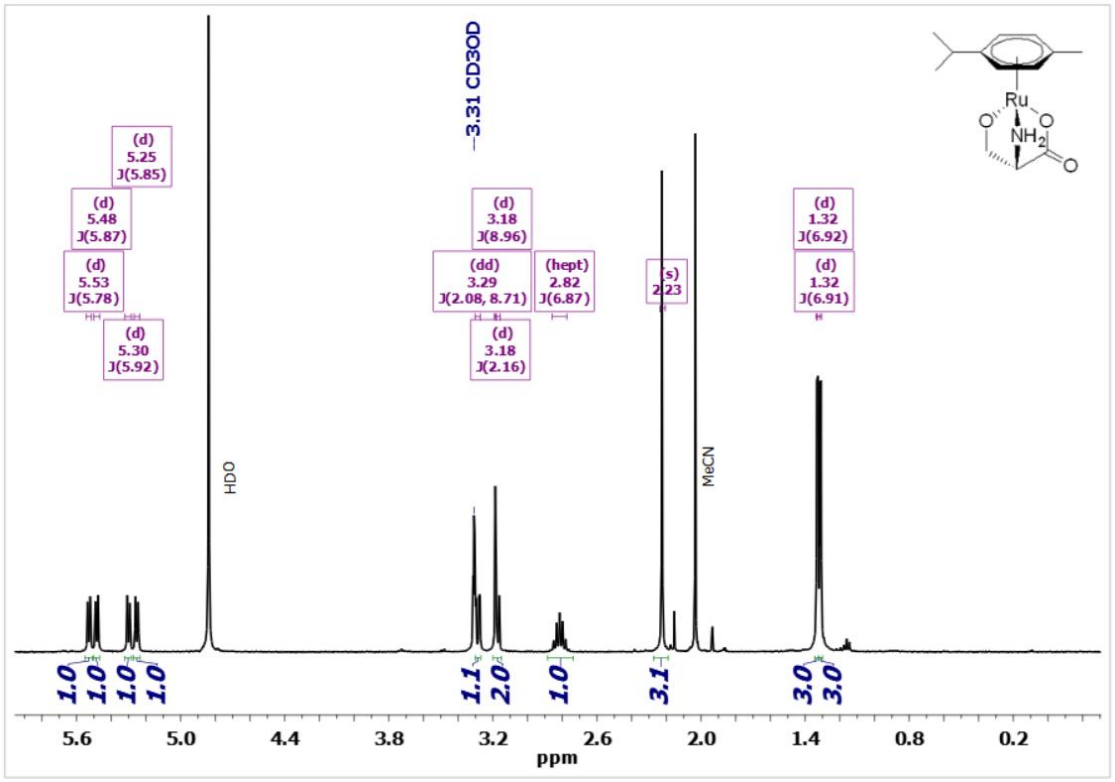

Figure S45. $^{13}C\{^{1}H\}$ NMR spectrum (101 MHz, CD_3OD) of [Ru(κ^3*N*,*O*,*O'*-Ser)(η^6-*p*-cymene)], **3h**.

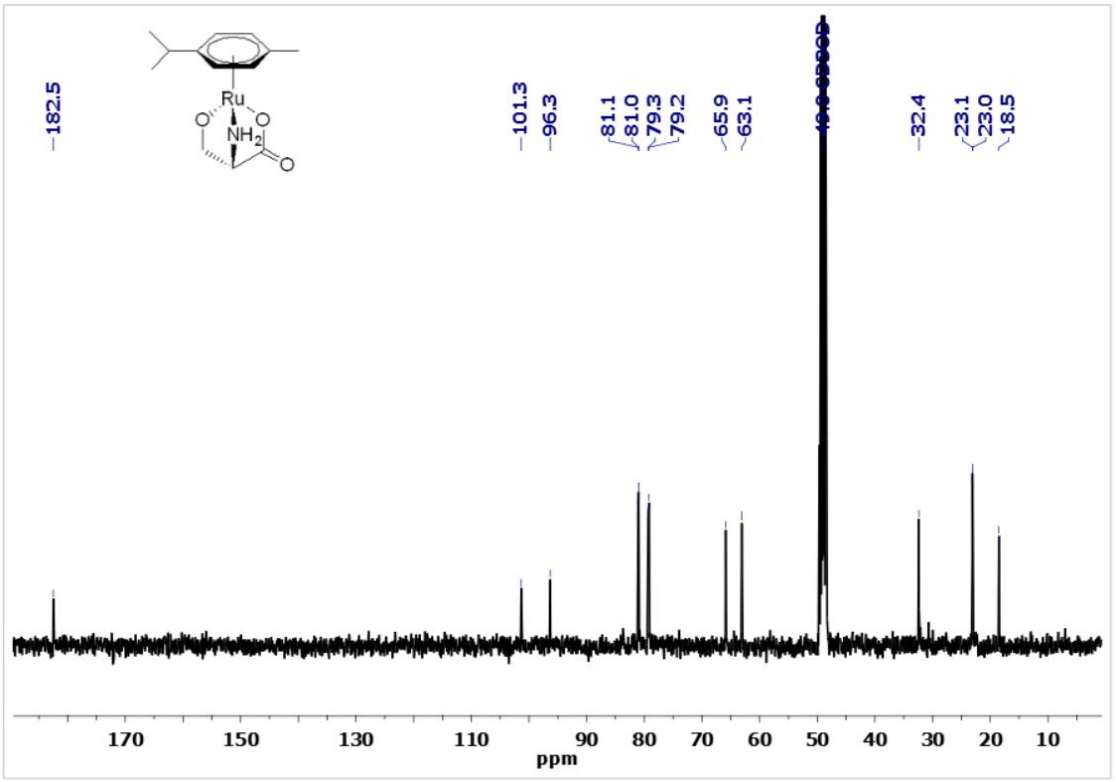

Figure S46. ^{1}H NMR spectrum (401 MHz, CD_3OD) of [Ru(κ^3*N*,*O*,*O'*-Thr)(η^6-*p*-cymene)], **4h**.

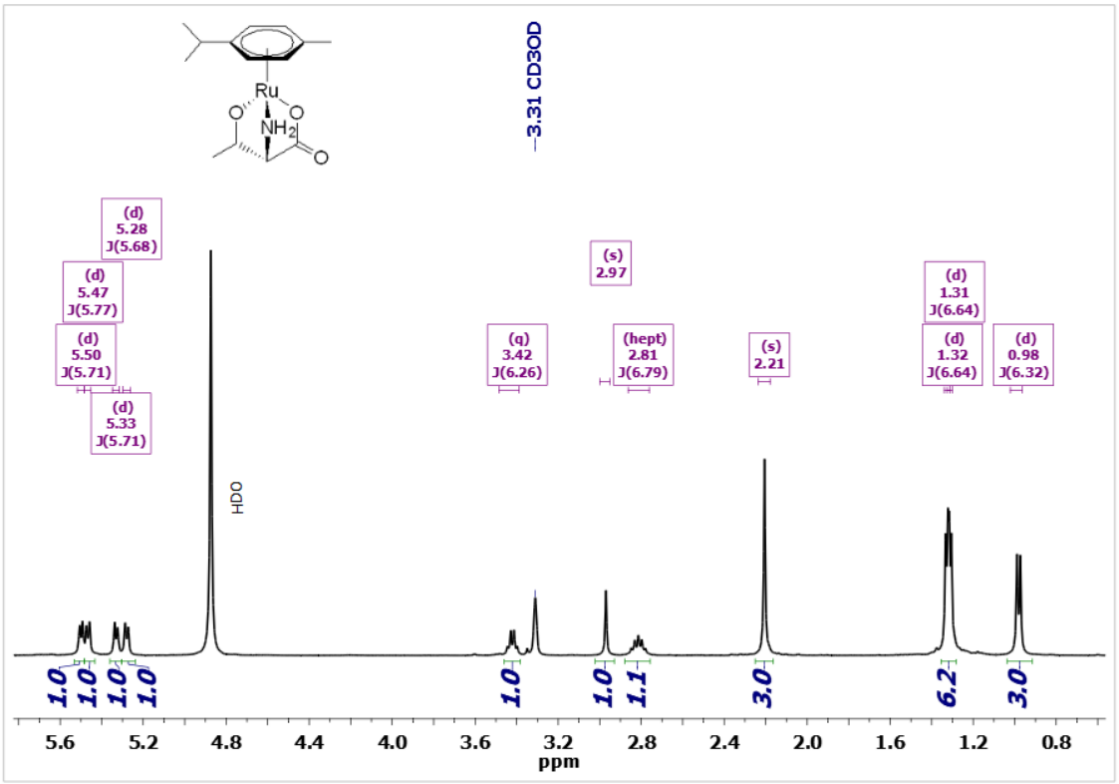

Figure S47. $^{13}C\{^{1}H\}$ NMR spectrum (101 MHz, CD_3OD) of [Ru(κ³*N*,*O*,*O'*-Thr)(η⁶-*p*-cymene)], **4h**.

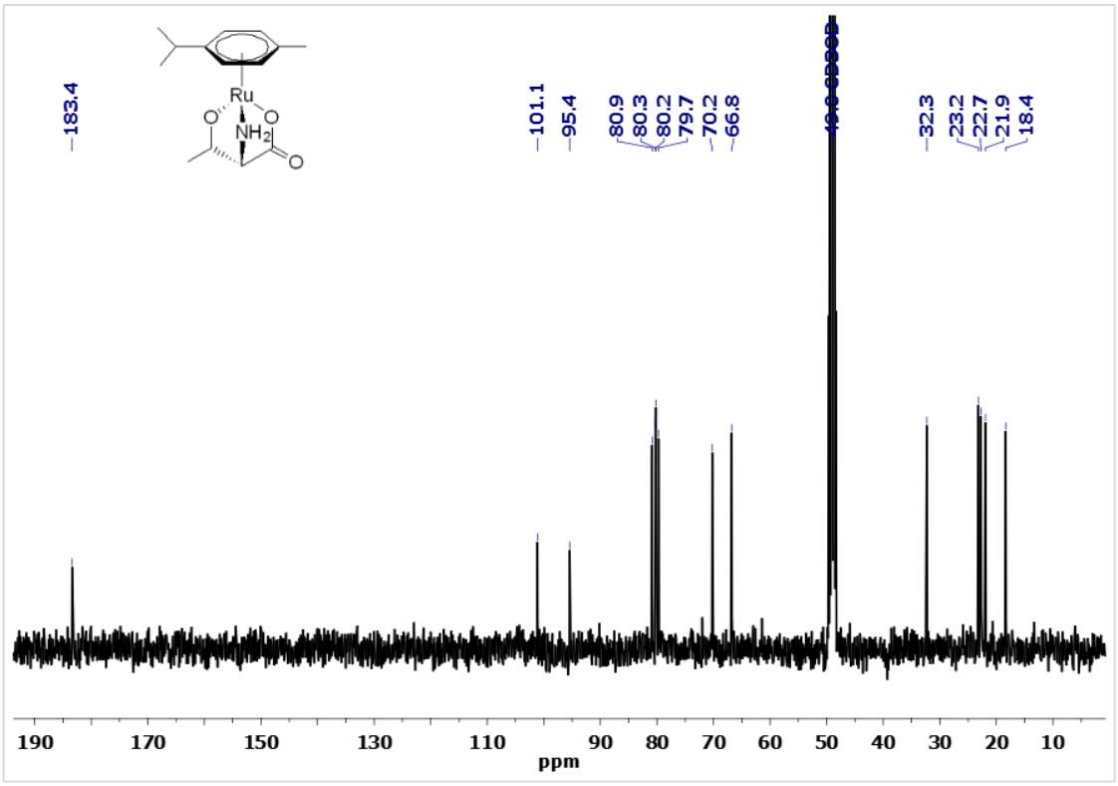

Figure S48. ^{1}H NMR spectrum (401 MHz, CD_3OD) of [Ru(κ³*N*,*O*,*O'*-Hom)(η⁶-*p*-cymene)], **5h**.

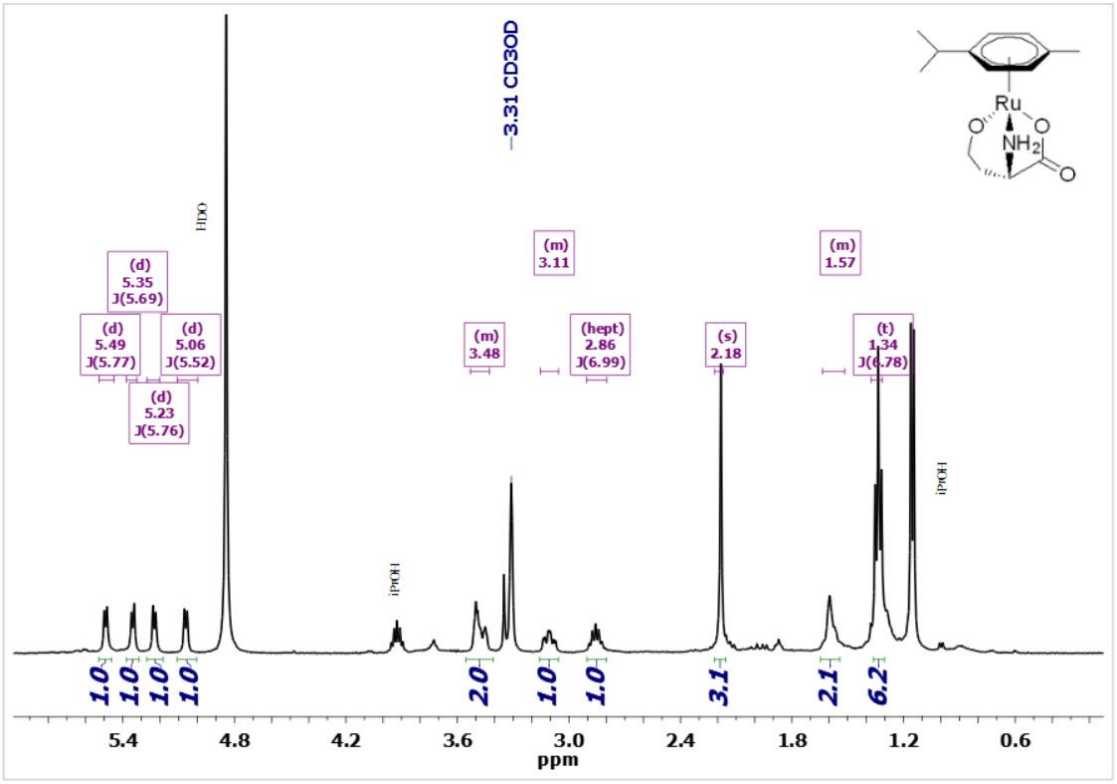

Figure S49. $^{13}C\{^{1}H\}$ NMR spectrum (101 MHz, CD_3OD) of [Ru(κ^3*N*,*O*,*O'*-Hom)(η^6-*p*-cymene)], **5h**.

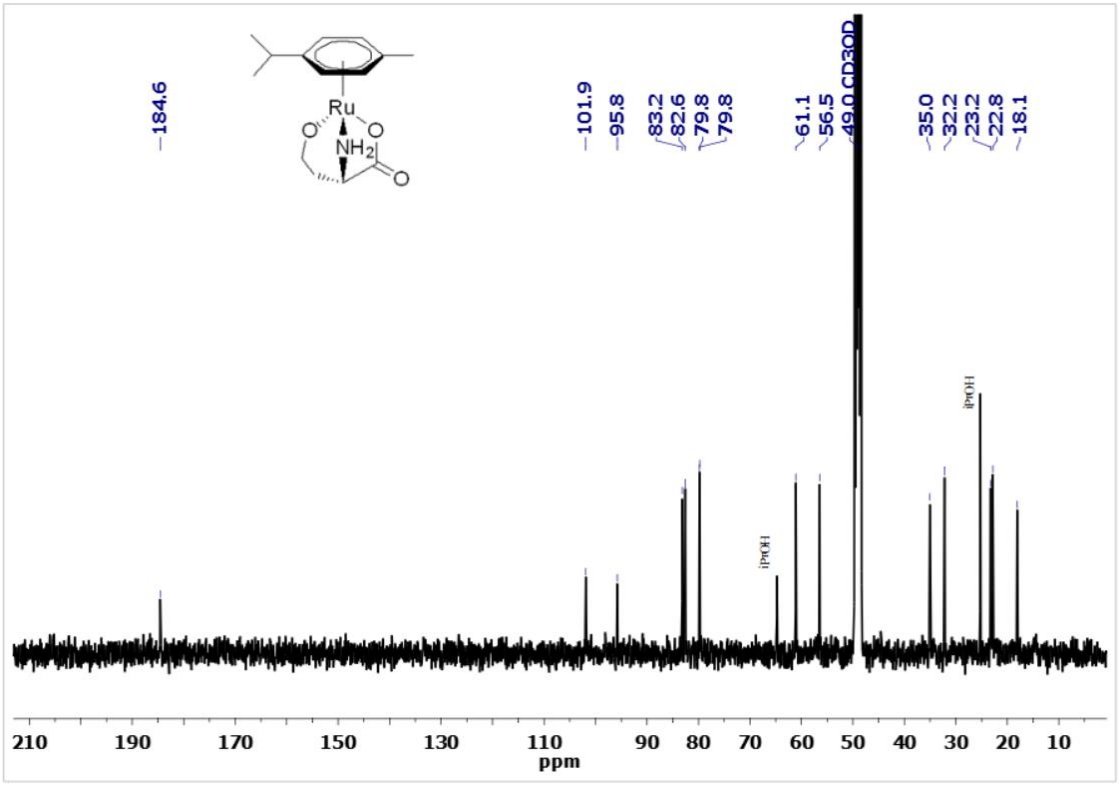

Figure S50. ^{1}H NMR spectrum (401 MHz, CD_3OD) of $[Ru_2(\mu\text{-}H)_2(\mu\text{-}Cl)(\eta^6\text{-}p\text{-cymene})_2]Cl$. Signal marked with asterisk (*) are due to traces of **3h**.

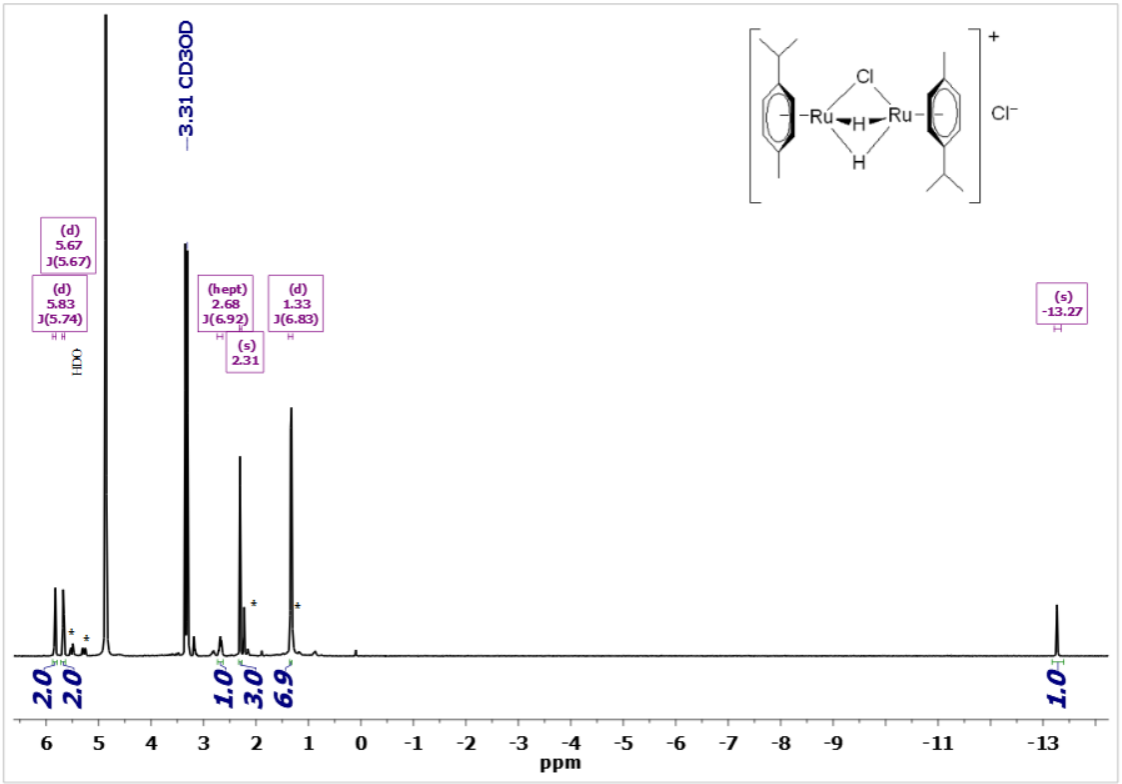

Figure S51. ^{1}H NMR spectrum (401 MHz, CD_3OD) of [Ru(κ^2*N*,*O*-Ser)(κ*P*-pta)(η^6-*p*-cymene)]Cl, [**3i**]Cl. Inset shows NH resonances in the freshly-prepared solution.

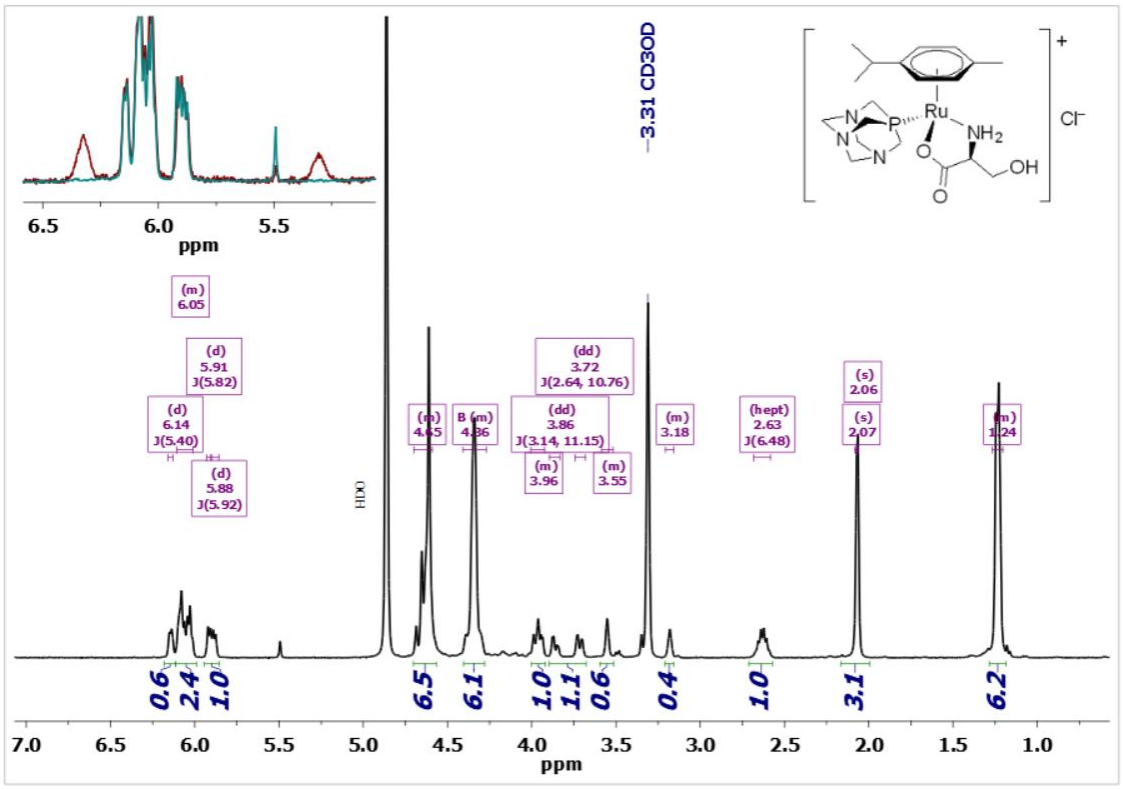

Figure S52. ^{13}C{^{1}H} NMR spectrum (101 MHz, D_2O) of [Ru(κ^2*N*,*O*-Ser)(κ*P*-pta)(η^6-*p*-cymene)]Cl, [**3i**]Cl.

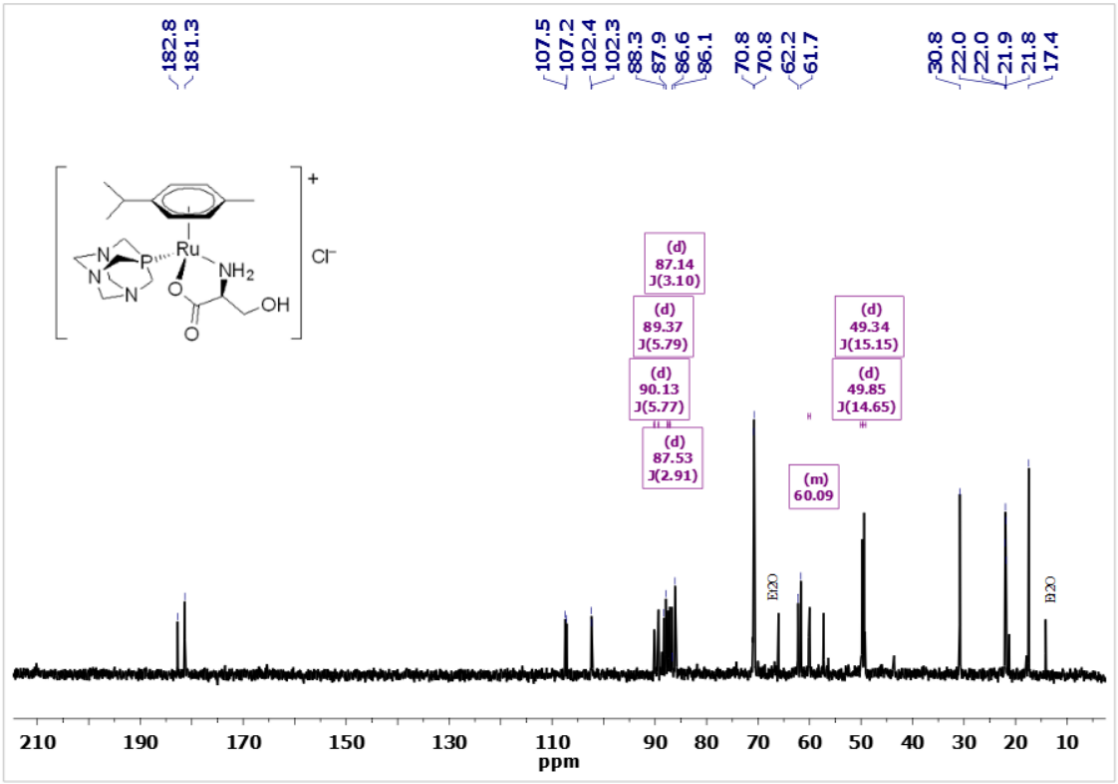

Figure S53. $^{31}P\{^{1}H\}$ NMR spectrum (162 MHz, CD_3OD) of [Ru(κ²*N*,*O*-Ser)(κ*P*-pta)(η⁶-*p*-cymene)]Cl, [**3i**]Cl.

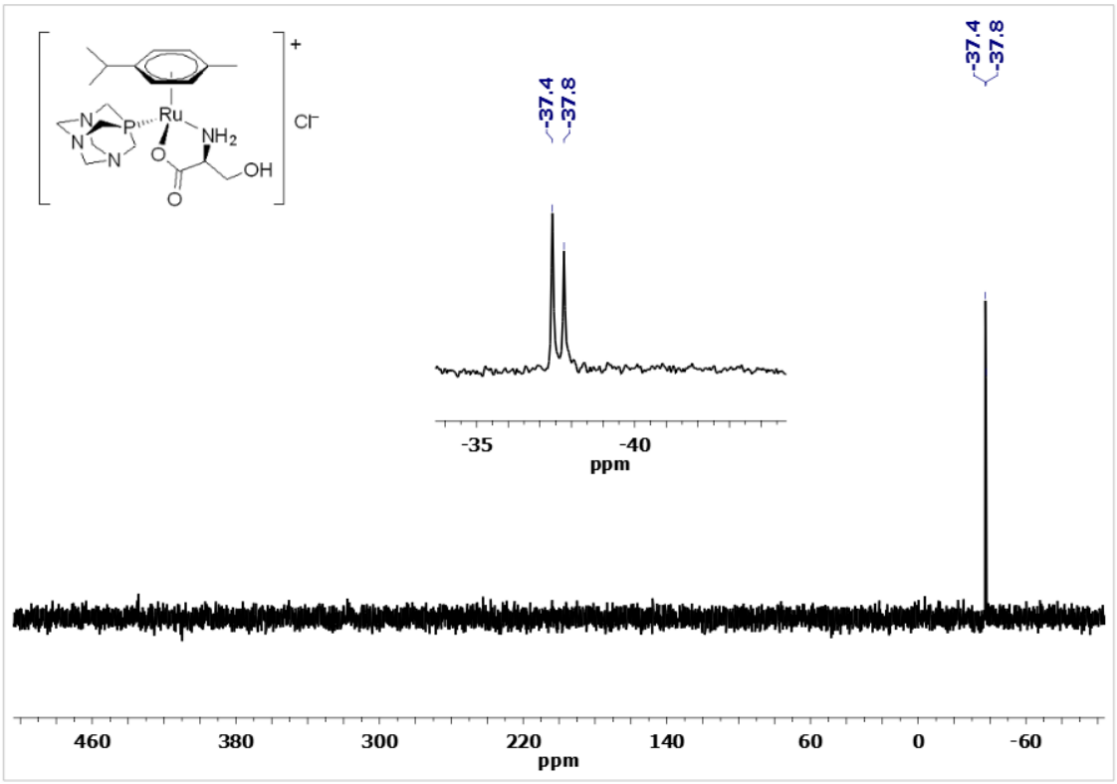

Figure S54. ^{14}N NMR spectra (29 MHz) of: KSCN in MeOH **(a)**; $[Ru(SCN)_2(\eta^6\text{-}p\text{-cymene})]_2$ in acetone **(b)**; [Ru(κ*N*-NCS)(κ²*N*,*O*-Pro)(η⁶-*p*-cymene)], **1d** in acetone **(c)**; [Ru(κ*N*-NCS)(κ²*N*,*O*-Hyp)(η⁶-*p*-cymene)], **2d** in MeOH **(d)**. Instrumental peak at − 72.2 ppm (*).

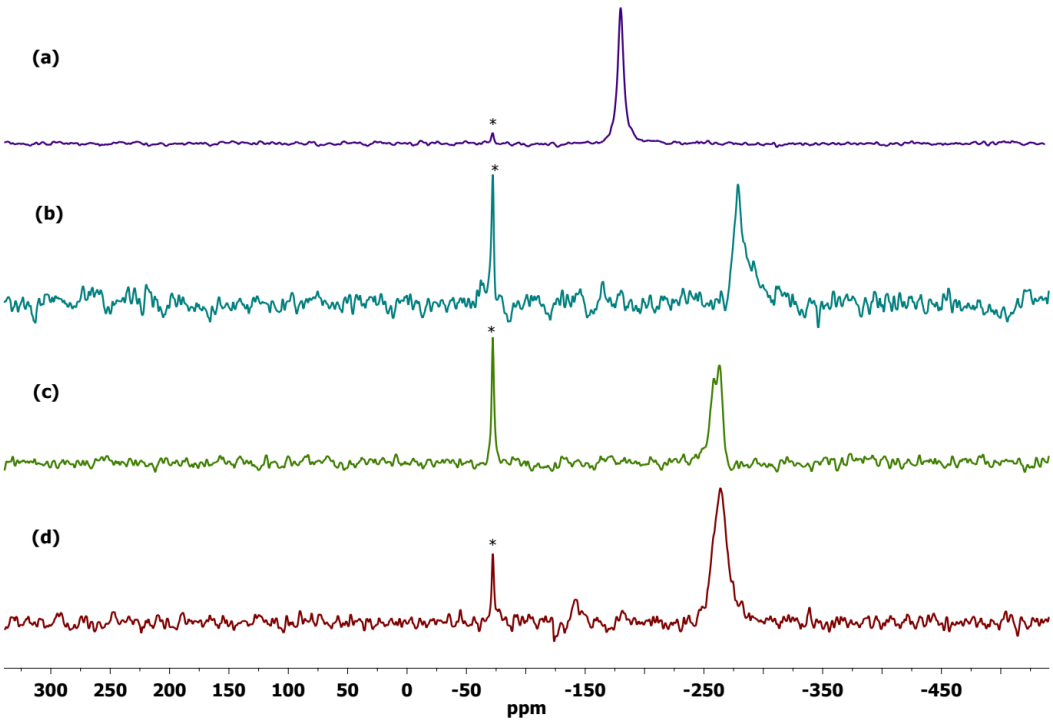

Figure S55. ^{14}N NMR spectra (29 MHz) of: NaN_3 in MeOH **(a)**; $[Ru(N_3)_2(\eta^6\text{-}p\text{-cymene})]_2$ in acetone **(b)**; $[Ru(N_3)(\kappa^2N,O\text{-Pro})(\eta^6\text{-}p\text{-cymene})]$, **1e** in MeOH **(c)**; $[Ru(N_3)(\kappa^2N,O\text{-Hyp})(\eta^6\text{-}p\text{-cymene})]$, **2e** in MeOH **(d)**. Instrumental peak at − 72.2 ppm (*).

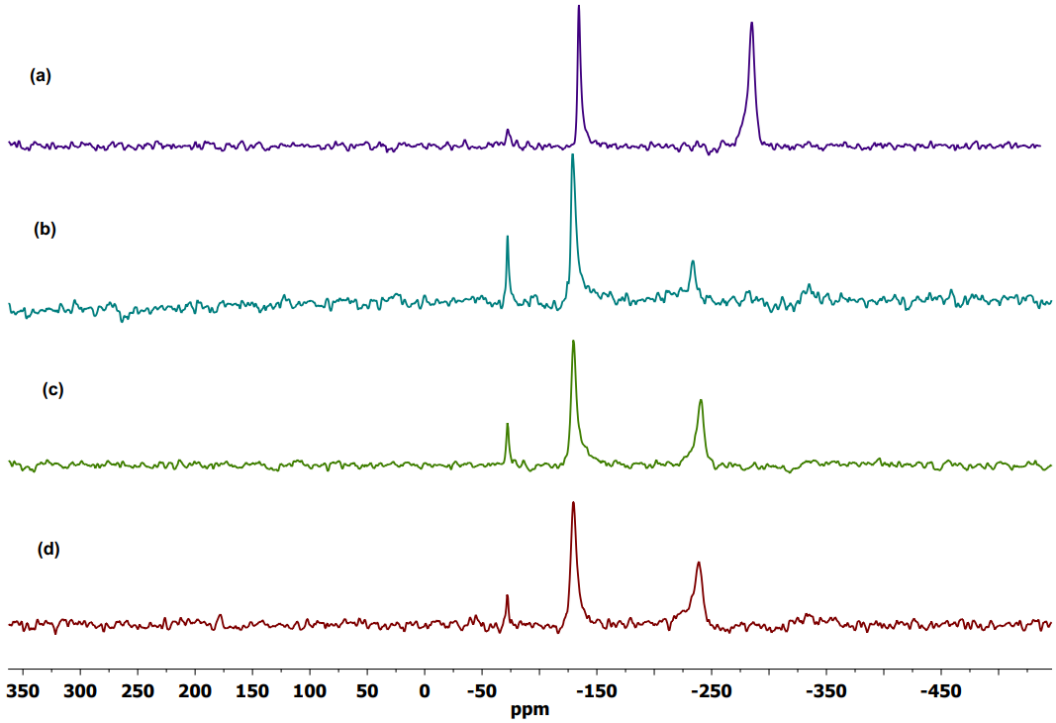

Figure S56. ^{14}N NMR spectra (29 MHz, MeOH) of: $NaNO_2$ **(a)**; $[Ru(\kappa N\text{-}NO_2)(\kappa^2N,O\text{-Pro})(\eta^6\text{-}p\text{-cymene})]$, **1f (b)**. Instrumental peak at − 72.2 ppm (*).

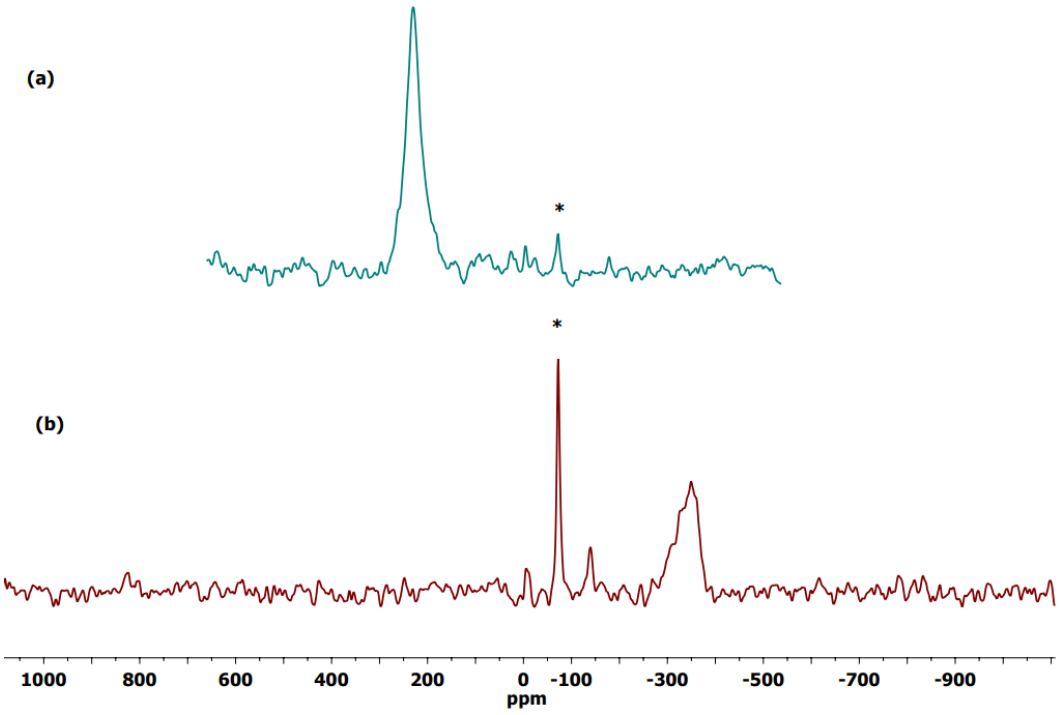

X-ray structural data.

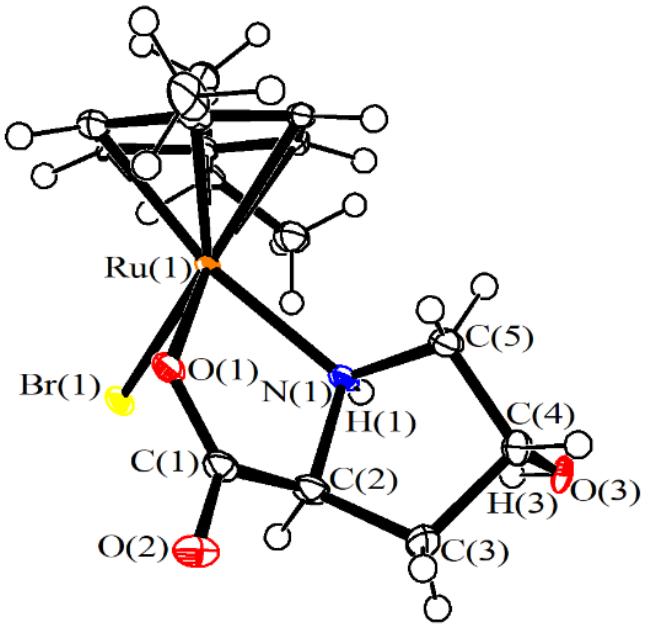

Figure S57. View of the X-ray structure of [RuBr(κ²*N*,*O*-Hyp)(η⁶-*p*-cymene)], **2b**. Displacement ellipsoids are at the 50% probability level. Main bond distances (Å) and angles (°): Ru(1)-$(\eta^6\text{-p-cymene})_{average}$ 2.18(6), Ru(1)-O(1) , 2.108(18) Ru(1)-N(1) 2.16(2), Ru(1)-Br(1) 2.525(3), O(1)-C(1) 1.29(3), C(1)-O(2) 1.24(3), C(1)-C(2) 1.53(4), C(2)-C(3) 1.51(4), C(3)-C(4) 1.60(4), C(4)-C(5) 1.51(4), N(1)-C(2) 1.55(3), N(1)-C(5) 1.49(4), C(4)-O(3) 1.46(2), Ru(1)-O(1)-C(1) 117.1(16), O(1)-C(1)-C(2) 119(2), C(1)-C(2)-N(1) 108(2), C(2)-N(1)-Ru(1) 109.6(17), O(1)-Ru(1)-N(1) 77.9(8).

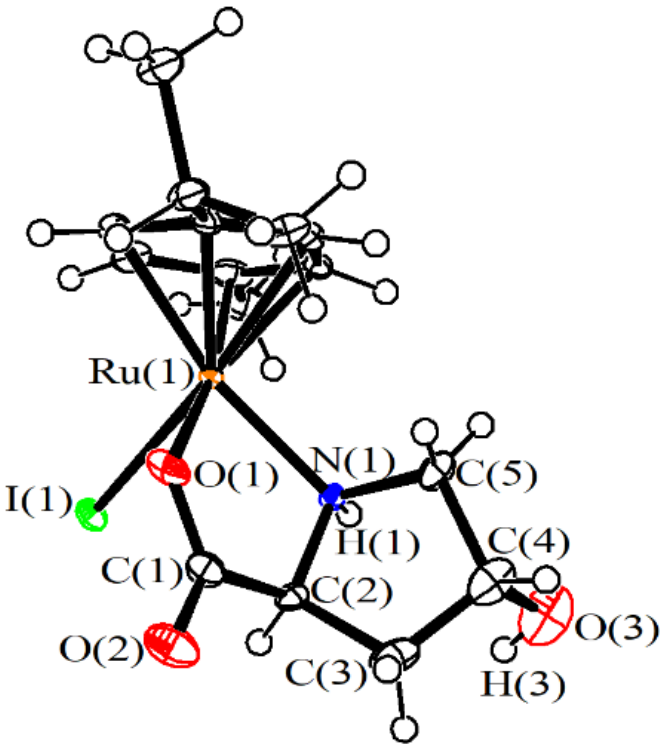

Figure S58. View of the X-ray structure of [RuI(κ²*N*,*O*-Hyp)(η⁶-*p*-cymene)], **2c**. Displacement ellipsoids are at the 50% probability level. Main bond distances (Å) and angles (°): Ru(1)-(η⁶-p-cymene)$_{average}$ 2.19(4), Ru(1)-O(1) 2.144(11), Ru(1)-N(1) 2.142(12, Ru(1)-I(1) 2.7434(15), O(1)-C(1) 1.30(2), C(1)-O(2) 1.24(2), C(1)-C(2) 1.52(2), C(2)-C(3) 1.56(2), C(3)-C(4) 1.52(3), C(4)-C(5) 1.52(2), N(1)-C(2) 1.466(18), N(1)-C(5) 1.495(19), C(4)-O(3) 1.46(2), Ru(1)-O(1)-C(1) 114.2(9), O(1)-C(1)-C(2) 118.4(13), C(1)-C(2)-N(1) 109.4(12), C(2)-N(1)-Ru(1) 110.5(9), O(1)-Ru(1)-N(1) 76.2(4).

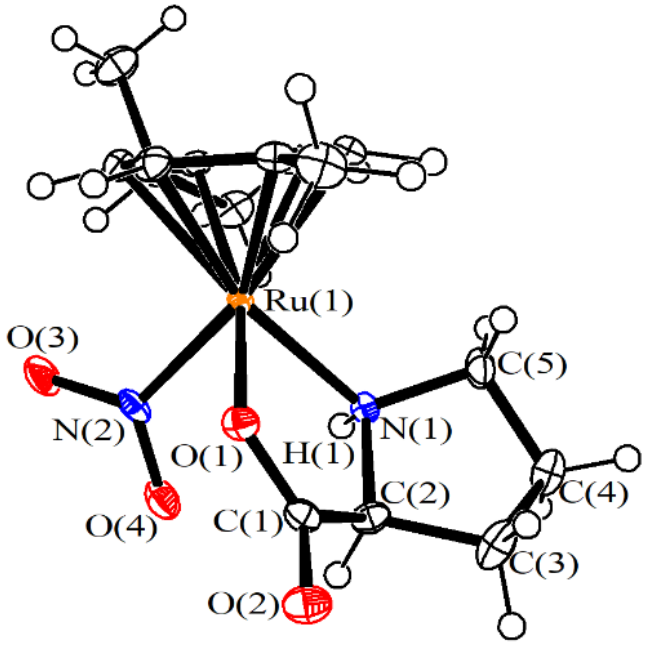

Figure S59. View of the X-ray structure of [Ru(NO_2)(κ^2*N*,*O*-Pro)(η^6-*p*-cymene)], **1f**. Displacement ellipsoids are at the 50% probability level. Main bond distances (Å) and angles (°): Ru(1)-(η^6-p-cymene)$_{average}$ 2.203(5), Ru(1)-O(1) 2.0694(17), Ru(1)-N(1) 2.1262(18), Ru(1)-N(2) 2.0888(18), O(1)-C(1) 1.289(3), C(1)-O(2) 1.236(3), C(1)-C(2) 1.521(3), C(2)-C(3) 1.536(3), C(3)-C(4) 1.530(4), C(4)-C(5) 1.522(3), N(1)-C(2) 1.514(3), N(1)-C(5) 1.501(3), N(2)-O(3) 1.247(3), N(2)-O(4) 1.242(3), Ru(1)-O(1)-C(1) 118.71(15), O(1)-C(1)-C(2) 117.5(2), C(1)-C(2)-N(1) 111.52(18), C(2)-N(1)-Ru(1) 111.08(14), O(1)-Ru(1)-N(1) 79.70(7), O(3)-N(2)-O(4) 118.5(2).

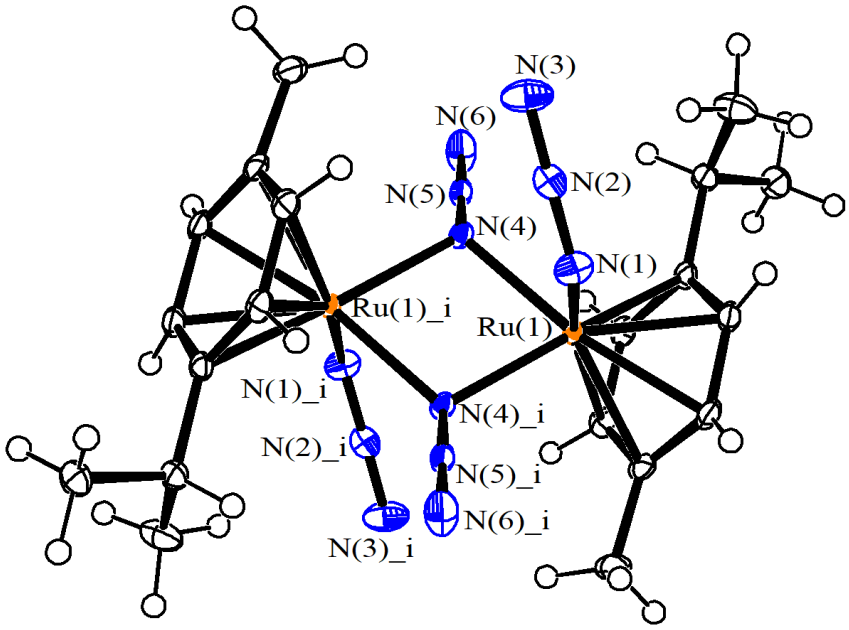

Figure S60. View of the X-ray structure of $[Ru(N_3)_2(\eta^6\text{-}p\text{-cymene})]_2$ (**Ru-N3**). Displacement ellipsoids are at the 50% probability level. Main bond distances (Å) and angles (°): Ru(1)-$(\eta^6$-p-cymene$)_{average}$ 2.183(4), Ru(1)-N(1) 2.1063(15), Ru(1)-N(4) 2.1314(14), Ru(1)-N(4)_i 2.1610(14), N(1)-N(2) 1.193(2), N(2)-N(3) 1.160(2), N(4)-N(5) 1.222(2), N(5)-N(6) 1.140(2), Ru(1)-N(1)-N(2) 120.67(12), N(1)-N(2)-N(3) 176.90(18), Ru(1)-N(4)-Ru(1)_i 104.97(6), Ru(1)-N(4)-N(5) 121.88(11), N(4)-N(5)-N(6) 177.27(19), N(4)-Ru(1)-N(4)_i 75.03(6). Symmetry transformation used to generate equivalent atoms: -x+1,-y+1,-z+1.

Table S3. Hydrogen bonds (Å and °) for **2b**, **2c**, **2d** and **2e.**

Complex	D-H···A	d(D-H)	d(H···A)	d(D···A)	<(DHA)
2b *	O(3)-H(3)...O(5)#1	0.84	1.90	2.72(2)	165.8
	N(1)-H(1)...O(5)#1	1.00	2.21	3.07(3)	142.6
	O(6)-H(6)...O(1)#2	0.84	2.04	2.84(3)	159.4
	N(2)-H(2A)...O(2)#2	1.00	1.98	2.95(3)	160.4
2c	N(1)-H(1)...O(2)#3	1.00	1.89	2.875(3)	166.3
	O(3)-H(3)...O(1)#3	0.84	2.11	2.935(3)	166.6
	C(2)-H(2)...O(1)#3	1.00	2.60	3.425(3)	139.5
2d	N(1)-H(1)...O(2)#4	1.00	2.11	2.942(9)	139.3
	O(3)-H(3)...O(2)#4	0.84	2.00	2.829(9)	167.7
2e	N(1)-H(1)...O(2)#5	1.00	1.82	2.799(17)	167.0
	O(3)-H(3)...O(1)#5	0.84	2.16	2.961(17)	159.1

Symmetry transformations used to generate equivalent atoms: #1 -x+1,y+1/2,-z+2; #2 -x+1,y-1/2,-z+1; #3 -x+1,y-1/2,-z+3/2; #4 x-1,y,z; #5 x-1/2,-y+1/2,-z+1

* Two independent molecules are present within the unit cell.

Speciation in water and in cell culture medium.

[RuCl(κ²*N*,*O*-Pro)(η⁶-*p*-cymene)], 1a, in D_2O.

1a. ^{1}H NMR (D_2O; with excess Cl^-): δ/ppm = *5.94*, 5.85 (d, *J* = 5.9 Hz, 1H); *5.74*, 5.68 (app-t, *J* = 6.7 Hz, 2H); *5.59*, 5.52 (d, *J* = 6.0 Hz, 1H); 4.07 (dd, *J* = 11.2, 5.9 Hz), *3.77* (d, *J* = 9.1 Hz) (1H); 3.44 (t, *J* = 8.6 Hz, 1H); 3.21 (td, *J* = 11.4, 5.9 Hz), *3.15–3.08* (m) (1H); 2.81 (hept, *J* = 6.9 Hz, 1H); 2.27–2.20 (m, 1H); 2.17, *2.15* (s, 3H); 2.06–1.97 (m, 1H); *1.89–1.79*, 1.79–1.65 (m, 2H); 1.34, 1.29 (d, *J* = 6.9 Hz, 6H). Isomer ratio = 7.

[1w]$^+$. ^{1}H NMR (D_2O): δ/ppm = 5.96–5.89 (m, 1H); 5.79–5.72 (m), 5.69 (d, *J* = 6.0 Hz) (2H); *5.59*, 5.51 (d, *J* = 5.8 Hz, 1H); 4.06 (dd, *J* = 10.8, 5.1 Hz), *3.77* (t, *J* = 8.4 Hz) (1H); 3.36–3.18 (m), 2.66–2.54 (m) (2H), 2.82 (hept, *J* = 6.9 Hz, 1H); 2.19, *2.18* (s, 3H), 2.16–2.07, *1.34 – 1.25* (m, 1H) 2.06–1.92 (m, 1H), 1.85–1.63 (m, 2H). Isomer ratio = 2.6. **Cl**$^-$. ^{35}Cl NMR (D_2O): δ/ppm = 0.44 ($\Delta\upsilon_{1/2}$ = 22 Hz).

Figure S61. ^{1}H NMR spectra (3-6 ppm region) of **1a** in D_2O: freshly prepared solution **(a)**, following $AgNO_3$ **(b)** or NaCl addition **(c)**. Spectra aligned to the **1a**/D_2O solution to compensate ionic strength effects on chemical shift.

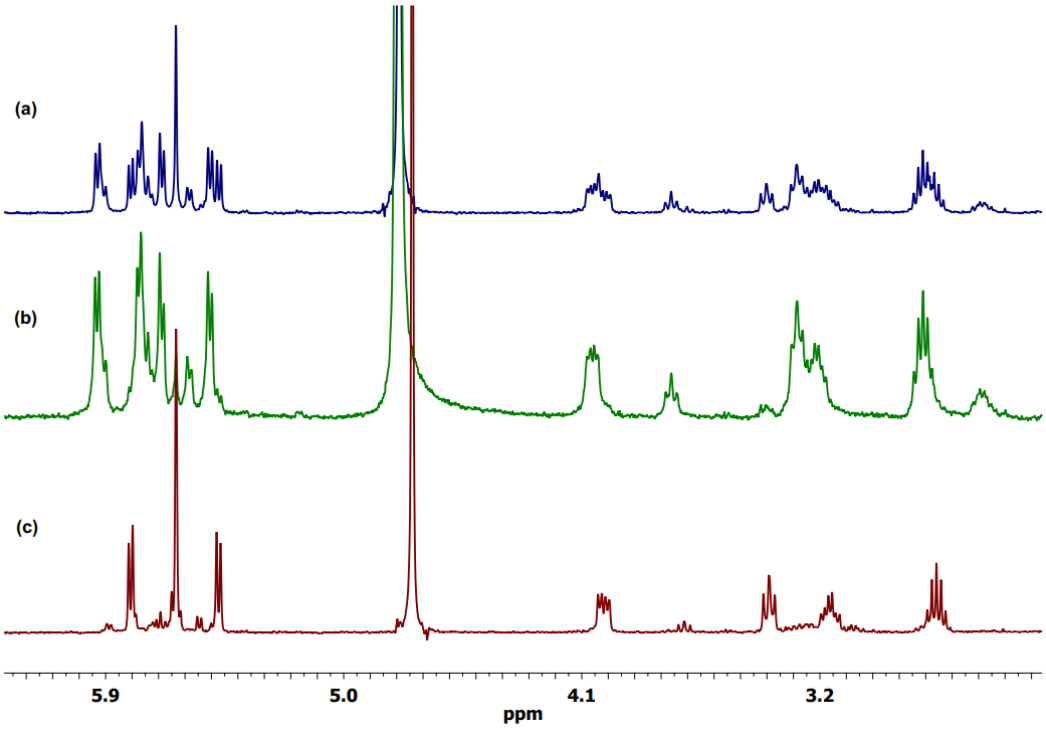

[RuBr(κ²*N*,*O*-Pro)(η⁶-*p*-cymene)], 1b, in D_2O.

1b. ^1H NMR (D_2O; with excess Br^-): δ/ppm = *5.86*, 5.81 (d, *J* = 5.9 Hz, 1H); *5.78*, 5.73 (d, *J* = 6.1 Hz, 1H); 5.69–5.63 (m, 1H); 5.57, *5.49* (d, *J* = 6.0 Hz, 1H); 4.06 (dd, *J* = 11.0, 5.8 Hz, 1H); 3.50–3.45, *3.39–3.32* (m, 1H); 3.21 (td, *J* = 11.5, 5.6 Hz, 1H); 2.82 (hept, *J* = 6.9 Hz, 1H); 2.25–2.15 (m), 2.18 (s), *2.16* (s) (4H), 2.06–1.96 (m, 1H); *1.87–1.78*, 1.76–1.63 (m, 2H); 1.33, 1.27 (d, *J* = 6.9 Hz, 6H). Isomer ratio = 6.

Br^-. ^{81}Br NMR (D_2O): δ/ppm = − 3.4 ($\Delta\upsilon_{1/2} \approx 10^3$ Hz).

Figure S62. ^1H NMR spectra (3-6 ppm region) of **1b** in D_2O: freshly prepared solution **(a),** following $AgNO_3$ **(b)** or NaBr addition **(c)**. Spectra aligned to the **1b**/D_2O solution to compensate ionic strength effects on chemical shift.

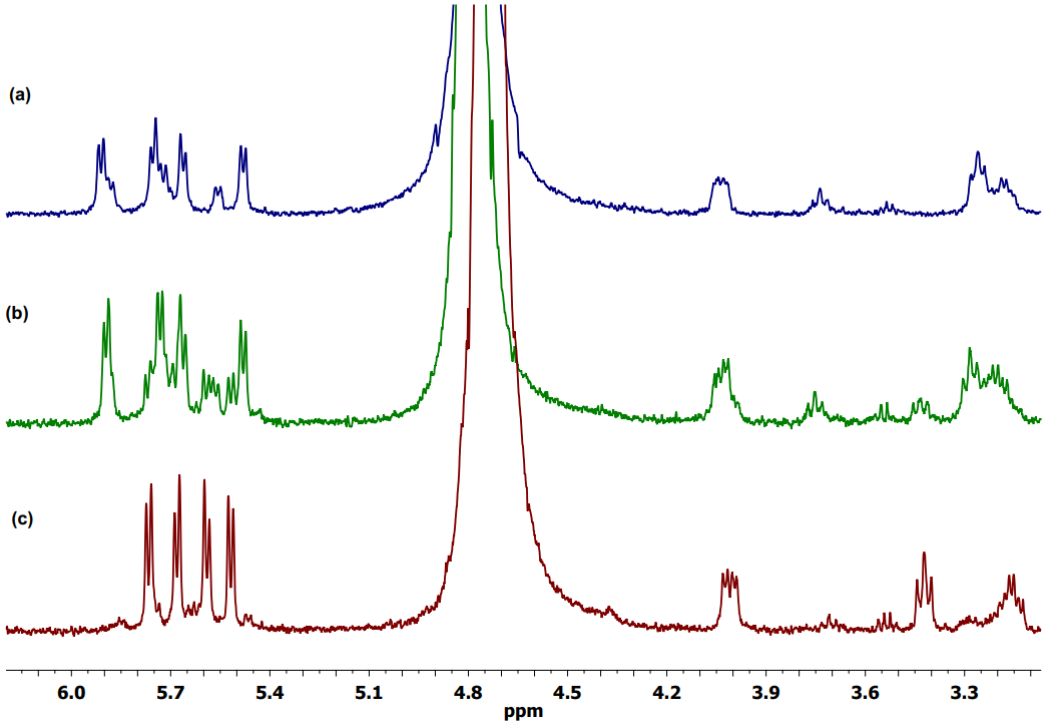

[RuI(κ^2*N*,*O*-Pro)(η^6-*p*-cymene)], 1c, in D_2O.

1c. ^{1}H NMR (D_2O; with excess I^-): δ/ppm = *5.97*, 5.91 (d, *J* = 6.0 Hz, 1H); *5.82* ,5.78 (d, *J* = 5.9 Hz, 1H); 5.74 (d, *J* = 5.9 Hz, 1H); *5.65*, 5.58 (d, *J* = 6.0 Hz, 1H); 4.06 (dd, *J* = 11.1, 5.8 Hz, 1H), 3.58–3.49 (m, 1H), 3.23 (td, *J* = 11.4, 5.4 Hz, 1H), 2.85 (hept, *J* = 7.0 Hz, 1H); 2.27–2.15 (m), 2.19 (s), 2.17 (s), (4H); 2.05–1.96 (m, 1H), 1.79–1.65 (m, 2H); 1.33, 1.27 (d, *J* = 6.9 Hz, 6H). Isomer ratio ≈ 16.

I$^-$. ^{127}I NMR (D_2O): δ/ppm = − 1.0 (br.).

Figure S63. ^{1}H NMR spectra (3-6 ppm region) of **1c** in D_2O: freshly prepared solution **(a)**; following $AgNO_3$ **(b)** or NaI addition **(c)**. Spectra aligned to the **1c**/D_2O solution to compensate ionic strength effects on chemical shift.

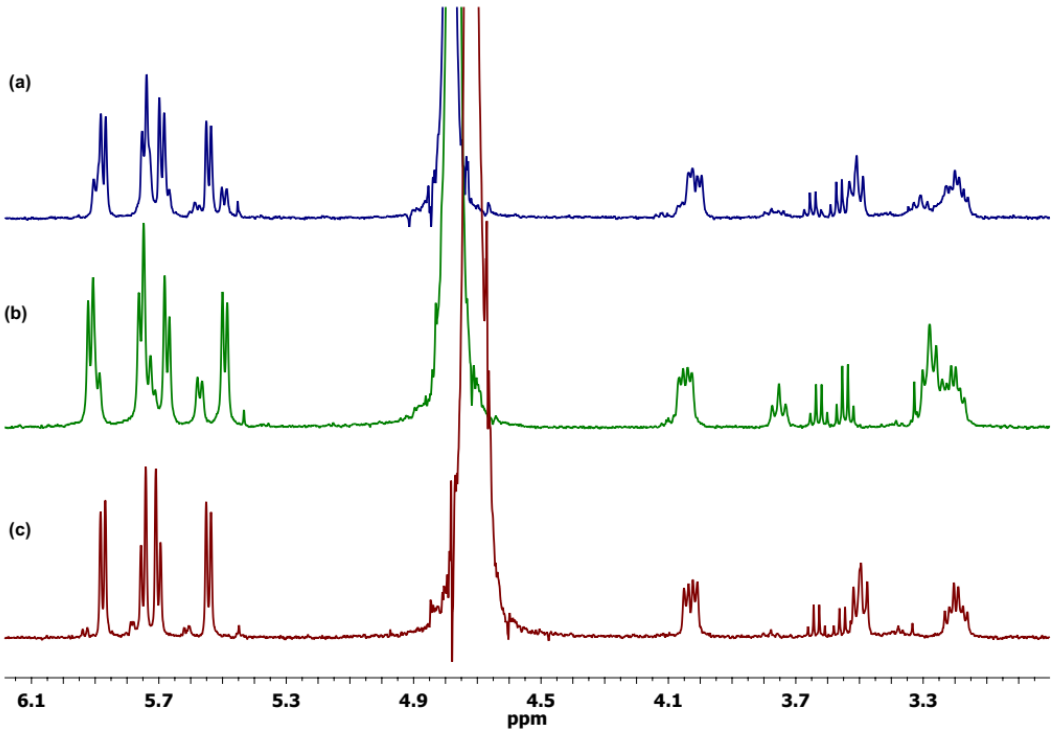

[Ru(κ*N*-NCS)(κ^2*N*,*O*-Pro)(η^6-*p*-cymene)], 1d, in D_2O or D_2O/CD_3OD 5:2 v/v.

1d. ^{1}H NMR (D_2O): δ/ppm = 5.85 (d), 5.81 (app-t), 5.76 (d) (2H); 5.69–5.65 (m, 1H); 5.62, 5.55 (d, 1H), 4.01–3.95, 3.79–3.72 (m, 1H); 3.41–3.30 (m), 2.82–2.70 (m); 2.13, 2.12 (s, 3H), 1.32–1.24 (m, 6H). Isomer ratio ≈ 1. Solubility of **1d** in D_2O was insufficient to carry out a detailed speciation study.

^{1}H NMR (D_2O/CD_3OD 5:2): δ/ppm = 5.86 (d, *J* = 5.9 Hz), *5.83–5.81* (m, 1H), 5.76 (d, *J* = 6.1 Hz) (2H); 5.70–5.65 (m, 1H); *5.62*, 5.56 (d, *J* = 5.8 Hz, 1H); 3.98 (dd, *J* = 11.2, 4.9 Hz), *3.73* (t, *J* = 8.7 Hz) (1H), 3.40–3.34, *3.26–3.17* (m, 1H); 3.09–3.00, *2.93–2.84* (m, 1H); 2.82–2.71 (m, 1H), 2.15, *2.14* (s, 1H); 2.05–1.93 (m, 1H), 1.84–1.62 (m, 2H); *1.32*, 1.29 (d, *J* = 6.8 Hz, 6H). Isomer ratio = 1.2.

Figure S64. ^{1}H NMR spectra (3-6 ppm region) of **1d** in D_2O/CD_3OD 5:2: freshly prepared solution **(a)**, following KSCN **(b)** or $AgNO_3$ addition **(c)**; 24 h after $AgNO_3$ addition **(d)**. Spectra aligned to the **1d**/D_2O solution to compensate ionic strength effects on chemical shift.

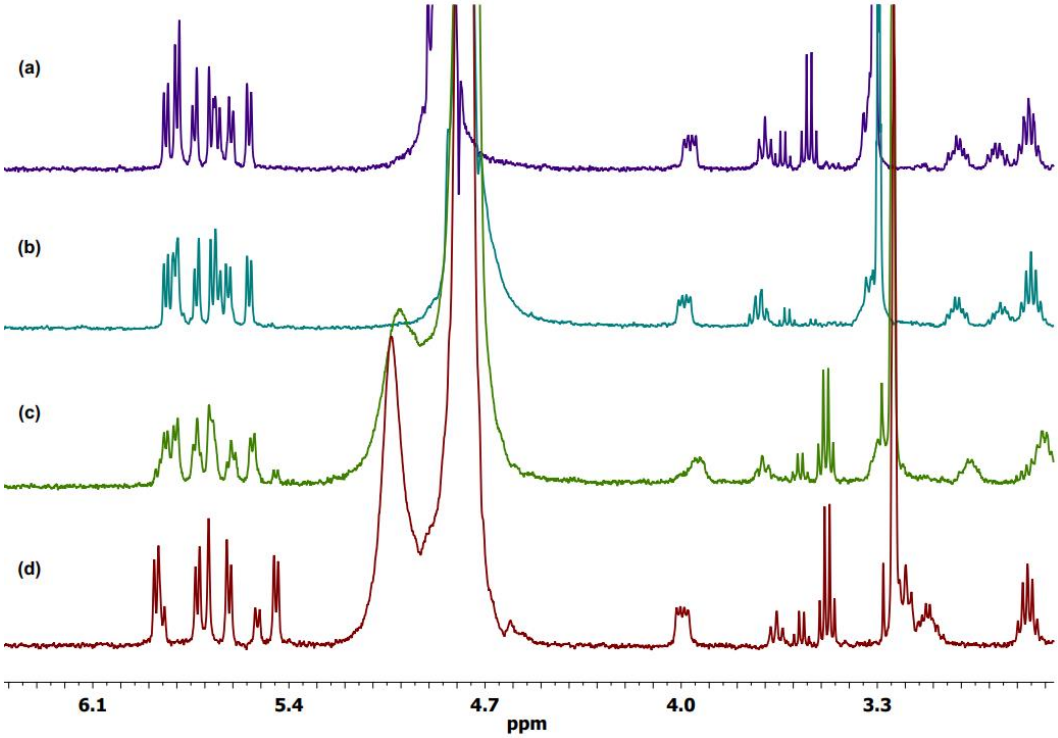

[Ru(N_3)(κ^2*N*,*O*-Pro)(η^6-*p*-cymene)], 1e, in D_2O.

1e. ^{1}H NMR (D_2O): δ/ppm = 5.77, *5.74* (d, *J* = 6.0 Hz, 1H); *5.71*, 5.67 (d, *J* = 6.0 Hz, 1H); 5.59, *5.57* (d, *J* = 6.1 Hz, 1H); *5.54*, 5.49 (d, *J* = 6.0 Hz, 1H); 3.96 (dd, *J* = 10.8, 5.3 Hz), 3.75 (t, *J* = 8.7 Hz) (1H); 3.33–3.27, *3.27–3.20* (m, 1H); 3.19–3.10, *2.71–2.62* (m, 1H); 2.78 (hept, *J* = 6.5 Hz, 1H), 2.26–2.16 (m, 1H); 2.16, *2.13* (s, 3H); 2.01–1.81 (m, 1H), 1.79–1.56 (m, 2H), 1.32–1.25 (m, 6H). Isomer ratio = 2.5.

Figure S65. ^{1}H NMR spectra (3-6 ppm region) of **1e** in D_2O: freshly prepared solution **(a)**; following NaN_3 **(b)** or $AgNO_3$ addition **(c)**; 24 h after $AgNO_3$ addition **(d)**. Spectra aligned to the **1e**/D_2O solution to compensate ionic strength effects on chemical shift.

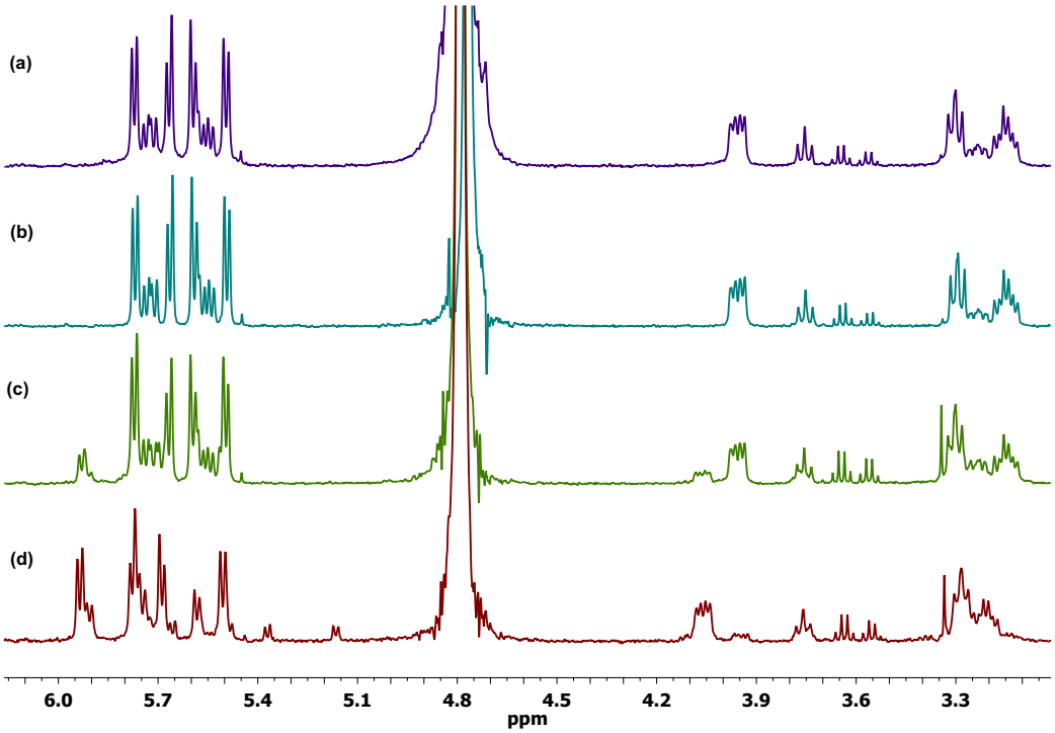

[RuCl(κ²*N*,*O*-Hyp)(η⁶-*p*-cymene)], 2a, in D_2O.

2a. ^{1}H NMR (D_2O, with excess Cl^-): δ/ppm = 5.85 (d, *J* = 6.0 Hz), 5.84–5.82 (m) (1H); *5.77* (d, *J* = 5.4 Hz), 5.73–5.67 (m) (2H); *5.62*, 5.55 (d, *J* = 6.1 Hz, 1H); 4.58–4.50, *4.44–4.38* (m, 1H); 4.06–3.96 (m, 1H); 3.66 (t, *J* = 9.0 Hz), *3.30* (d, *J* = 12.4 Hz) (1H); 3.42–3.36 (m, 1H); 2.81 (hept, *J* = 6.9 Hz, 1H); 2.25–2.19, *2.13–2.06* (m, 1H); 2.18, *2.16* (s, 3H), 2.03–1.93, *1.81–1.70* (m, 1H); 1.37 – 1.25 (m, 6H). Isomer ratio = 3.5.

[2w]⁺. ^{1}H NMR (D_2O): δ/ppm = 5.97–5.92 (m, 1H); 5.82–5.76 (m), 5.69 (d) (2H); *5.62*, 5.55 (d, *J* = 6.1 Hz, 1H); 4.51, *4.41* (s-br, 1H); 4.05–3.97 (m, 1H), 3.51, (app-t, *J* = 9.1 Hz), *2.89–2.75** (m) (0.6H); 3.36, *3.28* (d, *J* = 12.6 Hz, 1H), 2.89–2.75* (m, 1.4H); 2.20 (s, 3H); 2.18–2.08 (m, 1H), 2.01–1.85, *1.70–1.57* (m, 1H), 1.35–1.20 (m, 6H). *Superimposed. Isomer ratio = 1.5.

Cl^-. ^{35}Cl NMR (D_2O): δ/ppm = 0.34 ($\Delta\upsilon_{1/2}$ = 25 Hz).

Figure S66. ^{1}H NMR spectra (3-6 ppm region) of **2a** in D_2O: freshly prepared solution **(a)**; following $AgNO_3$ **(b)** or NaCl addition **(c)**. Spectra aligned to the **2a**/D_2O solution to compensate ionic strength effects on chemical shift.

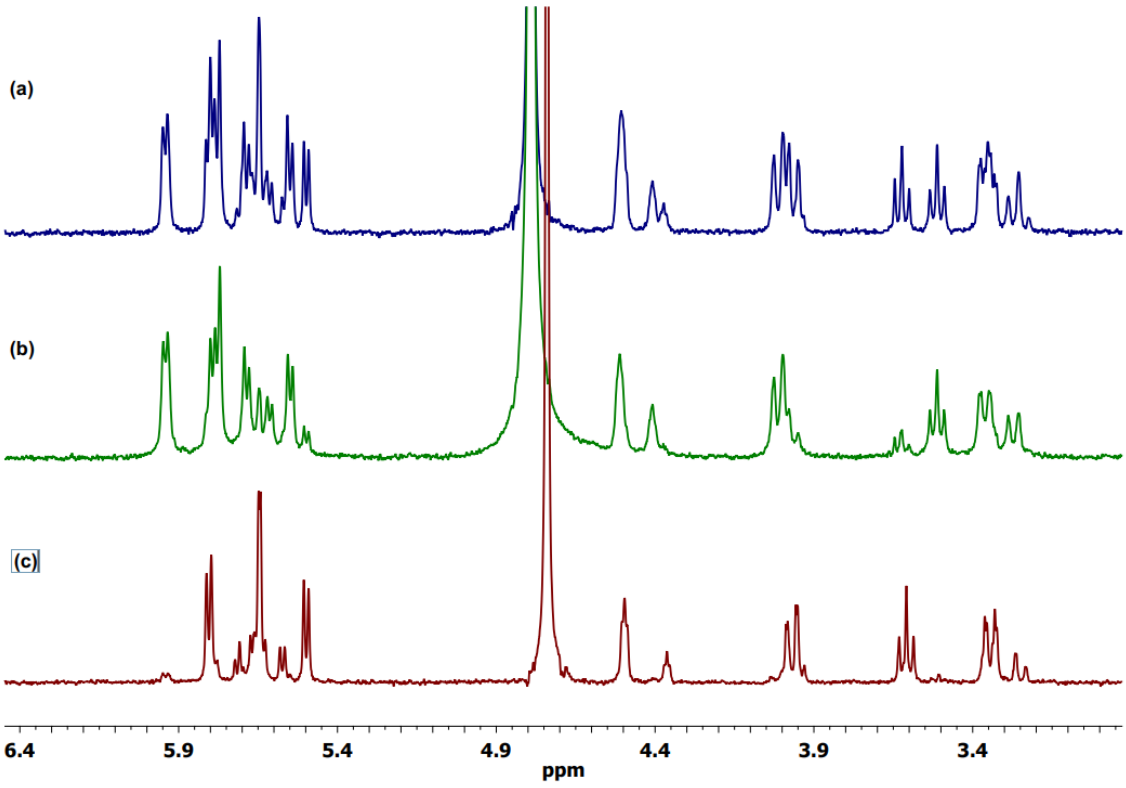

[RuBr(κ^2*N*,*O*-Hyp)(η^6-*p*-cymene)], 2b, in D_2O.

2b. ^{1}H NMR (D_2O, with excess Br^-): δ/ppm = *5.88* (br.), 5.78–5.73 (m), 5.69 (d, *J* = 5.9 Hz) (2H); *5.65*, 5.61, 5.55 (d, *J* = 5.9 Hz), *5.51* (br.) (2H); 4.53–4.47, *4.37–4.33* (m, 1H); 4.02–3.91 (m, 1H); 3.65 (t, *J* = 9.0 Hz), *3.28* (d, *J* = 12.3 Hz) (1H); *3.52–3.48*, 3.39–3.32 (m, 1H); 2.78 (hept, *J* = 6.8 Hz, 1H), 2.21–2.11 (m, 4H), 2.00–1.89; *1.83–1.72* (m, 1H); 1.34–1.20 (m, 6H). Isomer ratio = 5.

Br$^-$. ^{81}Br NMR (D_2O): δ/ppm = − 1.9 ($\Delta\upsilon_{1/2} \approx 8 \cdot 10^2$ Hz).

Figure S67. ^{1}H NMR spectra (3-6 ppm region) of **2b** in D_2O: freshly prepared solution **(a)**; following $AgNO_3$ **(b)** or NaBr addition **(c)**. Spectra aligned to the **2b**/D_2O solution to compensate ionic strength effects on chemical shift.

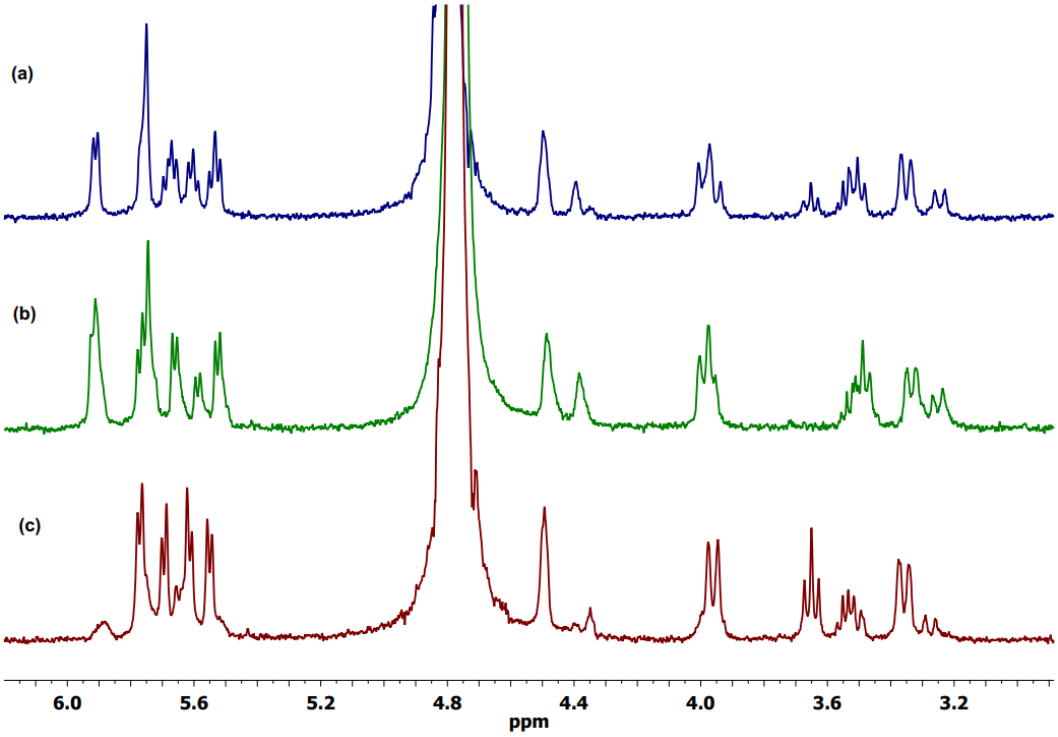

[RuI(κ^2*N*,*O*-Hyp)(η^6-*p*-cymene)], 2c, in D_2O.

2c. ^{1}H NMR (D_2O, with excess I^-): δ/ppm = *6.04*, 5.98 (d, *J* = 6.0 Hz, 1H); *5.93*, *5.87*, 5.85–5.81 (m, 2H); *5.73*, 5.65 (d, *J* = 5.9 Hz, 1H); 4.64–4.60, *4.45–4.40* (m, 1H); *4.10* (d, *J* = 8.1 Hz), 4.07 (dd, *J* = 12.6, 1.8 Hz) (1H); 3.79 (t, *J* = 9.0 Hz), *3.74* (d, *J* = 3.7 Hz) (1H); 3.51 (dd, *J* = 12.5, 2.8 Hz), *3.48–3.44* (m) (1H); 2.91 (hept, *J* = 6.8 Hz, 1H); 2.27 (s), *2.24* (s), 2.23–2.18 (m) (4H), 2.15–2.04 (m, 1H); 1.38 (d, *J* = 6.9 Hz), 1.32 (d, *J* = 7.0 Hz) (6H). Isomer ratio = 6.5.

Figure S68. ^{1}H NMR spectra (3-6 ppm region) of **2c** in D_2O: freshly prepared solution **(a)**; following $AgNO_3$ **(b)** or NaI addition **(c)**. Spectra aligned to the **2c**/D_2O solution to compensate ionic strength effects on chemical shift.

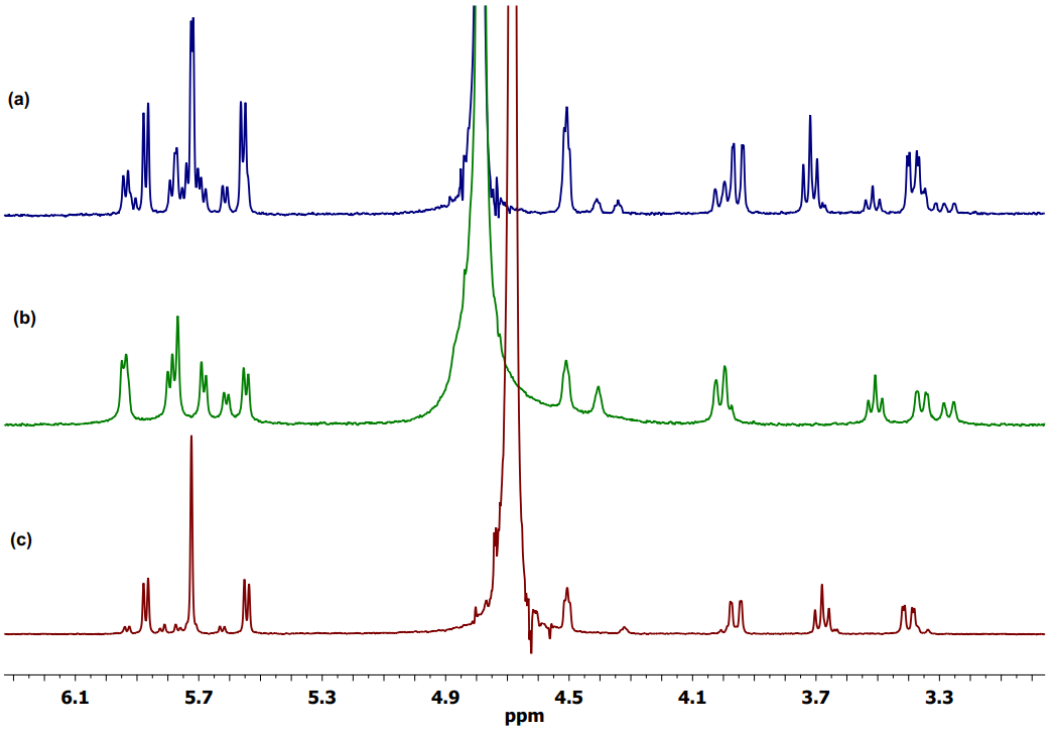

[Ru(κ*N*-NCS)(κ^2*N*,*O*-Hyp)(η^6-*p*-cymene)], 2d, in D_2O or D_2O/CD_3OD 5:2 v/v.

2d. ^{1}H NMR (D_2O): δ/ppm = 5.84 (app-t), *5.76* (d, *J* = 6.0 Hz) (2H); 5.68, *5.65*, *5.57* (d, *J* = 6.0 Hz, 2H); 4.55–4.45 (m, 1H); *4.07–3.97* (m); 3.92 (d, *J* = 12 Hz) (1H); 3.59 (app-t, *J* = 8.8 Hz), *3.42–3.31* (m) (1H); 3.23, *3.08* (dd, *J* = 12, 3 Hz, 1H); 2.77 (hept, *J* = 6.9 Hz, 1H); 2.26–2.16 (m, 1H); 2.14, *2.13* (s, 3H); 2.05–1.97, *1.79–1.60* (m, 1H); 1.34–1.25 (m, 6H). Isomer ratio = 1.5. Solubility of **2d** in D_2O was insufficient to carry out a detailed speciation study.

^{1}H NMR (D_2O/CD_3OD 5:2): δ/ppm = 5.86, 5.84, 5.77 (d, *J* = 6.1 Hz) (2H); 5.72–5.68 (m, 1H); *5.66*, 5.58 (d, *J* = 6.1 Hz, 1H); 4.53–4.44 (m, 1H); *3.99* (dd, *J* = 11.2, 7.7 Hz), 3.92 (d, *J* = 12.2 Hz) (1H); 3.60–3.53, *3.37–3.34* (m, 1H); 3.20, *3.09* (dd, *J* = 12.8, 3.5 Hz, 1H); 2.78 (hept, *J* = 6.9 Hz, 1H); 2.26–2.10 (m), 2.16 (s), *2.15* (s) (4H); 2.05–1.97, *1.79–1.69* (m, 1H); *1.32*, 1.29 (d, *J* = 6.9 Hz, 6H). *Superimposed to 2.16, 2.15. Isomer ratio = 1.3.

Figure S69. ^{1}H NMR spectra (3-6 ppm region) of **2d** in D_2O/CD_3OD 5:2: freshly prepared solution **(a)**, following KSCN **(b)** or $AgNO_3$ addition **(c)**; 24 h after $AgNO_3$ addition **(d)**. Spectra aligned to the **2d**/D_2O solution to compensate ionic strength effects on chemical shift.

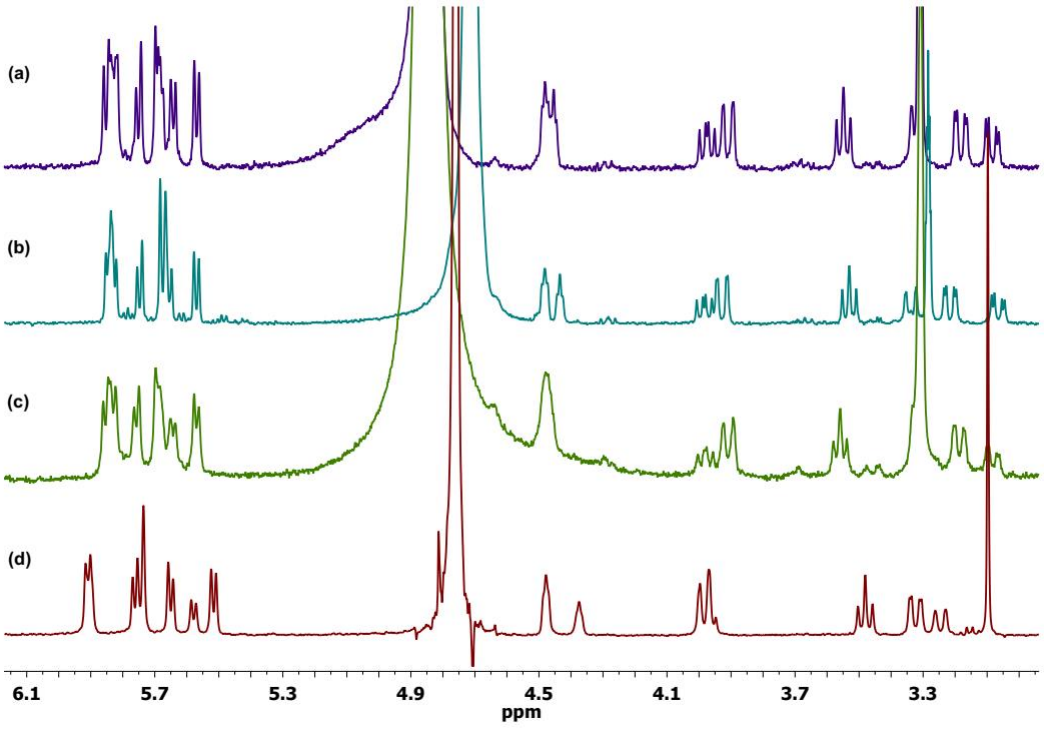

[Ru(N_3)(κ^2*N*,*O*-Hyp)(η^6-*p*-cymene)], 2e, in D_2O.

2e. ^{1}H NMR (D_2O): δ/ppm = 5.77 (app-t), *5.72*, 5.67 (d, *J* = 5.9 Hz) (2H); 5.60, *5.56*, 5.51 (d, *J* = 5.9 Hz, 2H); 4.49, *4.41* (app-t, *J* ≈ 3 Hz); *3.99* (dd, *J* = 10.9, 8.0 Hz), 3.90 (d, *J* = 10.6 Hz) (1H); 3.53 (app-t, *J* = 8.8 Hz), *3.21* (d, *J* = 14 Hz) (1H); 3.32, *2.92* (dd; *J* = 12.6, 2.8 Hz) (1H); 2.79 (hept, *J* = 6.9 Hz); 2.23–2.07 (m), 2.17 (s), *2.14* (s) (4H); 2.03–1.93, *1.76–1.66* (m, 1H); 1.35–1.24 (m, 6H). Isomer ratio = 2.

Figure S70. ^{1}H NMR spectra (3-6 ppm region) of **2e** in D_2O: freshly prepared solution **(a)**, following NaN_3 **(b)** or $AgNO_3$ addition **(c)**, 24 h after $AgNO_3$ addition **(d)**. Spectra aligned to the **2e**/D_2O solution to compensate ionic strength effects on chemical shift.

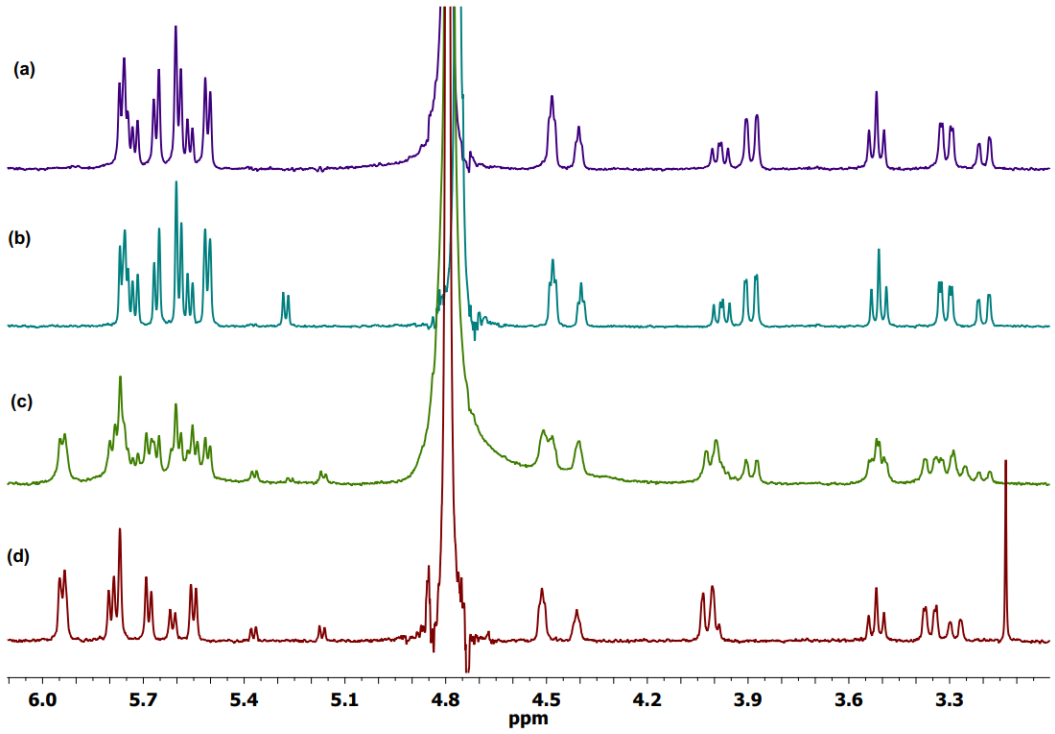

[RuX(κ^2*N*,*O*-Pro)(η^6-*p*-cymene)], X = Cl (1a), Br (1b), I (1c) in cell culture medium (DMEM-d).

Figure S71. ^{1}H NMR spectra (4-6 ppm region) of freshly prepared solutions of: **1a** in D_2O **(a); 1a (b)**, **1b (c)** or **1c (d)** in DMEM-d. Spectra aligned to the **1a**/D_2O solution to compensate ionic strength effects on chemical shift.

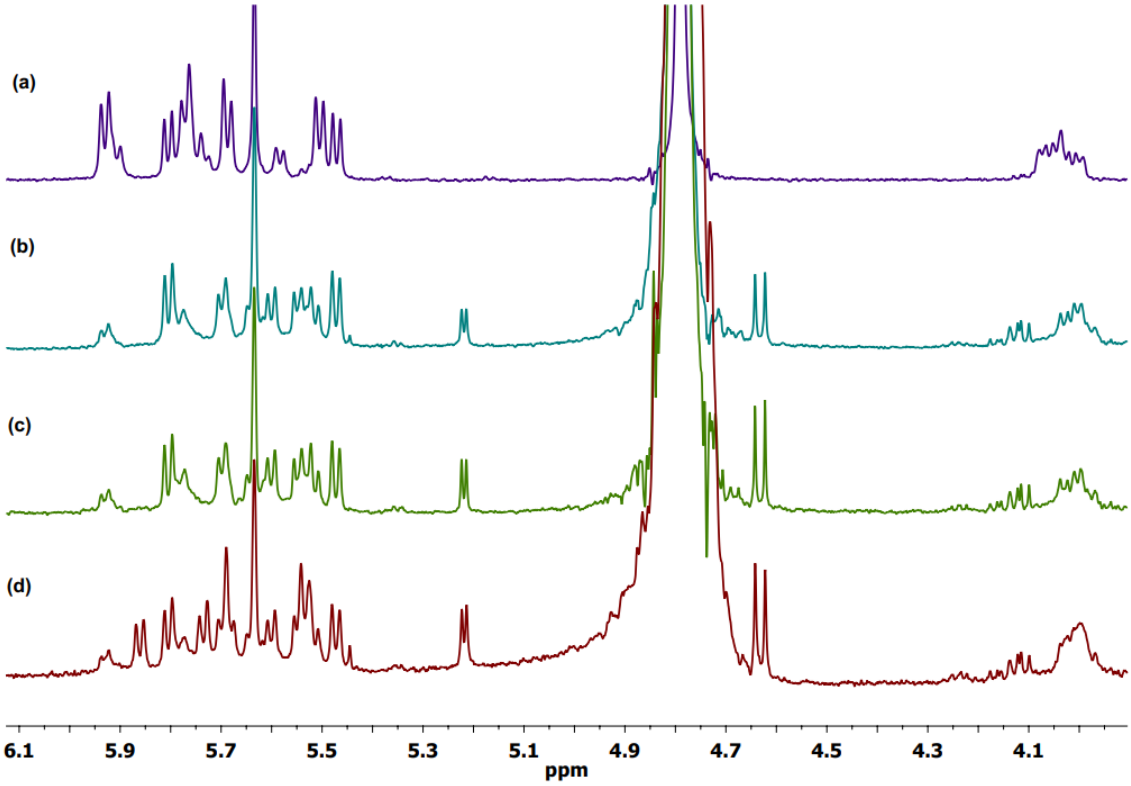

[RuX(κ^2*N*,*O*-Hyp)(η^6-*p*-cymene)], X = Cl (2a), Br (2b), I (2c) in cell culture medium (DMEM-d).

Figure S72. ^{1}H NMR spectra (4-6 ppm region) of freshly prepared solutions of: **2a** in D_2O **(a); 2a (b)**, **2b (c)** or **2c (d)** in DMEM-d. Spectra aligned to the **1a**/D_2O solution to compensate ionic strength effects on chemical shift.

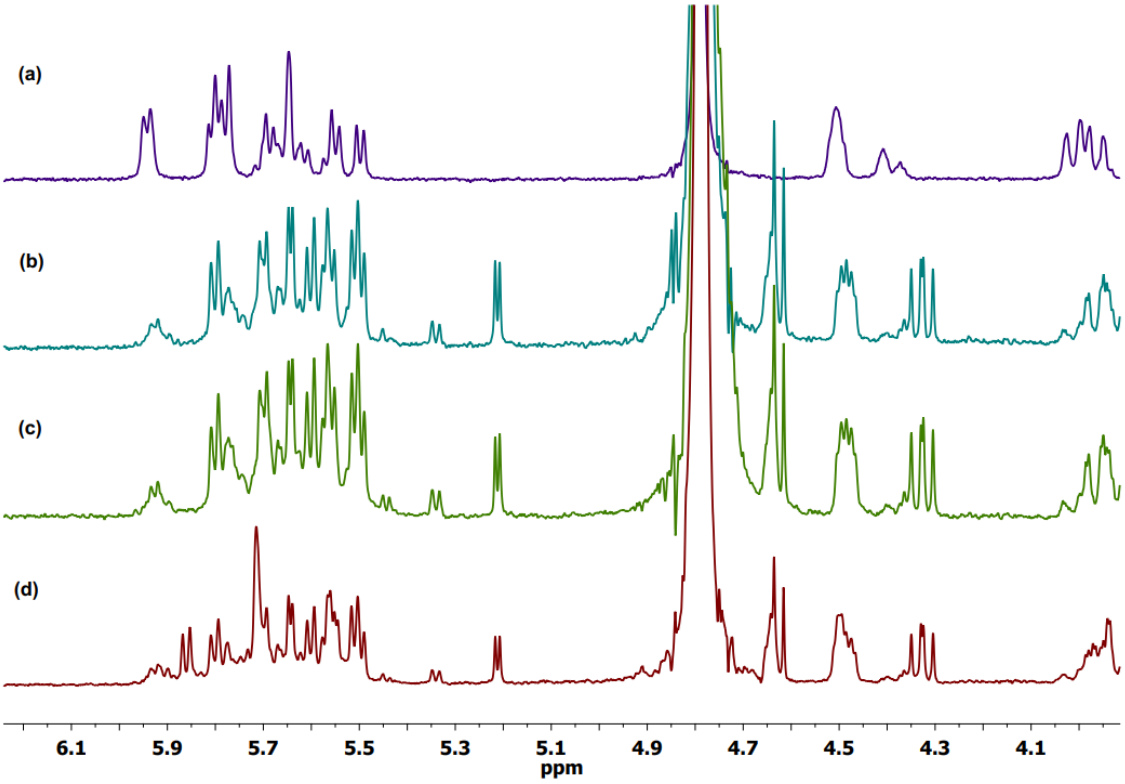

Stability in water and in cell culture medium.

[Ru(κ*N*-NCS)(κ^2*N*,*O*-Pro)(η^6-*p*-cymene)], 1d, in in D_2O/CD_3OD or DMEM-d/CD_3OD 5:2 v/v.

Figure S73. ^{1}H NMR spectra (3-6 ppm region) of: **1d** in D_2O/CD_3OD 5:2 v/v, freshly prepared solution **(a)** and after 48 h at 37 °C **(b)**; **1d** in DMEM-d/CD_3OD 5:2 v/v, freshly prepared solution **(c)** and after 24 h at 37 °C **(d)**; **1a** in D_2O **(e).** Spectral changes from **(a)** to **(b)** represent a variation in the diastereomeric ratio.

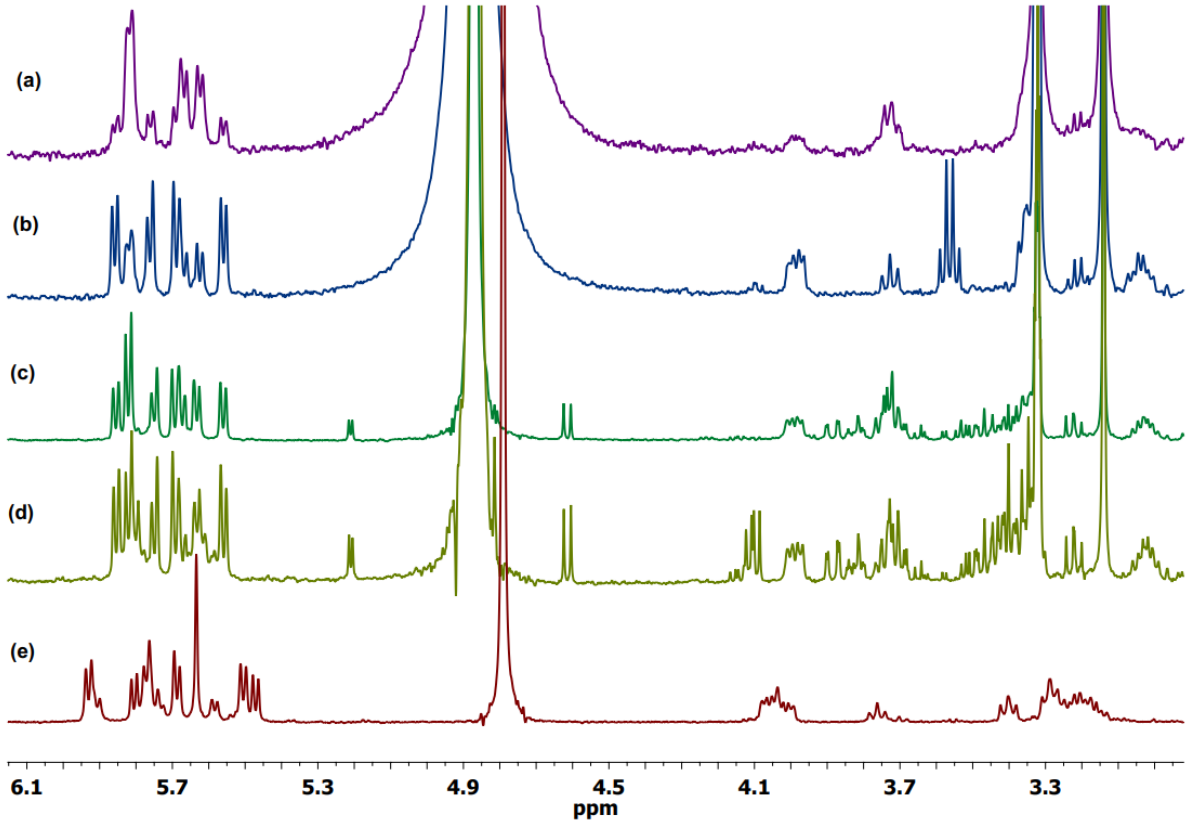

[Ru(N$_3$)(κ^2*N*,*O*-Pro)(η^6-*p*-cymene)], 1e, in D$_2$O and DMEM-d.

Figure S74. ^{1}H NMR spectra (3-6 ppm region) of: **1e** in D$_2$O, freshly prepared solution **(a)** and after 48 h at 37 °C **(b)**; **1e** in DMEM-d, freshly prepared solution **(c)** and after 24 h at 37 °C **(d)**; **1a** in D$_2$O **(e).**

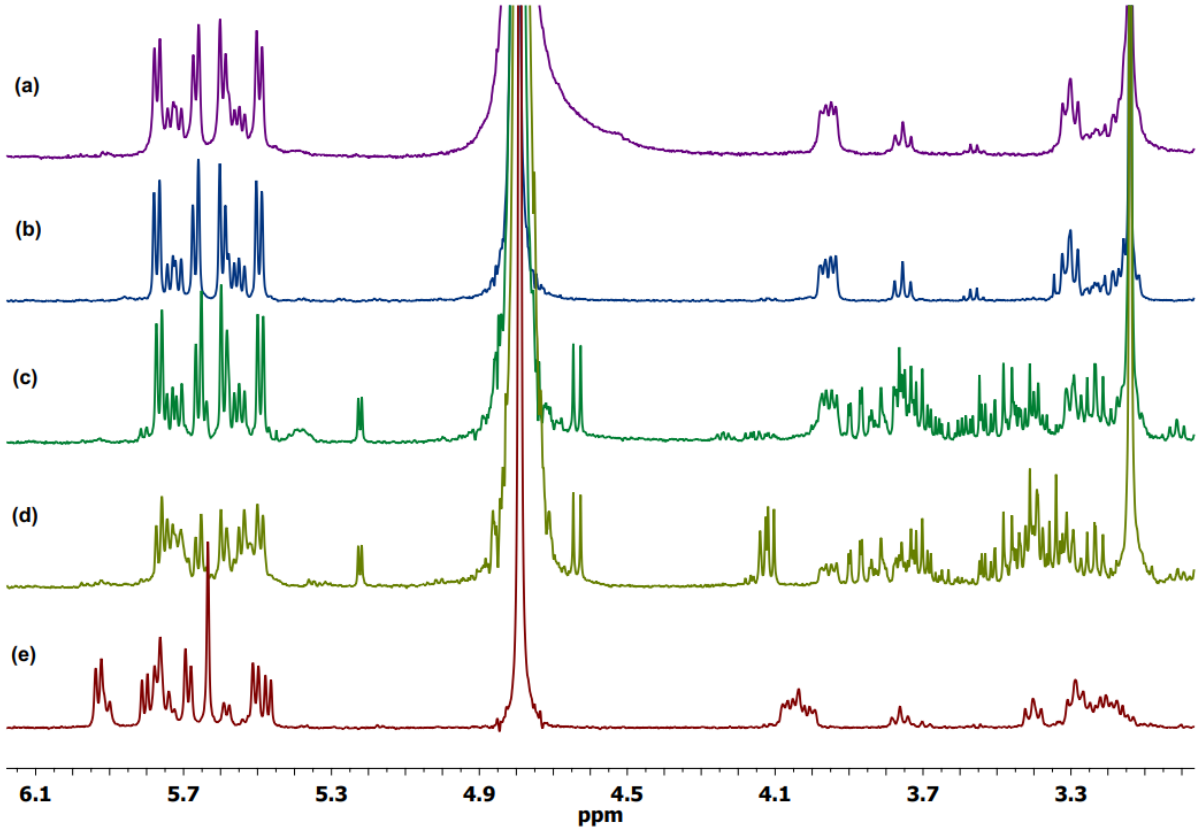

[Ru(κ*N*-NCS)(κ^2*N*,*O*-Hyp)(η^6-*p*-cymene)], 2d, in D_2O and DMEM-d.

Figure S75. ^{1}H NMR spectra (3-6 ppm region) of: **2d** in D_2O/CD_3OD 5:2 v/v, freshly prepared solution **(a)** and after 48 h at 37 °C **(b)**; **2d** in DMEM-d/CD_3OD 5:2 v/v, freshly prepared solution **(c)** and after 24 h at 37 °C **(d)**; **2a** in D_2O **(e).**

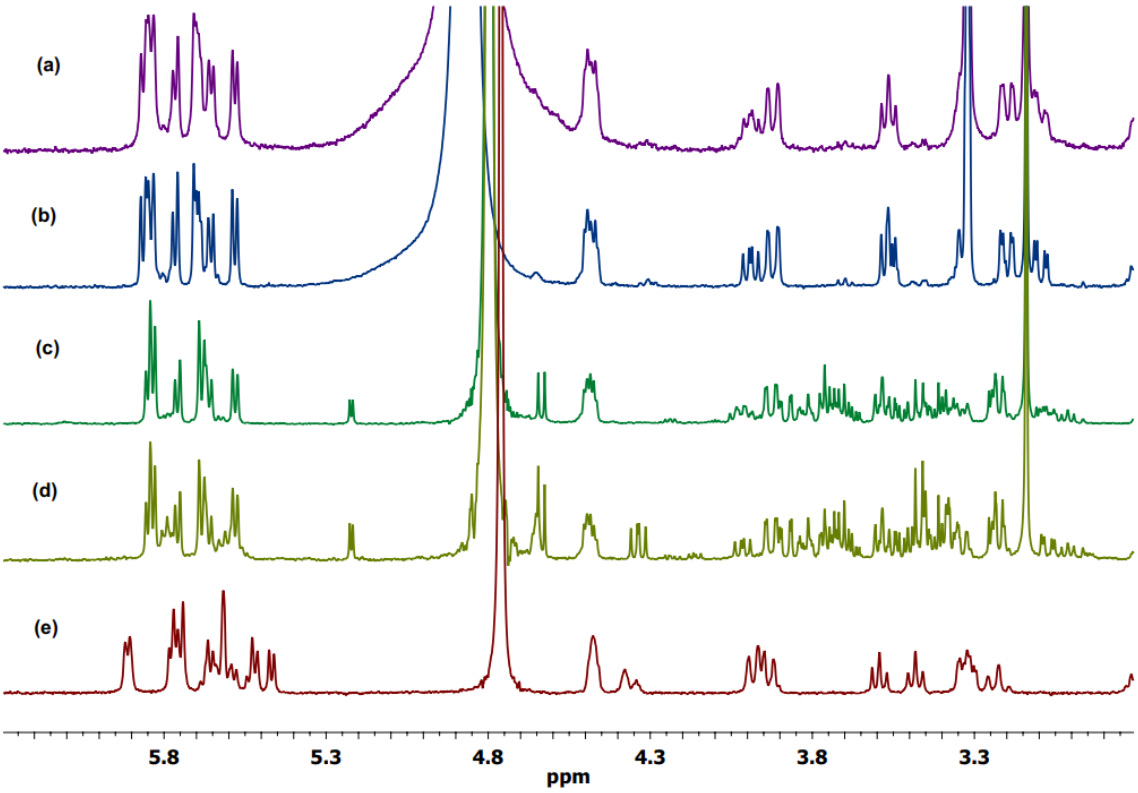

[Ru(N_3)(κ^2*N*,*O*-Hyp)(η^6-*p*-cymene)], 2e, in D_2O and DMEM-d.

Figure S76. ^{1}H NMR spectra (3-6 ppm region) of: **1e** in D_2O, freshly prepared solution **(a)** and after 48 h at 37 °C **(b)**; **2e** in DMEM-d, freshly prepared solution **(c)** and after 24 h at 37 °C **(d)**; **2a** in D_2O **(e).**

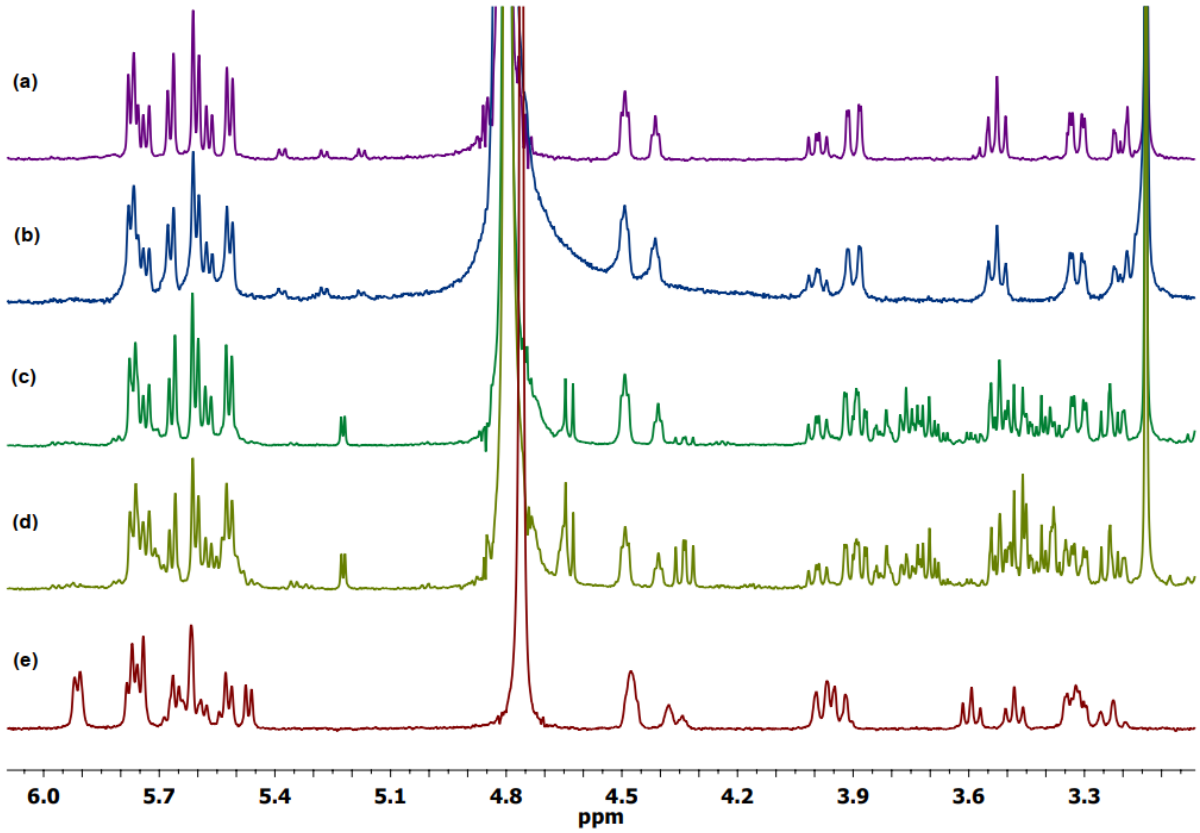

[Ru(κ^3*N*,*O*,*O'*-Ser)(η^6-*p*-cymene)], 3h, in D_2O and DMEM-d.

3h. ^{1}H NMR (D_2O): δ/ppm = 5.62, 5.59 (d, *J* = 6.2 Hz, 2H); 5.36 (d, *J* = 6.1 Hz, 2H); 3.31 (d, *J* = 2.4 Hz, 1H), 3.19 (d, *J* = 9.9, 2.6 Hz, 1H), 3.04 (d, *J* = 9.8 Hz, 1H), 2.79 (hept, *J* = 6.9 Hz, 1H), 2.22 (s, 3H); 1.28 (d, *J* = 6.9 Hz, 6H).

Figure S77. ^{1}H NMR spectra (3-6 ppm region) of: **3h** in D_2O, freshly prepared solution **(a)** and after 48 h at 37 °C **(b)**; **3h** in DMEM-d, freshly prepared solution **(c)** and after 24 h at 37 °C **(d)**; **3a** in D_2O **(e).**

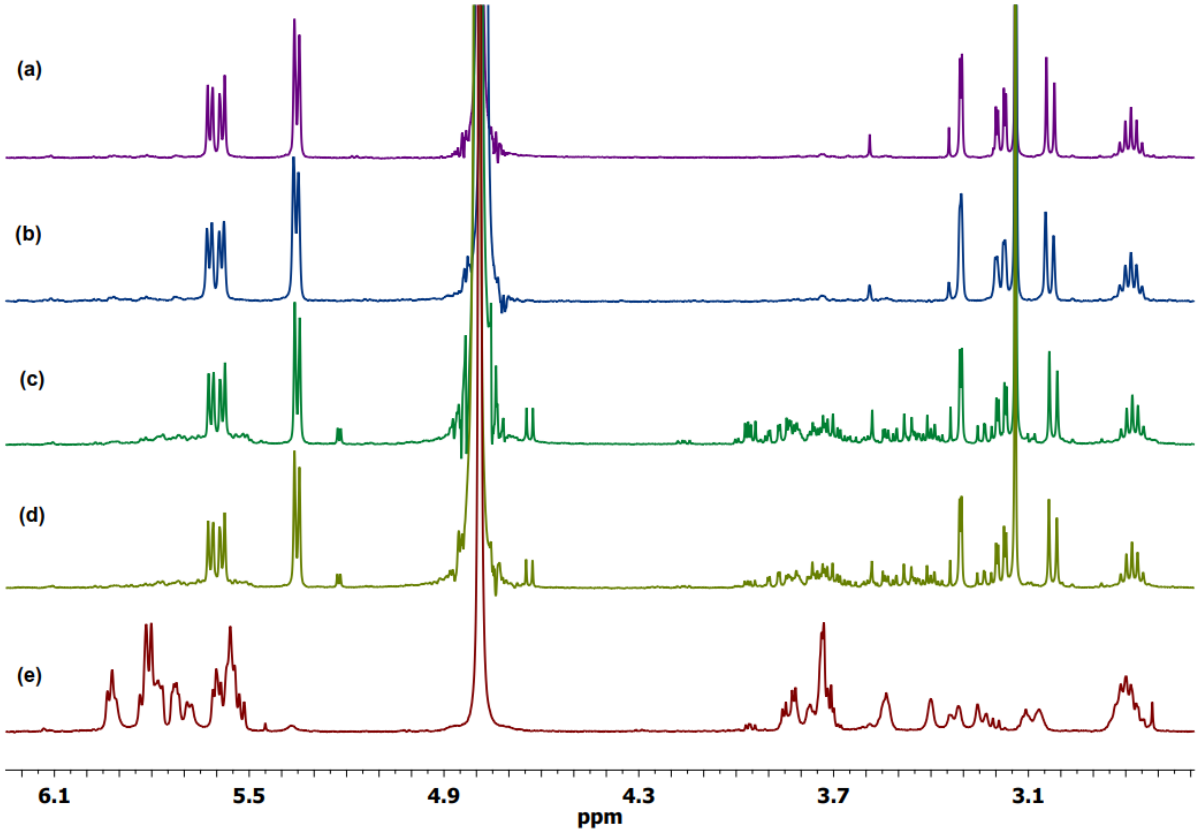

[Ru(κ^3*N,O,O'*-Thr)(η^6-*p*-cymene)], 4h, in D_2O and DMEM-d.

4h. ^{1}H NMR (D_2O): δ/ppm = 5.61, 5.51 (d, *J* = 5.9 Hz, 2H); 5.45, 5.35 (d, *J* = 5.9 Hz, 2H); 3.32 (q, *J* = 6.4 Hz, 1H), 3.08 (s, 1H), 2.80 (hept, *J* = 6.9 Hz, 1H), 2.22 (s, 3H); 1.29, 1.28 (d, *J* = 6.9 Hz, 6H); 0.97 (d, *J* = 6.4 Hz, 3H).

Figure S78. ^{1}H NMR spectra (3-6 ppm region) of: **4h** in D_2O, freshly prepared solution **(a)** and after 48 h at 37 °C **(b)**; **4h** in DMEM-d, freshly prepared solution **(c)** and after 24 h at 37 °C **(d)**; **4a** in D_2O **(e).**

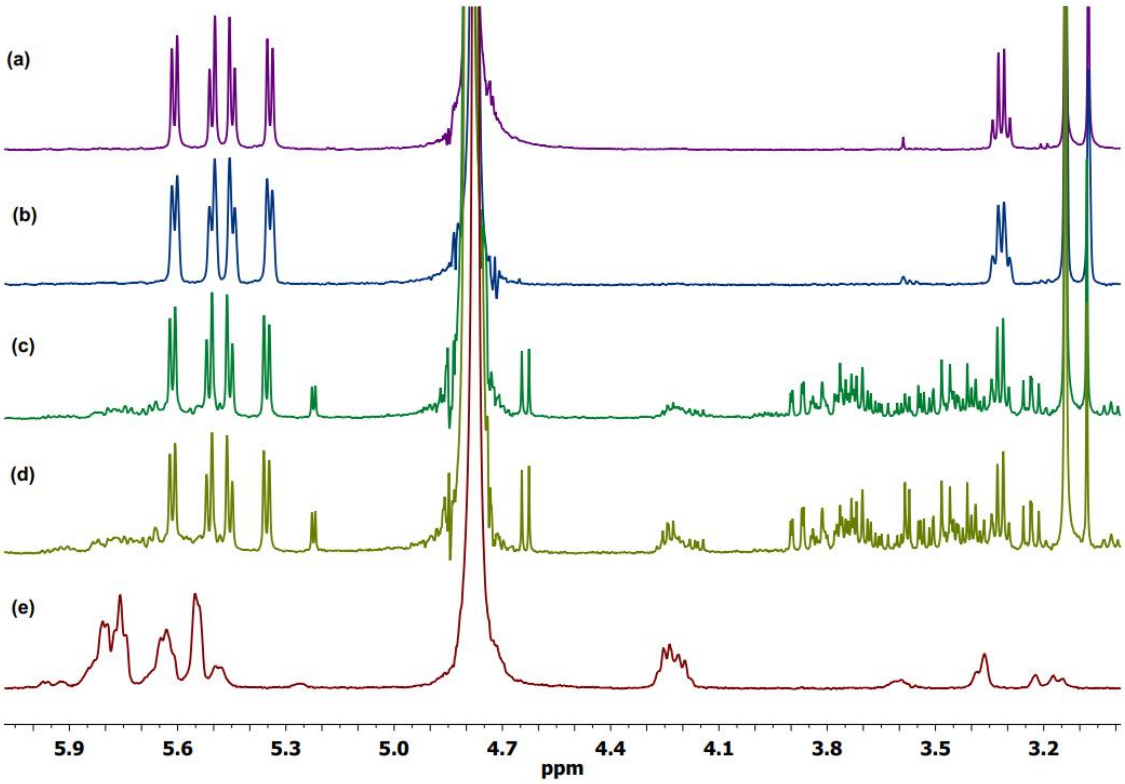

[Ru(κ^2*N*,*O*-Ser)(κ*P*-pta)(η^6-*p*-cymene)]Cl, [3i]Cl in D_2O and DMEM-d.

[3i]$^+$. ^{1}H NMR (D_2O): δ/ppm = 6.17–6.06 (m, 3H), 5.89 (t, *J* = 5.6 Hz, 1H); *4.62*, 4.60 (s, 6H); 4.37–4.24 (m, 6H), 4.06–3.95 (m, 1H); 3.93, 3.31 (t, *J* = 3.7 Hz, 1H), 3.88 (dd, *J* = 12.0, 3.4 Hz), 3.76–3.71 (m) (1H); 2.59 (hept, *J* = 7.1 Hz, 1H); *2.05*, 2.03 (s, 2H); 1.18 (t, *J* = 6.2 Hz, 6H). ^{31}P{^{1}H} NMR (D_2O): δ/ppm = –36.4, *–36.7*. Isomer ratio = 1.3.

Figure S79. ^{1}H NMR spectra (3-6 ppm region) of: **[3i]$^+$** in D_2O, freshly prepared solution **(a)** and after 48 h at 37 °C **(b)**; [**3i**]$^+$ in DMEM-d, freshly prepared solution **(c)** and after 24 h at 37 °C **(d)**; **3a** in D_2O **(e).**

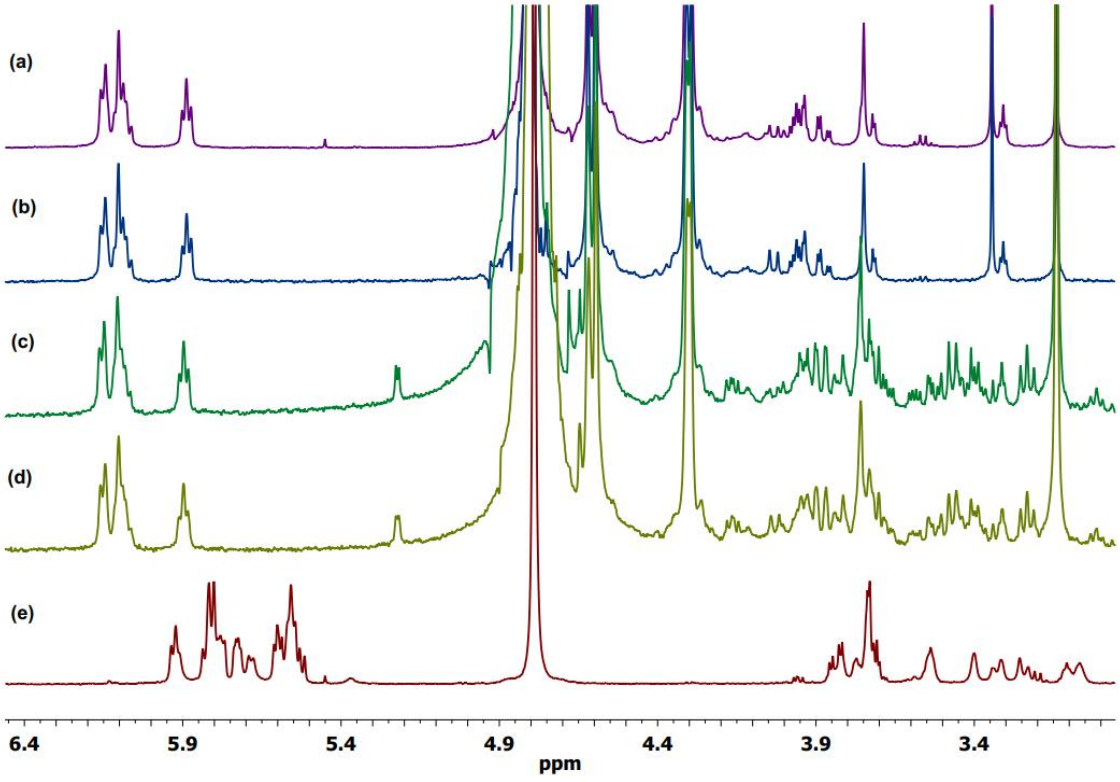

UV-Vis spectra of 4d for Log P_{ow} measurement

Figure S80. UV-Vis spectra of [Ru(κ*N*-NCS)(κ²*N*,*O*-Hyp)(η⁶-*p*-cymene)], **2d** for Log P_{ow} measurement: initial spectrum in the aqueous stock solution (blue line), spectra after partition in the aqueous phase (light blue / cyan lines) and in the octanol phase (yellow / orange lines); x3 replicates.

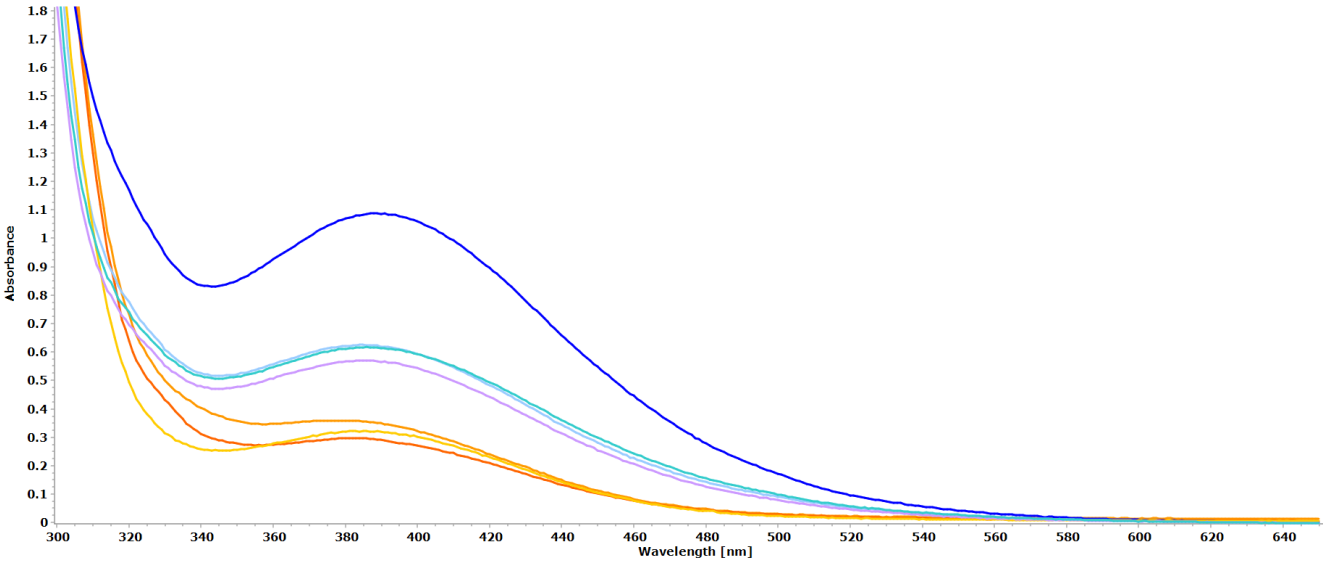

Mass spectra following incubation with Cyt c

Figure S81. Deconvoluted ESI mass spectrum of Cyt c in 2 mM ammonium acetate solution, pH 6.8, incubated with compound **1a** for 72 h at 37 °C. The final protein concentration was 10^{-7} M with a complex to protein molar ratio of 3:1. 0.1% v/v of formic acid was added just before infusion.

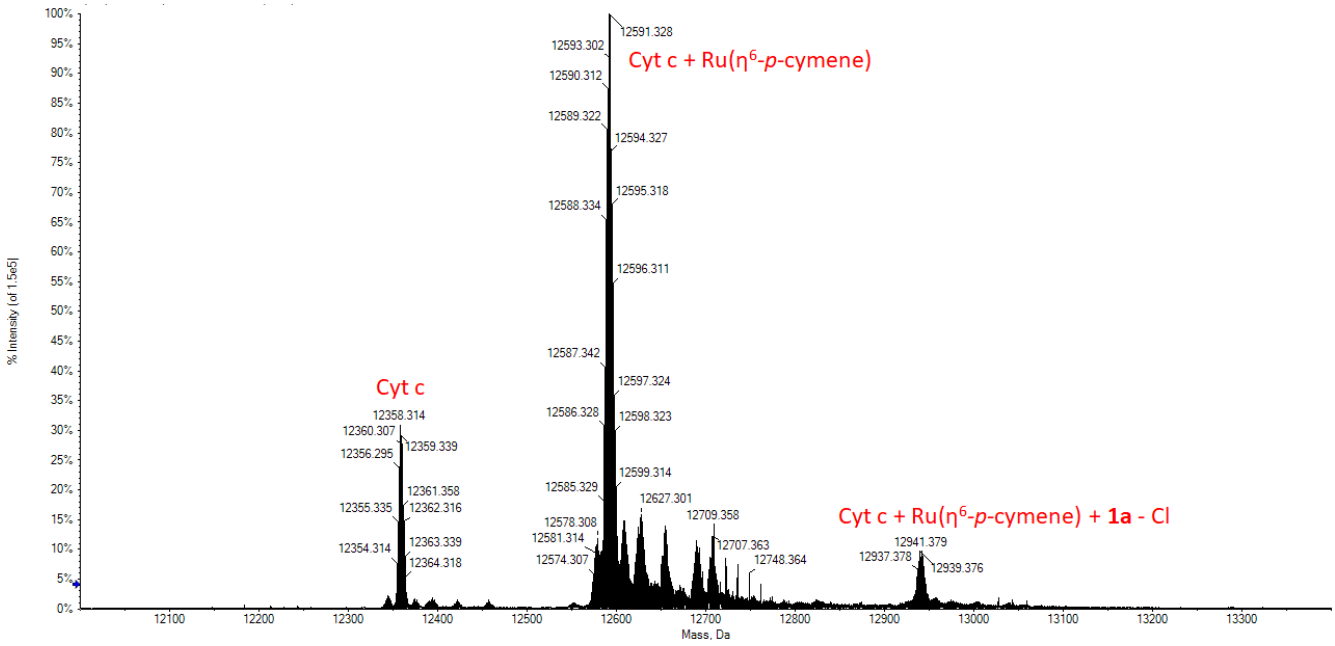

Figure S82. Deconvoluted ESI mass spectrum of Cyt c in 2 mM ammonium acetate solution, pH 6.8, incubated with compound **1d** for 24 h at 37 °C. The final protein concentration was 10^{-7} M with a complex to protein molar ratio of 3:1. 0.1% v/v of formic acid was added just before infusion.

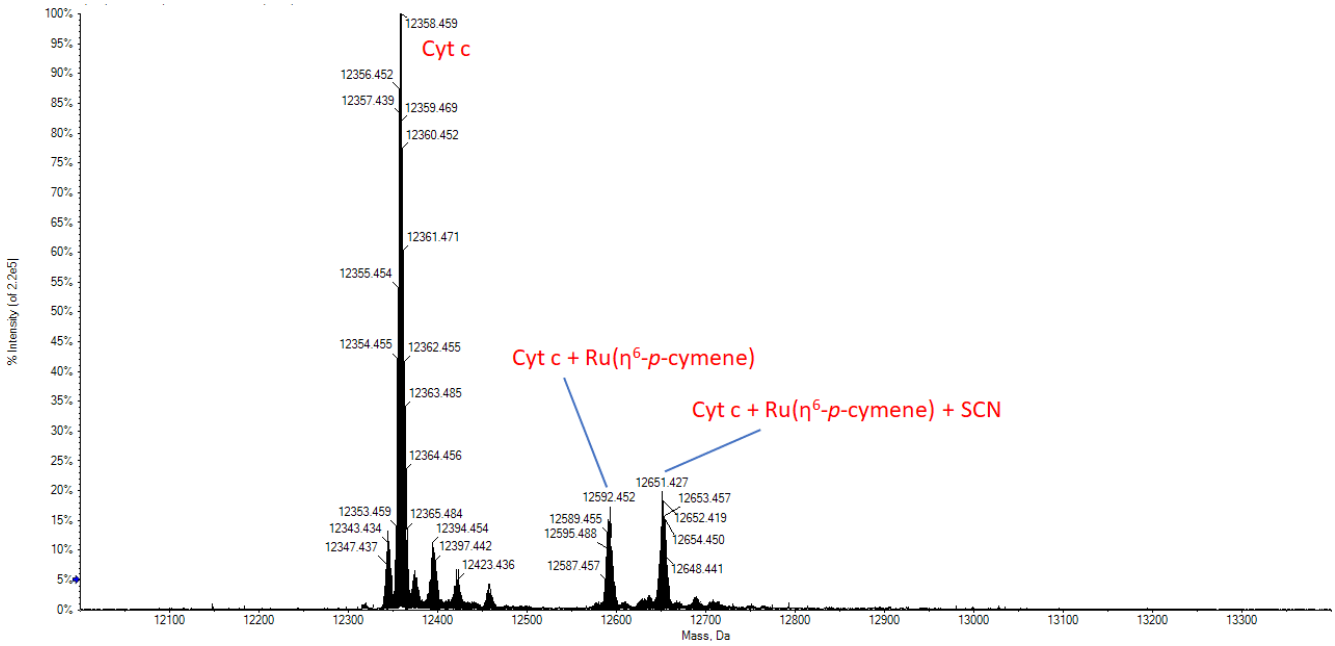

Figure S83. Deconvoluted ESI mass spectrum of Cyt c in 2 mM ammonium acetate solution, pH 6.8, incubated with compound **1d** for 72 h at 37 °C. The final protein concentration was 10^{-7} M with a complex to protein molar ratio of 3:1. 0.1% v/v of formic acid was added just before infusion.

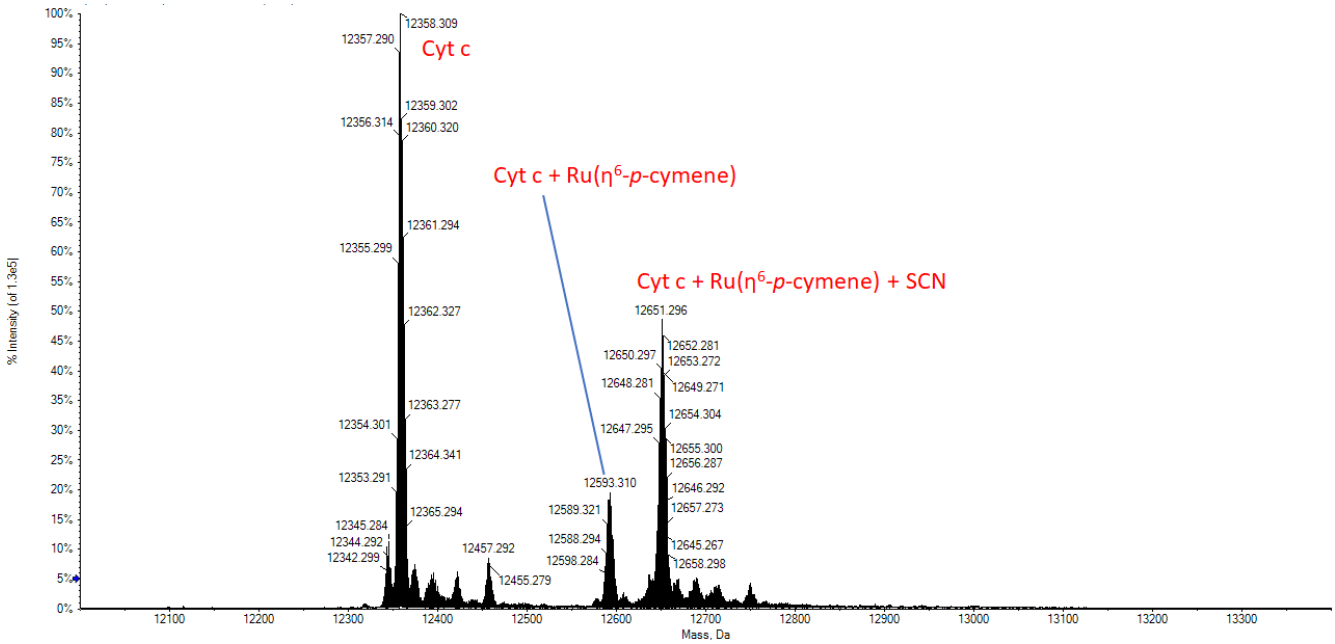

Figure S84. Deconvoluted ESI mass spectrum of Cyt c in 2 mM ammonium acetate solution, pH 6.8, incubated with compound **4h** for 24 h at 37 °C. The final protein concentration was 10^{-7} M with a complex to protein molar ratio of 3:1. 0.1% v/v of formic acid was added just before infusion.

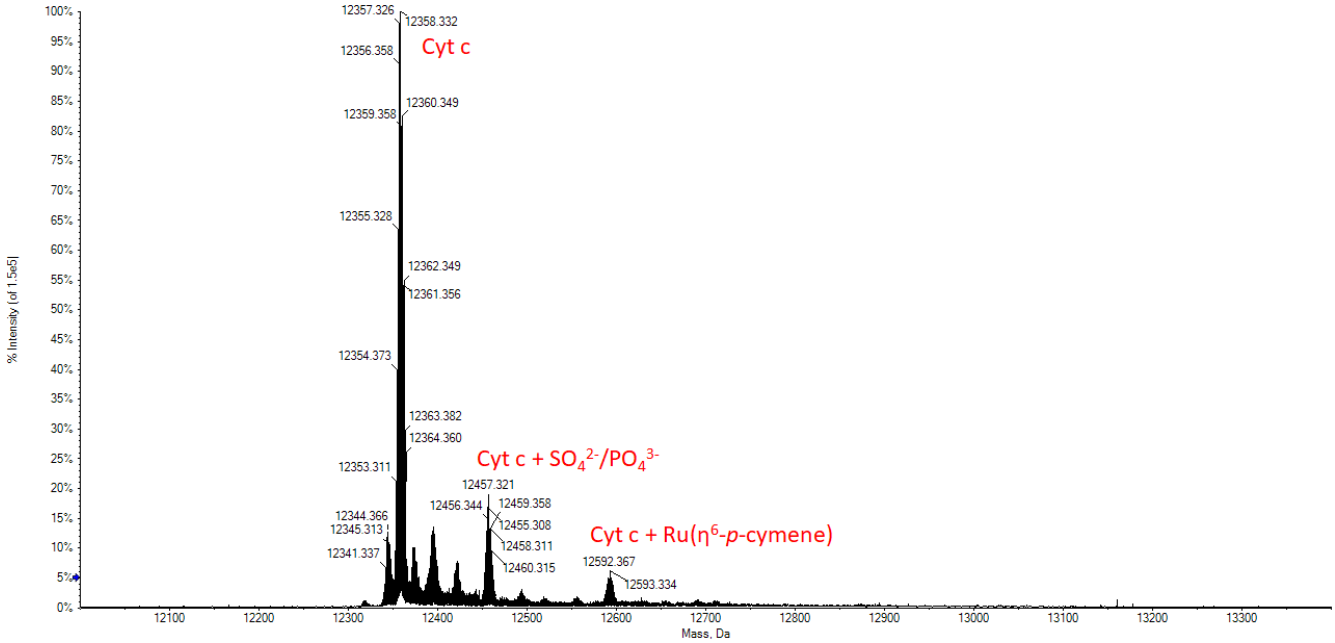

Figure S85. Deconvoluted ESI mass spectrum of Cyt c in 2 mM ammonium acetate solution, pH 6.8, incubated with compound **4h** for 72 h at 37 °C. The final protein concentration was 10^{-7} M with a complex to protein molar ratio of 3:1. 0.1% v/v of formic acid was added just before infusion.

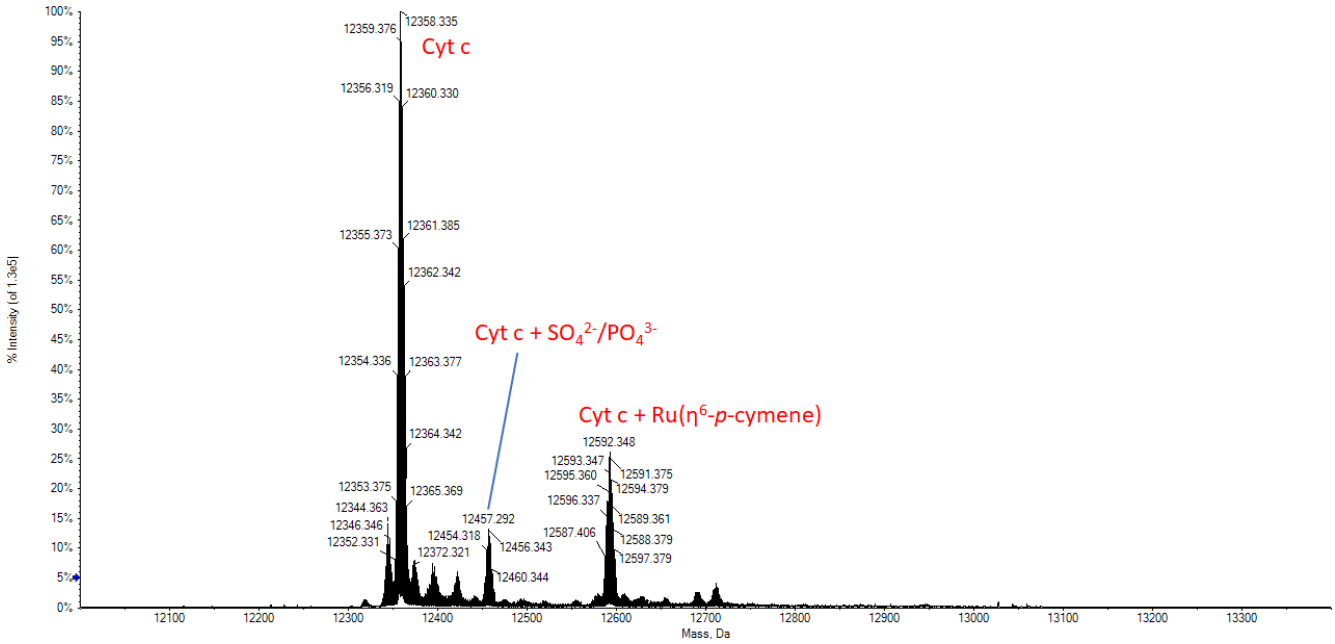

Figure S86. Deconvoluted ESI mass spectrum of Cyt c in 2 mM ammonium acetate solution, pH 6.8, incubated with compound [**3i**]Cl for 24 h at 37 °C. The final protein concentration was 10^{-7} M with a complex to protein molar ratio of 3:1. 0.1% v/v of formic acid was added just before infusion.

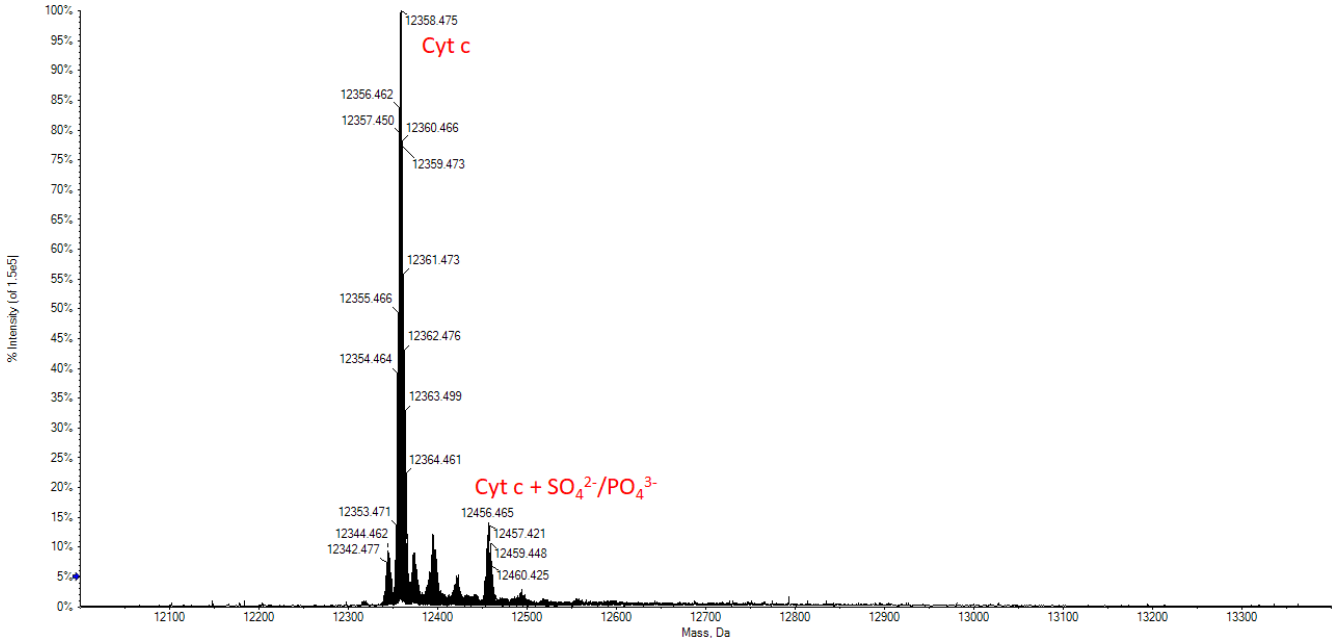

Figure S87. Deconvoluted ESI mass spectrum of Cyt c in 2 mM ammonium acetate solution, pH 6.8, incubated with compound [**3i**]Cl for 72 h at 37 °C. The final protein concentration was 10^{-7} M with a complex to protein molar ratio of 3:1. 0.1% v/v of formic acid was added just before infusion.

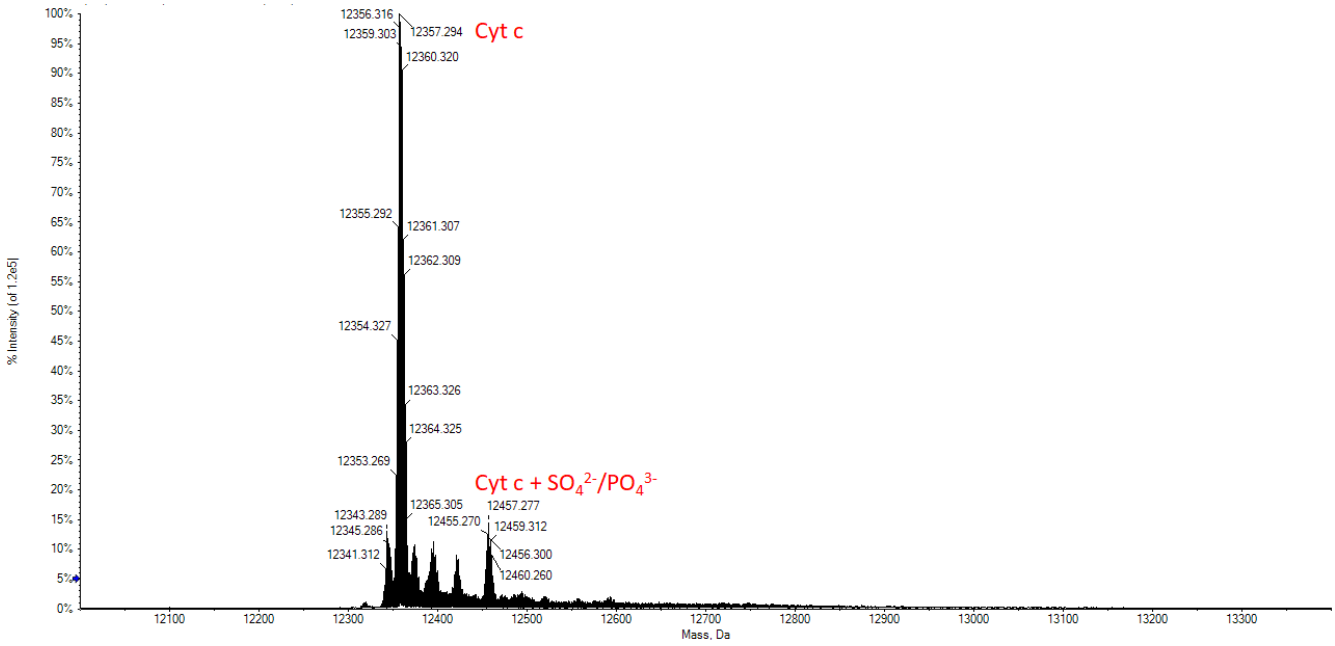

References.

1 L. Biancalana, I. Abdalghani, F. Chiellini, S. Zacchini, G. Pampaloni, M. Crucianelli and F. Marchetti, *Eur. J. Inorg. Chem.* 2018, 3041–3057.

2 (a) NaN_3: R. T. M. Fraser, *Anal. Chem*. 1959, **31**, 1602–1603; (b) KCN: G. E. Leroi and W. Klemperer, *J. Chem. Phys*. 1961, **35**, 774 and SDBSWeb: https://sdbs.db.aist.go.jp (National Institute of Advanced Industrial Science and Technology, 05/2021); (c) $[Ru(N_3)_2(\eta^6\text{-}C_6Me_6)]_2$: P. Govindaswamy, H. P. Yennawar and M. Rao Kollipara, *J. Organomet. Chem.* 2004, **689**, 3108–3112.

3 J. Feeney and A. S. V. Burgen, *Eur. J. Biochem*. 1973, **34**, 107-111.